Kaunas University of Technology
Faculty of Chemical Technology

Lithuanian University of Health Sciences
Faculty of Pharmacy

Synthesis and Structure-Activity Relationships of 2-Aminothiazole and Imidazole Derivatives Based on 3-Bromoaniline

Master's Final Degree Project

Salman Ibnu Abbas
Project author

Rsch. Dr. Kazimieras Anusevičius
Supervisor

Kaunas, 2026

Kaunas University of Technology
Faculty of Chemical Technology

Lithuanian University of Health Sciences
Faculty of Pharmacy

Synthesis and Structure-Activity Relationships of 2-Aminothiazole and Imidazole Derivatives Based on 3-Bromoaniline

Master's Final Degree Project

Medicinal Chemistry (6281CX001)

Salman Ibnu Abbas
Project author

Rsch. Dr. Kazimieras Anusevičius
Supervisor

Rsch. Dr. Mariia Stanitska
Reviewer

Kaunas, 2026

Kaunas University of Technology
Faculty of Chemical Technology

Lithuanian University of Health Sciences
Faculty of Pharmacy

Salman Ibnu Abbas

Synthesis and Structure-Activity Relationships of 2-Aminothiazole and Imidazole Derivatives Based on 3-Bromoaniline

Declaration of Academic Integrity

I confirm the following:

1. I have prepared the final degree project independently and honestly without any violations of the copyrights or other rights of others, following the provisions of the Law on Copyrights and Related Rights of the Republic of Lithuania, the Regulations on the Management and Transfer of Intellectual Property of Kaunas University of Technology (hereinafter – KTU) and Lithuanian University of Health Sciences (hereinafter – LSMU) and the ethical requirements stipulated by the Code of Academic Ethics of KTU and LSMU;

2. All the data and research results provided in the final degree project are correct and obtained legally; none of the parts of this project are plagiarised from any printed or electronic sources; all the quotations and references provided in the text of the final degree project are indicated in the list of references;

3. I have not paid anyone any monetary funds for the final degree project or the parts thereof unless required by the law;

4. I understand that in the case of any discovery of the fact of dishonesty or violation of any rights of others, the academic penalties will be imposed on me under the procedure applied at KTU or LSMU; I will be expelled from the KTU or LSMU and my final degree project can be submitted to the Office of the Ombudsperson for Academic Ethics and Procedures in the examination of a possible violation of academic ethics.

Salman Ibnu Abbas

Confirmed electronically

Salman Ibnu Abbas. Synthesis and Structure-Activity Relationships of 2-Aminothiazole and Imidazole Derivatives Based on 3-Bromoaniline. Master's Final Degree Project / supervisor Rsch. Dr. Kazimieras Anusevičius; Faculty of Chemical Technology, Kaunas University of Technology; Lithuanian University of Health Sciences, Faculty of Pharmacy

Study field and area (study field group): Chemistry, Physical Sciences.

Keywords: 2-aminothiazole, chalcone, imidazole-2-thione, anticancer activity.

Kaunas, 2026. 62 pages.

Summary

A series of novel 3-bromoaniline-based heterocyclic derivatives was synthesised and structurally characterised using ^{1}H and ^{13}C NMR spectroscopy, FTIR analysis, and elemental analysis. The compounds were divided into three main classes: 2-aminothiazole derivatives **5a–h**, chalcone derivatives **9a–k**, and imidazole-2-thione derivatives **11–17a,b**. Chemical transformations of the obtained intermediate compounds **4**, **8**, and **11** were carried out, enabling the stepwise introduction of the desired functional fragments into the molecular structure. The chalcone derivatives **9a–k** were synthesised by the condensation of 5-acetylthiazole **8** with various substituted aldehydes, allowing for systematic structural modification.

The anticancer activity of the synthesised compounds **4-17** was evaluated in the human non-small cell lung cancer A549 cell line. The results revealed a clear structure-activity relationship: several compounds reduced cell viability to less than 50%. The anticancer activity of the synthesised compounds was evaluated in the human non-small cell lung cancer A549 cell line. The results revealed a clear structure–activity relationship, with several compounds reducing cell viability to below 50%. The most pronounced antiproliferative activity was observed for (*E*)-3-((3-bromophenyl)(5-(3-(2,6-dichlorophenyl)acryloyl)-4-methylthiazol-2-yl)amino)propanoic acid (**9e**), 3-((3-bromophenyl)(5-cinnamoyl-4-methylthiazol-2-yl)amino)propanoic acid (**9a**), and 1-(3-bromophenyl)-4-(naphthalen-2-yl)-1,3-dihydro-2*H*-imidazole-2-thione (**11a**). Enhanced antiproliferative activity was associated with the presence of heterocyclic azole systems, particularly thione-containing moieties, as well as halogen-substituted aryl groups. These results suggest that 3-bromoaniline-based heterocyclic derivatives are a promising basis for the development of new anticancer drugs.

Salman Ibnu Abbas. 2-Aminotiazolo ir imidazolo darinių, gautų iš 3-bromanilino, sintezė ir struktūros-aktyvumo ryšių analizė. Baigiamasis magistro projektas / vadovas / m. d. dr. Kazimieras Anusevičius; Kauno technologijos universitetas, Cheminės technologijos fakultetas; Lietuvos sveikatos mokslų universitetas, Farmacijos fakultetas.

Studijų kryptis ir sritis (studijų krypčių grupė): chemija, fiziniai mokslai.

Reikšminiai žodžiai: 2-aminotiazolas, chalkonas, imidazol-2-tionas, priešvėžinis aktyvumas.

Kaunas, 2026. 62 p.

Santrauka

Susintetinta nauja 3-bromanilino pagrindu sudarytų heterociklinių darinių serija, kurios struktūra patvirtinta ^{1}H ir ^{13}C BMR spektroskopija, FTIR analize ir elementų analize. Junginiai suskirstyti į tris pagrindines klases: 2-aminotiazolo dariniai **5a–h**, chalkono dariniai **9a–k** ir imidazolo-2-tiono dariniai **11–17a,b**. Atliktos gautų tarpinių junginių **4**, **8** ir **11** cheminės transformacijos, kurios leido nuosekliai įvesti norimus fragmentus į molekulės struktūrą. Chalkono dariniai **9a–k** buvo susintetinti kondensuojant 5-acetiltiazolą (**8**) su įvairiais pakeistais aldehidais, leidžiančiais sistemingai modifikuoti.

Susintetintų junginių **4–17** priešvėžinis aktyvumas buvo įvertintas žmogaus nesmulkialąstelinio plaučių vėžio (NSCLC) A549 ląstelių linijoje. Rezultatai rodo aiškų struktūros ir aktyvumo ryšį, nes keli junginiai sumažino ląstelių gyvybingumą iki mažiau nei 50 %. Ryškiausias antiproliferacinis aktyvumas nustatytas junginiams – 3-((3-bromfenil)(5-cinamoil-4-metiltiazol-2-il)amino)propano rūgštis (**9a**), (*E*)-3-((3-bromfenil)(5-(3-(2,6-dichlorfenil)akriloil)-4-metiltiazol-2-il)amino)propano rūgščiai (**9e**), 3-((3-bromfenil)(5-cinamol-4-il)aminotiazol(5-cinamol-4-il)metil-1-(3-bromfenil)-4-(naftalen-2-il)-1,3-dihidro-2*H*-imidazol-2-tionui (**11a**). Nustatyta, kad padidėjęs antiproliferacinis aktyvumas susijęs su heterociklinių azolo fragmentų, ypač tiono grupių, taip pat halogenu pakeistų arilo grupių, buvimu. Gauti rezultatai rodo, kad 3-bromanilino pagrindo heterocikliniai dariniai yra perspektyvus pagrindas kuriant naujus priešvėžinius vaistus

Table of contents

Abbreviations

ABC – ATP-binding cassette

ADMET – Absorption, distribution, metabolism, excretion, and toxicity

AKT – Protein kinase B

AraC – Cytarabine (arabinosylcytosine)

ATCC – American Type Culture Collection

BCL-2 – B-cell lymphoma 2 protein

CDK – Cyclin-dependent kinase

CML – Chronic myelogenous leukemia

DMSO – Dimethyl sulfoxide

DOX – Doxorubicin

EGFR – Epidermal growth factor receptor

FASN – Fatty acid synthase

FTIR – Fourier transform infrared spectroscopy

HER2 – Human epidermal growth factor receptor 2

IC_{50} – Half maximal inhibitory concentration

JAK/STAT – Janus kinase/signal transducer and activator of transcription

MAPK – Mitogen-activated protein kinase

MTT – 3-(4,5-dimethylthiazol-2-yl)-2,5-diphenyltetrazolium bromide

NCI – National Cancer Institute

NMR – Nuclear Magnetic Resonance

NSCLC – Non-Small Cell Lung Cancer

PI3K – Phosphatidylinositol 3-kinase

P-gp – P-glycoprotein (ABCB1)

Rb – Retinoblastoma protein

ROS – Reactive oxygen species

RTK – Receptor tyrosine kinase

SAR – Structure-activity relationship

SD – Standard deviation

TLC – Thin layer chromatography

TMP – 3,4,5-trimethoxyphenyl

TMS – Tetramethylsilane

VEGFR – Vascular endothelial growth factor receptor.

Introduction

Cancer remains a major global health problem and a leading cause of mortality worldwide. It is characterised by uncontrolled cell proliferation, often accompanied by invasion of surrounding tissues and metastasis to distant organs. Under normal physiological conditions, cell division is tightly regulated; however, genetic mutations, inactivation of tumour suppressor genes, and disruptions in signalling pathways can result in abnormal cell growth. Although current treatments, including chemotherapy, radiotherapy, and targeted therapy, have demonstrated considerable efficacy, significant limitations persist, such as poor selectivity, drug resistance, and adverse side effects. Therefore, the development of novel small molecules with improved anticancer activity and enhanced safety profiles remains essential in medicinal chemistry [1], [2].

Heterotricyclic compounds play an important role in drug discovery, especially those containing nitrogen and sulphur atoms. These structural motifs are widely found in clinically approved drugs and are valuable scaffolds for the development of anticancer drugs. Heterocyclic compounds exhibit diverse mechanisms of action, including inhibition of protein kinases, DNA replication, and tubulin polymerisation, making them important candidates for anticancer drug development [3]. In recent years, anticancer therapy has shifted from nonselective cytotoxic agents to more targeted approaches. Key molecular targets, such as epidermal growth factor receptor (EGFR), tubulin, and topoisomerase II, regulate essential cellular processes, including cell division and signalling. Their inhibition disrupts tumour growth and may improve therapeutic selectivity while reducing side effects [4]. Chalcones, a class of α,β-unsaturated flavonoids, are known for their antiproliferative activity, mainly attributed to their interaction with tubulin and Michael acceptor properties. These properties make them attractive scaffolds for the development of anticancer drugs. In this study, a series of novel 3-bromoaniline-based heterocyclic derivatives containing thiazole, chalcone and imidazole-2-thione pharmacophores were synthesised and evaluated in the A549 lung cancer cell line to investigate structure-activity relationships. Cancer is characterised by uncontrolled cell proliferation resulting from genetic mutations and dysregulation of signalling pathways. The ability of cancer cells to evade apoptosis and develop resistance to conventional therapies remains a major challenge. Therefore, targeted therapeutic strategies have become a major focus of medicinal chemistry, aiming to selectively interfere with tumour-specific pathways and improve treatment outcomes [5][6], [7].

The project objective is to synthesise new 2-aminothiazole, chalcone-thiazole hybrid and imidazole-2-thione derivatives based on the 3-bromoaniline scaffold and evaluate their anticancer activity *in vitro* against A549 cells.

Research tasks:

1. To synthesise thioureic acid derivatives from 3-bromoaniline and study their reactions with α-haloketones, as well as to determine the properties of the obtained products.
2. To synthesise imidazole-2-thione derivatives based on the 3-bromoaniline fragment and to study the properties of the synthesised compounds;
3. To evaluate the anticancer activity of the synthesised compounds *in vitro* against a human non-small cell lung cancer (A549) cell line;
4. To analyse structure-activity relationships to identify biologically important structural features.

1. Literature review

1.1. Problems and challenges related to chemotherapy in malignancy

Cancer remains a leading cause of death worldwide in the 21st century. In 2022, about 20 million new cases were reported, with 9.7 million cancer-related deaths worldwide [8]. This information highlights the significant problem of cancer on health care systems. Malignancy is characterised by unrestrained cell proliferation, invasion of adjacent tissues, and metastasis to distant organs. Cancer expansion is a multi-step procedure involving the accumulation of genetic alterations, epigenetic changes, dysregulated signalling pathways, and irregular intercellular communication [9]. Around 200 different types of cancer have been recognised, each exhibiting exceptional molecular features, biological behaviour, and clinical responses, which complicates the expansion of universal therapeutic approaches [9]. At the molecular level, cancer is related to the modifications in the signalling pathways changeable cellular homeostasis, proliferation, differentiation, existence, and apoptosis. Among the most extensively studied pathways are the phosphatidylinositol 3-kinase (PI3K)/AKT/mTOR pathway, the Ras/MAPK cascade, and the Janus kinase/signal transducer and activator of transcription (JAK/STAT) signalling system [9], [10].

Chemotherapy remains one of the main treatment methods, and it is widely employed either alone or in combination with surgical treatment and radiation therapy. Nevertheless, despite its clinical reputation, chemotherapy is accompanied by significant barriers that reduce treatment effectiveness. Conventional chemotherapeutic agents primarily target quickly multiplying cells but lack specificity between malignant and normal proliferating cells. As a result, vigorous tissues such as the gastrointestinal epithelium, hair follicles, and reproductive cells are often exaggerated, leading to adverse effects, together with nausea, vomiting, fatigue, and immunosuppression [11].

In response to these restrictions, medicinal chemistry efforts have progressively focused on the design and synthesis of low-molecular-weight compounds with enhanced anticancer activity and selectivity. Heterocyclic compounds play a dominant role in drug discovery due to their structural diversity and capability to interact with biological targets. Notably, many FDA-approved drugs contain heterocyclic scaffolds [12], [13]. Heterocycles containing nitrogen and sulphur atoms display a robust interaction with biological targets through hydrogen bonding, π–π stacking, and hydrophobic interactions, by means of management with active-site residues. Among these, thiazole, chalcone, and imidazole scaffolds are extensively recognised pharmacophores in anti-cancer drug expansion due to their structural adaptability and broad biological activity [12].

The incorporation of thiazole, chalcone, and imidazole scaffolds into small-molecule frameworks, therefore, represents a valuable strategy for the development of multi-target anticancer agents with promising therapeutic potential [10], [11], [12].

1.2. Signalling pathways and metabolic reprogramming in cancer biology

Cancer development is driven by the accumulation of molecular alterations that promote cell survival and proliferation. The hallmarks of cancer include independence from growth signals, evasion of apoptosis, limitless replicative potential, invasion, and metastasis [15]. These changes are mediated by dysregulation of signalling pathways, cell-cycle control, and metabolism (Fig. 1.1).

The PI3K/AKT/mTOR pathway is frequently dysregulated in cancer. Activation of receptor tyrosine kinases leads to PI3K-mediated formation of phosphatidylinositol-3,4,5-trisphosphate, which activates AKT and downstream signalling, promoting cell growth and survival. PTEN negatively regulates this pathway, and its loss results in sustained pathway activation and tumour progression [14].

Disruption of cell-cycle control is another key feature. Cyclin-dependent kinases (CDKs) regulate progression through the cell cycle, and their overactivation, combined with loss of inhibitors such as p21 and p27, leads to uncontrolled proliferation. CDKs are therefore important targets in anticancer drug development [15].

Metabolic reprogramming is characterised by increased glycolysis and glutamine utilisation, supporting rapid energy production and biosynthesis required for cell growth [18] [17]. Alterations in lipid metabolism and redox homeostasis further contribute to tumour progression and resistance to oxidative stress [18][19]

Resistance to apoptosis is regulated by the balance between pro- and anti-apoptotic proteins. Overexpression of BCL-2 family proteins promotes tumour survival and therapy resistance. Activation of apoptosis involves mitochondrial membrane permeabilisation, cytochrome c release, and caspase activation. Targeting these processes represents a key anticancer strategy [21].

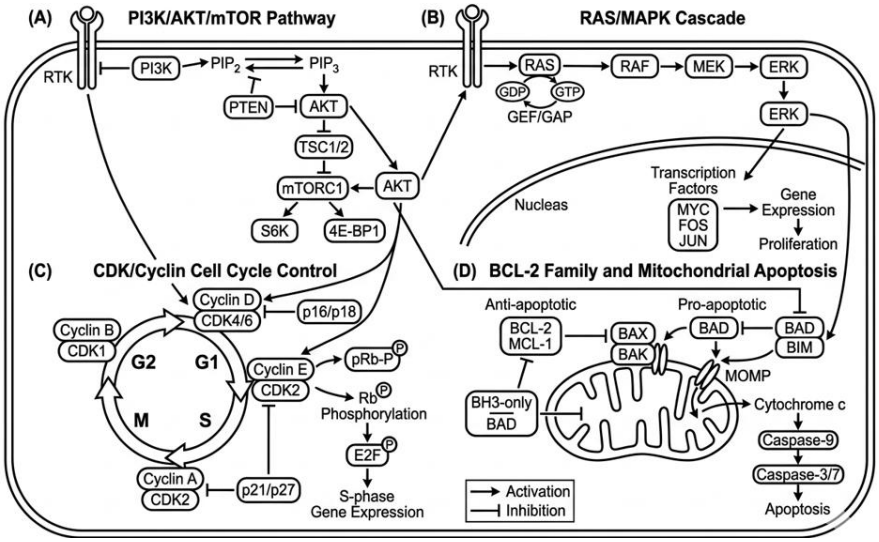

Fig. 1.1. The central role of important oncogenic signalling pathways and their deregulation in cancer cells. Arrows indicate activation (→) and inhibition (⊣).

These cancer signalling and metabolic pathways deliver well-defined targets for small molecule mediations. CDK inhibitors normally contain heterocyclic nitrogen-holding scaffolds, which enable the formation of hydrogen bonding within the ATP -binding hinge region of kinases. In the case of PI3K/AKT/mTOR pathway inhibitors widely used in heterocyclic core to interact with kinase active sites through hydrogen bonding, hydrophobic, lipophilic and electrostatic interactions [16], [17]. BCL-2 inhibitors occupy at BH3- binding site due to their strong hydrophobic aromatic system and show pro-apoptotic activities [21]. These signalling pathways support us in designing the heterocyclic thiazole, chalcone, and imidazole scaffolds and derivatives. This scaffold exhibits a wide range of electronic, hydrophobic interactions with cancer-linked molecular targets.

1.3. Small-molecules as therapeutic targets

The development of anticancer therapy has shifted from non-selective cytotoxic agents towards targeted small molecules acting on specific oncogenic pathways. This changeover was justified by the clinical accomplishment of imatinib, a BCR-ABL tyrosine kinase inhibitor that was used in the treatment of chronic myeloid leukaemia [15]. Targeted treatments are intended to inhibit specific proteins connected with tumour development, by this means reducing toxicity likened with conventional chemotherapy, which primarily affects quickly dividing cells.

Small-molecule anticancer agents comprise kinase inhibitors, polymerase inhibitors, and apoptosis-regulating complexes. These fragments are typically structurally adaptable and capable of interacting with well-defined binding sites on target proteins [22], [23]. Specifically, cyclin-dependent kinases (CDKs) represent key regulators of the cell cycle, and their dysregulation contributes to uncontrolled cell multiplication. CDK inhibitors, such as palbociclib, have demonstrated clinical efficacy, predominantly in hormone receptor-positive breast cancer [24] [24] [25] [26] Apoptosis-related targets, together with BCL-2 family proteins (BCL-2, BCL-XL, and MCL-1), characterise an additional significant class of therapeutic targets [6] Heterocyclic frameworks containing nitrogen and sulphur atoms, such as imidazole, chalcone, and thiazole, are normally found in anticancer agents due to their capability to form hydrogen bonds, π–π connections, and electrostatic interactions with biological marks [7].

These belongings support the usage of thiazole, chalcone, and imidazole pharmacophores in the design and synthesis of novel compounds with possible anticancer activity.

1.4. Clinically approved drugs include fragments encompassing thiazole, chalcone or imidazole rings.

Thiazole and imidazole are connected heterocycles characterised by core pharmacophores in many clinically accepted anti-cancer representatives. Some of the drug structures are shown in Fig. 1.1. Dasatinib, used in the treatment of severe myeloid leukaemia and Philadelphia chromosome-positive acute lymphoblastic leukaemia, encompasses an aminothiazole moiety that allows key hydrogen bonding within the BCR-ABL kinase hinge region [26],[27].

Dabrafenib is a clinically approved thiazole-containing inhibitor of mutant BRAF kinase (V600E), normally related to melanoma, and acts by overcoming MAPK signalling, by this means reducing tumour cell propagation [28]. In contrast, ixabepilone, a semi-synthetic correspondent of epothilone B encompassing a thiazole unit, exhibits. Its activity through microtubule stabilisation, followed by mitotic arrest and tumour cell death [29].

Imidazole by-products also display significant anticancer activity. Dacarbazine is a triazene prodrug used for the treatment of metastatic melanoma in addition to Hodgkin lymphoma, which acts via DNA methylation, subsequent metabolic activation [30]. Ketoconazole, even though recently developed as an antifungal agent, has demonstrated importance in oncology through inhibiting the action of CYP17A1, by this means reducing androgen production and tumour growth in prostate cancer [31].

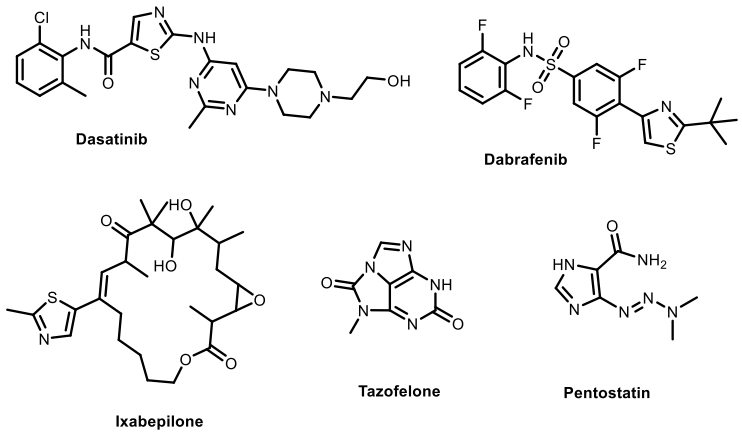

Fig. 1.2. Clinically available Anti-Cancer drugs approved by FDA

In contrast to the thiazole and imidazole-based drugs, chalcone derivatives are principally considered as investigational anticancer scaffolds and widely approved therapeutics. Chalcones contain an α,β-unsaturated carbonyl system, which functions as a Michael acceptor and enables communications with cellular nucleophiles. These structural characteristics are associated with numerous anticancer mechanisms. Which including inhibition of tumour cell proliferation, improvement of apoptosis, induction of oxidative stress, and interference with tubulin polymerisation [32]. Chalcones are structurally multipurpose and can be easily modified, making them suitable for the synthesis of hybrid molecules with improved biological activity. Clinically used drugs such as dasatinib, dabrafenib, ixabepilone, and ketoconazole underline the therapeutic relevance of heterocycles, including thiazole and imidazole, in anticancer drug design. Consequently, the development of novel thiazole-, imidazole-, and chalcone-based derivatives represents a promising approach for the synthesis of low-molecular-weight compounds with potential anti-cancer activity.

1.5. Thiazole moiety in anticancer drug design

In medicinal chemistry, thiazole-containing compounds signify an important class of scaffolds for anticancer drug expansion due to their structural adaptability and ability to interact with multiple biological targets. Thiazole is a five-membered aromatic heterocycle containing nitrogen and sulphur atoms, which exhibits favourable electronic properties for molecular interactions. The thiazole core is commonly synthesised via Hantzsch-type cyclisation reactions, typically relating to the condensation of α-haloketones with thiourea derivatives, allowing structural modification through substitution at different positions of the ring [33],[34]. Such substitutions, including electron-donating and electron-withdrawing groups, significantly influence the biological activity of the resulting compounds. The anticancer activity of thiazole derivatives is primarily associated with their interactions with targets such as protein kinases, tubulin, DNA-associated enzymes, and apoptosis-regulating proteins. The nitrogen atom acts as a hydrogen bond acceptor, while the sulphur atom and aromatic π-system contribute to hydrophobic interactions, enhancing binding affinity to biological targets [35].

Due to their availability, structural flexibility, and biological relevance, thiazole scaffolds are widely used in the development of novel anticancer drugs with improved activity, selectivity, and structure-activity relationships.

The Hantzsch method was used for the synthesis of thiazole derivative **3**, as shown in Scheme 1.1. 1-(5-Methyl-2-(pyridin-3-yl)thiazol-4-yl)ethan-1-one (**3**) was synthesised from pyridine-3-

carbothioamide (**1**) by the reaction with 2-chloro-1-phenylethan-1-one (**2**) in ethanol in the presence of triethylamine reflux [39].

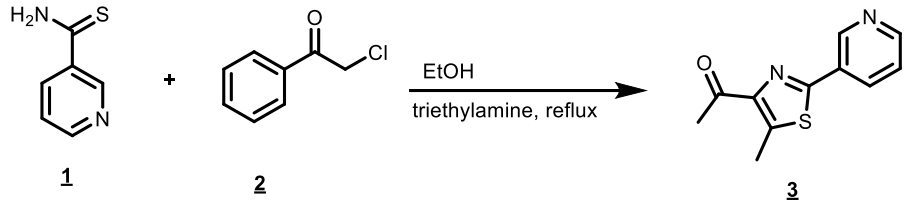

1 **2** **3**

Scheme. 1.1. General synthetic method of thiazole fragments.

Kassem *et al* [36] reported the synthesis of 2-methyl-5-aminothiazole hydrosulphate (**6**), which was obtained via condensation followed by cyclisation of aminoacetonitrile (**4**) with ethyl dithioacetate (**5**). The reaction was carried out in methanol at room temperature in the presence of triethylamine to afford the corresponding 5-aminothiazoles **6** with good yield, as shown in Scheme 1.2.

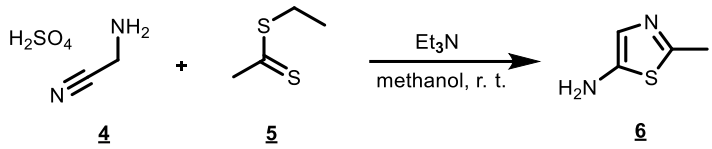

4 **5** **6**

Scheme 1.2. Synthesis of 2-methyl-5-aminothiazole hydrosulphate (**6**)

Ayoub Boualli *et al* [37], [38]. reported the synthesis of a series of 2-aminothiazole derivatives **9** from thiosemicarbazide derivative **7**. The compounds **9** were obtained by treating of different of 2-benzylidenehydrazine-1-carbothioamide **7** with phenacyl bromide derivative **8** in ethanol at room temperature for 24 h, affording the desired products in good yield (Scheme 1.3). After evaluating the synthesised compounds of series **9**, it was found that compound DBT9 significantly increased apoptosis in MCF-7 breast cancer cells, from 6.3% ± 1.1% in untreated controls to 57.8% ± 6.3% after treatment.

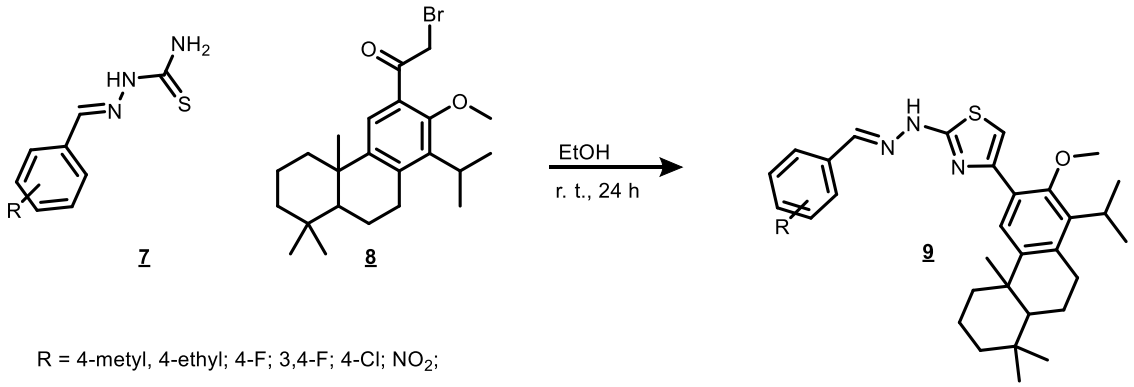

7 **8** **9**

R = 4-metyl, 4-ethyl; 4-F; 3,4-F; 4-Cl; NO_2;

Scheme 1.3. Syntheses of 2-aminothiazole derivatives **9**

The synthesis of novel thiazolyl hydrazones **11** was reported by the authors [39], as shown in Scheme 1.4. (*E*)-2-(4-((4-methylpiperazin-1-yl)methyl)benzylidene)hydrazine-1-carbothioamide (**10**) was reacted with various bromoacetophenones in ethanol under reflux for 6 h, affording the corresponding compounds **11** in good yield up to 85%.

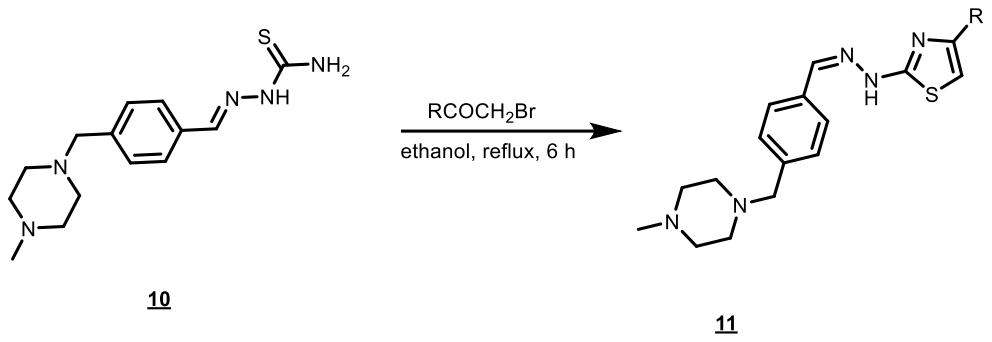

10 **11**

R = **a)** C_6H_5; **b)** 4-FC_6H_4; **c)** 4-ClC_6H_4; **d)** 4-BrC_6H_4; **e)** 4NO_2-C_6H_4;

Scheme 1.4. Syntheses of hitherto new thiazolyl hydrazones.

A series of 2-aminothiazole derivatives **11** was synthesised and evaluated for anticancer activity. The compounds **11** were tested against relevant cancer models, including A549 cells. Among the synthesised compounds, compound **11**, bearing a 4-fluorophenyl substituent, exhibited significant activity against the EGFR kinase binding site.

The synthesis of compound **13** was described by the authors [40], as shown in Scheme 1.5. The compound **13** was obtained by condensing 2-[2-(1-(2-hydroxyphenyl)ethylidene)hydrazinyl]-1,3-thiazol-4(5*H*)-one (**12**) with 5-bromo-2-hydroxybenzaldehyde in acetic acid in the presence of condensed sodium acetate at reflux for 4–6 h. Compound **13** was subsequently acetylated with acetic anhydride at reflux for 1–2 h to give the corresponding acetylated derivative **14**, as shown in Scheme 1.5.

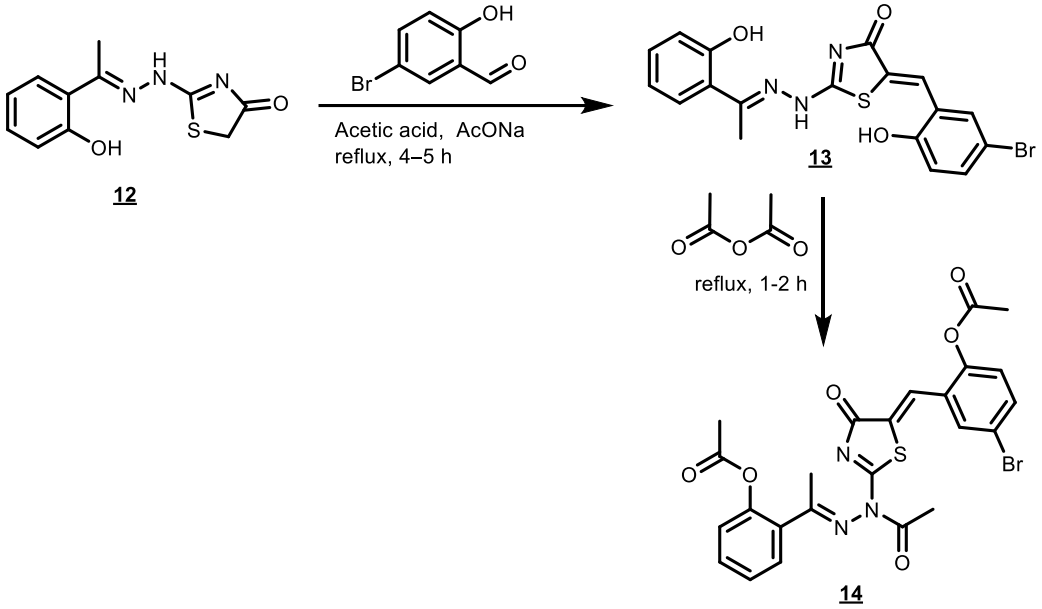

12 **13** **14**

Scheme 1.5. Synthesis of compound **14** from compound **13**.

Upon evaluation, compound **14** exhibited a broad spectrum of activity, especially antiproliferative properties. It was found to induce apoptosis in HepG2 and MCF-7 cells and to exhibit significant anti tubulin activity. These outcomes further demonstrate the importance of thiazole scaffolds in the expansion of anticancer drugs [40].

1.6. Chalcones moiety in the development of anticancer scaffolds

Chalcones signified as a important scaffolds in medicinal chemistry due to their simple framework, ease of synthesis, and wide-ranging of biological activities. They encompassed with two aromatic rings connected by an α,β-unsaturated carbonyl system, which help as a the key pharmacophore and functions as a Michael acceptor, permitting interactions with biological targets [41]. Chalcone derivatives have been described to exhibit anticancer activity through mechanisms such as inhibition of tubulin polymerization and modulation of signalling pathways [42]. Their structural features allows the formation of hybrid molecules with improved biological properties. Therefore, chalcone derivatives remain valuable candidates intended for further investigation and structure-activity relationship studies in anticancer drug development [43].

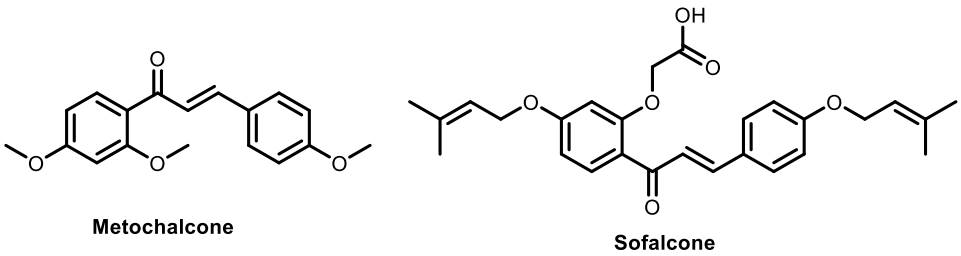

Fig. 1.3. commercially available chalcone derived drug approved by FDA.

Chalcone-based hybrids are well recognized for their anticancer activity, predominantly their ability to interrelate with multiple biological targets. This multifunctional property allows them to inhibit a variability of receptors and signalling pathways, making these compounds particularly important in surpass drug resistance related with compensatory signalling and tumour heterogeneity. Chalcones are most commonly synthesised via the Claisen-Schmidt condensation reaction, in which substituted benzaldehydes **15** react with substituted acetophenones **16** in the presence of bases such as NaOH or KOH to form α,β-unsaturated carbonyl derivatives **17** [40] (Scheme 1.6.).

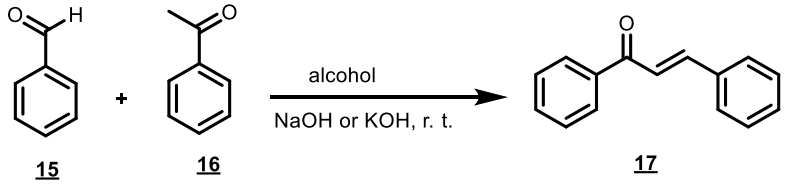

Scheme 1.6. Synthesis of chalcones **17**.

Kaur et al stated that intermediate **18** has reacted with 4-methoxybenzaldehyde in methyl alcohol using KOH as a base at room temperature to synthesise the product **19** was represented in (Scheme 1.7). Compound **19** showed important anticancer activity compared to various cell lines, such as MCF-7, HepG2, and HCT116. It remained also found to encourage apoptosis, by confirming its possible as an anticancer agent.

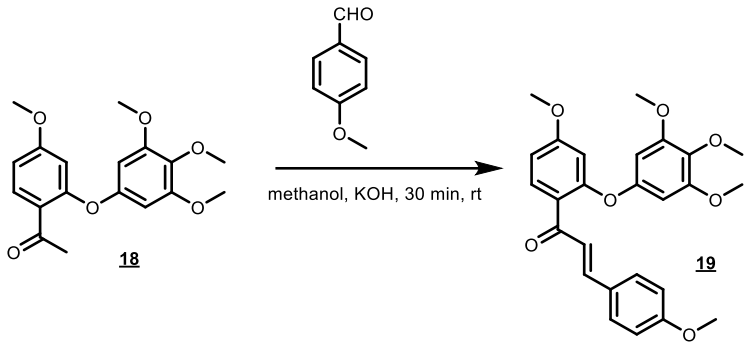

Scheme 1.7. Synthesis of compound **19** by condensation reaction.

As from reported [41]of acetylation reaction of compound **20** as shown in Scheme 1.8. The synthesised compound **21** from 1-[4-methoxy-2-(3,4,5-trimethoxyphenoxy)phenyl]ethan-1-one (**20**) via reaction with an acyl chloride in THF for 8 h with good yield.

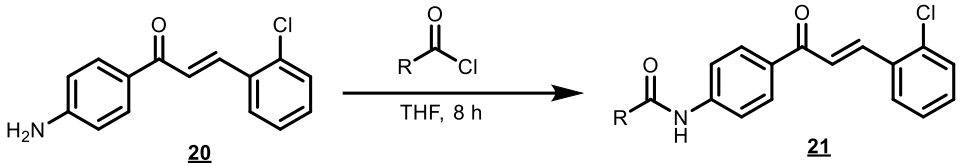

R_1 = C_6H_5; 4-CH_3-C_6H_4; 4-FC_6H_4; 4-Cl-C_6H_4; 4-$CH_3COC_6H_4$;

Scheme 1.8. Acetylation of 1-[4-methoxy-2-(3,4,5-trimethoxyphenoxy)phenyl]ethan-1-one (**20**)

The conducted studies demonstrated that chalcone analogues bearing an α,β-unsaturated ketone exhibit enhanced anticancer activity. Compound **21** was identified as the most potent derivative, showing significant antiproliferative effects against NCI-H460, A549, and H1975 cell lines. Its activity was associated with ROS-mediated, caspase-3-dependent proptosis and supported by favourable *in vivo* safety, indicating its potential as a lead compound.

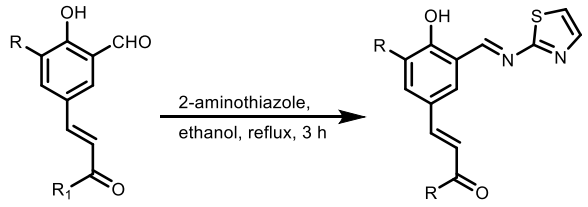

Scheme 1.9. Synthesis of chalcone-thiazole hybrid **23**.

The studies [42] reported that chalcone derivatives can be synthesised via acid-catalysed condensation reactions. In this approach, compound **23** was obtained by reacting compound **22** with 2-aminothiazoles in ethanol under reflux for 3 h (Scheme 1.9). The synthesised chalcone-thiazole hybrids exhibited significant antibacterial activity against *Staphylococcus aureus*. It exhibited low haemolytic activity and negligible toxicity to mammalian cells, and *in vivo* studies showed efficacy comparable to vancomycin, highlighting its potential as a primary antibacterial agent.

Chalcone-thiazole hybrids have been reported to exhibit anticancer activity, primarily through the induction of apoptosis [43] For example, a series of thiazole–chalcone derivatives **26a-f** described in the literature [44] [44] demonstrated significant anticancer activity (Scheme 1.10). These compounds

26a-f showed high selectivity, induced apoptosis, and inhibited cyclin-dependent kinases, highlighting their potential as promising antitumour agents.

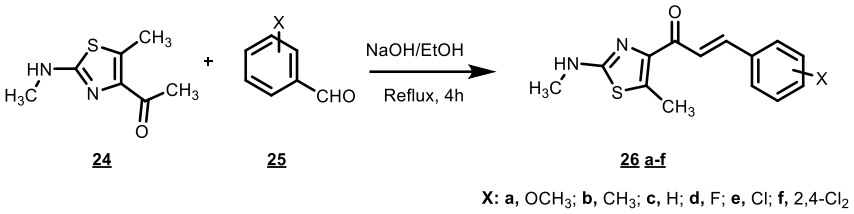

Scheme 1.10. Synthesis of thiazolyl chalcone derivatives **26a–f**.

Fathi *et al.* [45] reported the synthesis of bisarylchalcone derivatives **28** obtained from 4,4′-(ethane-1,2-diylbis(oxy))dibenzaldehyde (**27**) through condensation with various substituted acetophenones. The reaction was carried out in DMF using 40% KOH as a base under microwave irradiation for approximately Scheme 1.11.

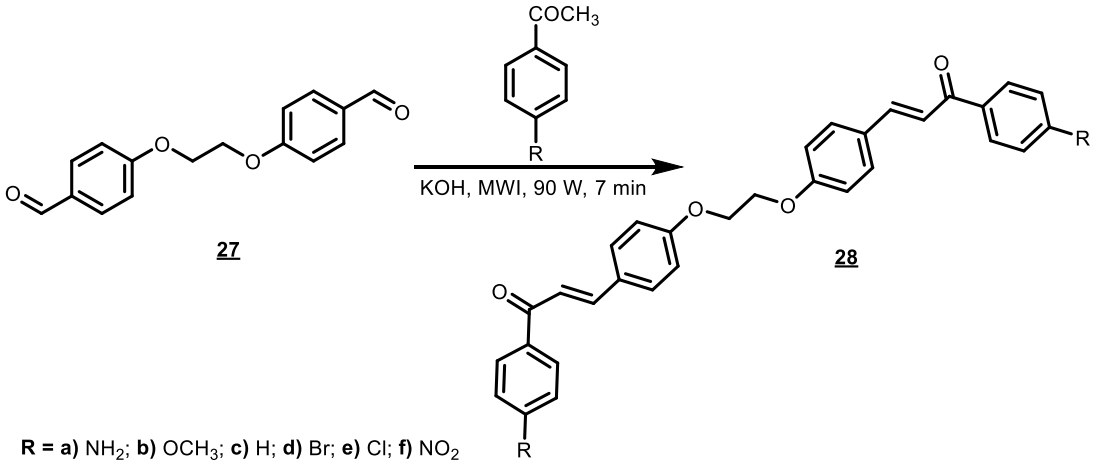

Scheme 1.11. Synthesis of different bischalcone type derivatives **28**

All the synthesised compounds exhibited significant anticancer activity [45]. In particular, (2*E*,4*E*,6*E*)-1-(4-aminophenyl)-7-(2-(4-((*E*)-3-(4-aminophenyl)-3-oxoprop-1-en-1-yl)phenoxy)ethoxy)-4-methylhepta-2,4,6-trien-1-one **28** demonstrated pronounced cytotoxic activity in in vitro studies against the CAL51 breast adenocarcinoma cell line.

1.7. Imidazole-based compounds in cancer therapy

Imidazole derivatives are nitrogen-containing heterocyclic compounds that play a significant role in medicinal chemistry. Several imidazole-based structures are present in FDA-approved anticancer drugs due to their function as key heterocyclic pharmacophores [55].

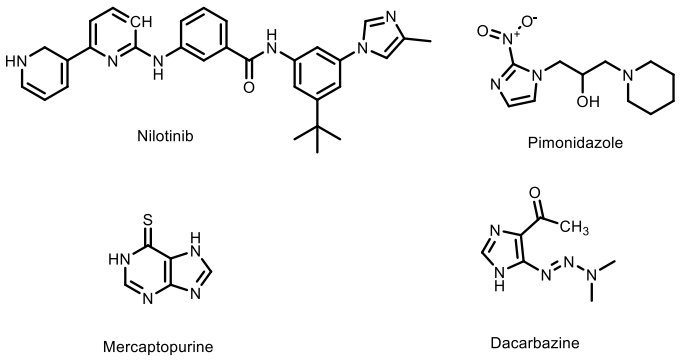

Fig. 1.4. Clinically approved anticancer drugs containing imidazole moieties

Imidazole is a nitrogen-containing heterocycle with two nitrogen atoms, which allows hydrogen bonding and coordination with metal ions, thereby facilitating interaction with the active sites of enzymes. Due to these properties, imidazole scaffolds can bind to a variety of biological targets. The anticancer activity of imidazole derivatives is mainly determined by their structural properties, and substituted imidazoles have shown cytotoxic activity against various cancer cell lines, including breast and lung cancer [47]. Recent studies have shown that imidazole-based hybrids obtained by combining imidazole with other pharmacophores, such as chalcone, thiazole, and benzimidazole, exhibit enhanced anticancer activity and selectivity [48]. Therefore, imidazole derivatives are promising scaffolds for the development of anticancer drugs due to their structural versatility and ability to interact with a variety of biological targets.

Imidazole **31** can be synthesised by cyclisation of α-keto aldehydes, which are obtained by oxidation of aryl methyl ketones with selenium dioxide (SeO_2) [49], followed by treatment with ammonium acetate in ethanol at room temperature as shown in Scheme 1.12.

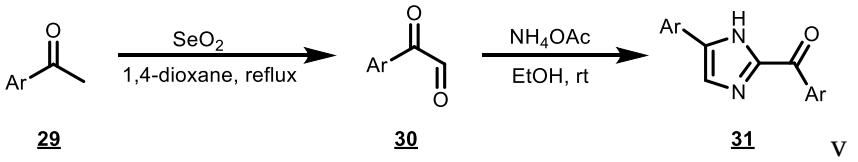

Scheme 1.12. Shows the general synthesis method of imidazole **31**

Substituted 1,2-diphenylethane-1,2-dione (**32**) was reacted with substituted aldehydes (33) in the presence of ammonium acetate to give trisubstituted imidazoles **34** as shown in Scheme 1.13. The reaction was carried out under suitable conditions, and in some cases, A-MFGO was used as a catalyst to facilitate the coupling process [50].

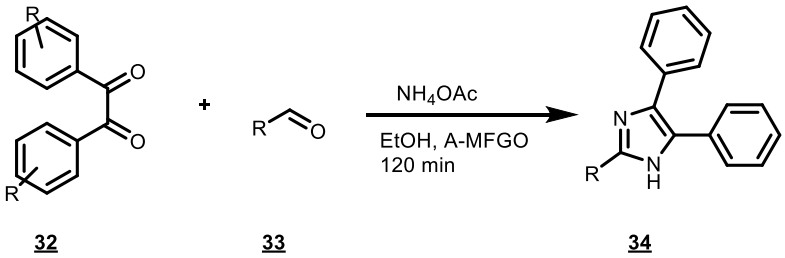

Scheme 1.13. The synthesis of trisubstituted imidazoles **34**

The synthesis of compound **35** was reported [51], as shown in Scheme 1.14. The compound was obtained by reaction with 3,4,5-trimethoxyphenyl isocyanate (**36**) in the presence of acetic acid and

zinc as a catalyst at room temperature for approximately 2 h, affording the desired 1-acetyl-1,3-dihydro-3,4-diaryl-2*H*-imidazol-2-ones **37**. The synthesised imidazole derivatives exhibited significant anticancer activity, with selected compounds demonstrating cytotoxicity comparable to standard drugs and effective tumour inhibition *in vitro* and *in vivo*.

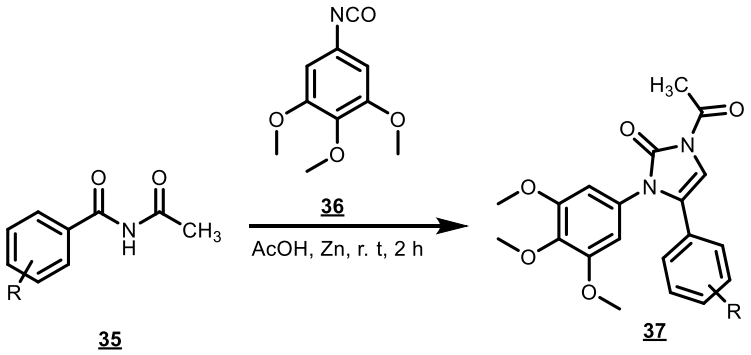

R = a) 4-OCH_3; **b)** 3,4-$(OCH_3)_2$; **c)** 3-NO_2 and 4-OCH_3; **d)** H; **f)** 4-Br; **g)** 4 -Cl; **h)** 4-NO_2; **i)** 2,4-F

Scheme 1.14. Synthesis of imidazole derivatives **37**

According to the reported study [52], compound **40** was synthesised starting from phenylenediamine **38**, which was reacted with chloroacetic acid to yield a benzimidazole intermediate **39**. The compound **39** was additionally transformed into the desired compound **40** through response with secondary amines via a dithiocarbonates intermediate, as shown in Scheme 1.15.

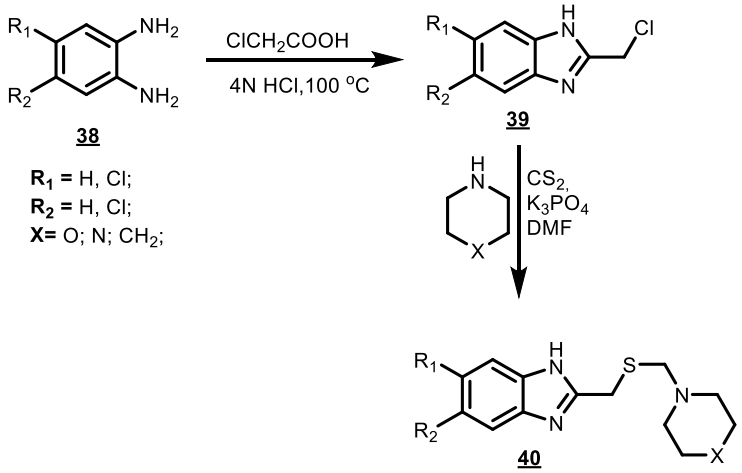

R_1 = H, Cl;
R_2 = H, Cl;
X= O; N; CH_2;

Scheme 1.15. Synthesis scheme for compound **40**

Benzimidazole derivatives **40** covering dithiocarbonate and Thio propyl linkers were synthesised and assessed for anticancer activity (Scheme 1.15). Numerous compounds showed significant cytotoxicity in contrast to MCF-7 cells, with selected by-products showing IC_{50} values below 10 µg/mL. Their activity was back upped by binding connections with the Pin1 enzyme and established by molecular docking, which indicate their potential as promising anticancer agents [61].

The synthesis of 1*H*-benzimidazole derivatives **42** was labelled, as shown in Scheme 1.16. Compound **42** was synthesised from sodium hydroxy(4-hydroxyphenyl)methanesulfonate (**41**) by reaction with several o-phenylenediamines. Among the synthesised compounds, the methyl-substituted derivative displayed notable topoisomerase I inhibitory activity, representing its potential anticancer belongings.

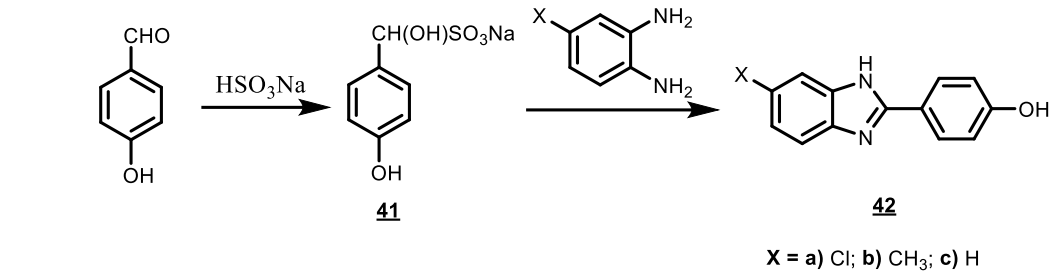

Scheme 1.16. Synthesis of (1*H*-benzimidazole derivatives **42**

According to the literature [53], compound **43** was treated with 2-hydroxybenzimidazole in the along with of caesium carbonate in DMF solution to develop compound **45**, as shown in Scheme 1.17. This intermediate was then further transformed to obtain the final product, which exhibited androgen receptor (AR) antagonist activity.

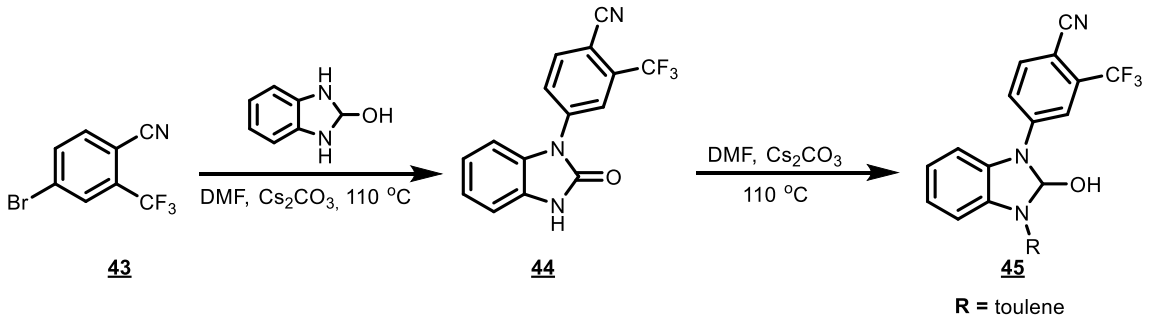

Scheme 1.17. Synthesis of benzimidazole derivative **45**

Androgen receptor signalling plays a critical role in the progression of prostate and certain breast cancers by regulating cell growth, differentiation, and survival [53]. As a result, AR has become an important therapeutic target. Oxo benzimidazole derivatives **45** were developed as potent AR antagonists using structure-based drug discovery approaches (Scheme 1.17). Among them, selected compounds showed significant cytotoxic activity against prostate (PC-3, LNCaP) and breast (MCF-7, MDA-MB-231) cancer cell lines. These results highlight the potential of oxobenzimidazole scaffolds for the development of targeted anticancer therapies.

1.8. Summary of the literature review

The literature review highlights that thiazole, chalcone and imidazole scaffolds are the main structural frameworks for the development of modern anticancer drugs. Their chemical versatility and ability to interact with multiple biological targets allow the modulation of key pathways in cancer progression, including cell cycle regulation, apoptosis and signalling cascades. Numerous studies have shown that the incorporation of functional groups and hybridisation of these heterocyclic motifs significantly enhance biological activity, selectivity and target affinity.

In particular, thiazole-based compounds contribute to the inhibition of kinases, chalcone derivatives form reactive α, β-unsaturated systems, and imidazole scaffolds facilitate strong interactions with the active sites of enzymes. Overall, these results confirm that thiazole, chalcone and imidazole derivatives are promising platforms for the development of novel multifunctional anticancer drugs with improved efficacy and reduced drug resistance.

2. Experimental part

2.1 Chemistry

Reagents and solvents were purchased from Sigma-Aldrich (St. Louis, MO, USA) and used without further purification. Elemental analysis (C, H, N, S) was performed on an EA3100 series CHNSO analyser (EuroVector S.p.A., Pavia, Italy) using Weaver software CFR 21 art.11, and the results were consistent with the theoretical values with an accuracy of ±0.3%. IR spectra (ν, cm^{-1}) were recorded on a Vertex70 FT–IR spectrometer (Bruker, JAV, Billerica, MA, USA) using KBr pellets. NMR spectra were recorded on a Bruker Avance III (400, 101 MHz) spectrometer (Bruker BioSpin AG, Fällanden, Switzerland). Chemical shifts were reported in (δ) ppm relative to tetramethylsilane (TMS), with the residual solvent as internal reference (DMSO-d_6, δ = 2.50 ppm for ^{1}H NMR and δ =39.50 ppm for ^{13}C NMR). Data are reported as follows: chemical shift, multiplicity, integration, coupling constant [Hz], and assignment. The reaction course and purity of the synthesised compounds were monitored by TLC using aluminium plates pre-coated with Silica gel (F254, Merck KGaA, Darmstadt, Germany). Melting points were determined using a Mel-Temp melting point apparatus (Laboratory Devices Inc., Holliston, MA, USA) in capillary tubes sealed at one end and are uncorrected.[58]

The main reagents used in this study, along with their suppliers and purities, are listed in Table 2.1.

Table 2.0. Chemicals and Reagents Used in the Experimental Work

Chemical/Reagent	**Manufacturer/ seller**	**Purity**	**Purpose in Synthesis**
3-Bromoaniline	„sigma-Aldrich”	98%	Core precursor scaffold
Potassium thiocyanate	„sigma-Aldrich”	97%	Thiocyanate source for cyclisation
Substituted aldehydes	„sigma-Aldrich”	98%	Chalcone formation
Substituted ketones	„sigma-Aldrich”	99%	Condensation reactions
Ammonium acetate	„sigma-Aldrich”	98%	Imidazole cyclisation
Ethanol	„sigma-Aldrich”	99%	Reaction solvent
Methanol	„sigma-Aldrich”	99%	Recrystallisation solvent
Chloroform	„sigma-Aldrich”	98%	Extraction and purification
DMSO	„sigma-Aldrich”	98%	Solubility and analysis
Acetic acid	„sigma-Aldrich”	98%	
Hydrochloric acid	„sigma-Aldrich”	99.5%	
Sodium hydroxide	„sigma-Aldrich”	98%	
Potassium carbonate	„sigma-Aldrich”	98%	
Silica gel TLC plates			Reaction monitoring

Method for the synthesis of 3-(1-(3-bromophenyl)thioureido)propanoic acid (4)

A mixture of 3-bromoaniline (**1**) (0.1 mol, 17.20 g), acrylic acid (0.11 mol, 7.92 g) and toluene (100 ml) was stirred at 50 °C for 24 h. The reaction mixture was slowly poured into 5% aqueous sodium hydroxide solution, mixed, and the layers were separated. The organic layer was washed with distilled water. The aqueous layer was combined with alkali and extracted with toluene (2 × 20 ml). The aqueous fraction was acidified with glacial acetic acid to pH 6. The resulting resin was allowed to settle, the supernatant was decanted, and the residue was washed with distilled water (2 × 50 ml) by repeated decantation. 3-((3-Bromophenyl)amino)propanoic acid (**2**) was used in the next reaction without further purification. The resin of the 3-((3-bromophenyl)amino)propanoic acid (**2**) was dissolved in glacial acetic acid (100 ml), and potassium thiocyanate (0.1 mol, 9.72 g) was added to the solution. The reaction mixture was heated under reflux for 48 h. Subsequently, 15% hydrochloric acid (30 ml) was added to the reaction mixture, and heating was continued for another 30 min. The mixture was cooled, and the precipitate was filtered and washed with water and diethyl ether. 1-(3-bromophenyl)-2-thioxotetrahydropyrimidin-4(1*H*)-one (**3**) (0.05 mol, 14.26 g)was dissolved in 5% aqueous sodium hydroxide solution (50 ml) by heating to boiling. The alkaline solution was cooled and filtered, and the filtrate was slowly acidified with 10% acetic acid to pH 6. The resulting precipitate was filtered and washed with water. 3-(1-(3-Bromophenyl)thioureido)propanoic acid (**4**) was recrystallised from water.

1-(3-Bromophenyl)-2-thioxotetrahydropyrimidin-4(1*H*)-one (3)

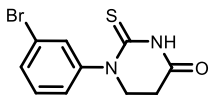

Off white, yield 17.96 g (63%), m. p. 200–203 °C, ^{1}H NMR (400 MHz, DMSO-d_6) δ (ppm) 11.35 (s, 1H, NH), 7.65 (s, 1H, H_{ar}), 7.54 (d, J = 6.4 Hz, 1H, H_{ar}), 7.46–7.30 (m, 2H, H_{ar}), 3.91 (t, J = 6.9 Hz, 2H, NCH_2), 2.82 (t, J = 6.9 Hz, 2H, CH_2CO). ^{13}C NMR (101 MHz, DMSO-d_6) δ (ppm) 179.58 (C=S), 167.03 (C=O), 146.36, 130.96, 130.46, 130.29, 126.54, 121.23 (C_{ar}), 48.64 (NCH_2), 30.34 ($\underline{C}H_2CO$). FTIR (ν, cm^{-1}): 3141 (NH), 1432 (C=O). Anal. Calc for $C_{10}H_9BrN_2OS$ (285.16 g/mol): C, 42.12%, H, 3.18%, N, 9.82%, S,11.24%. Found: C, 42.24%; H, 3.13%; N, 9.73%; S,11.02%.

3-(1-(3-Bromophenyl)thioureido)propanoic acid (4)

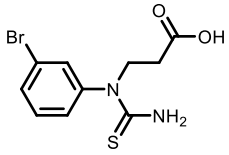

White solid, yield 13.19 g (87%), m. p. 154–155 °C, ^{1}H NMR (400 MHz, DMSO-d_6) δ (ppm) 12.29 (s, 1H, OH), 7.55 (d, J = 8.1 Hz, 1H, H_{ar}), 7.49 (s, 1H, H_{ar}), 7.39 (t, J = 8.0 Hz, 1H, H_{ar}), 7.25 (d, J = 7.9 Hz, 1H, H_{ar}), 6.85 (br. s, 2H, NH_2), 4.15 (t, J = 7.5 Hz, 2H, NCH_2), 2.54 (t, J = 7.6 Hz, 2H, CH_2CO). ^{13}C NMR (101 MHz, DMSO-d_6) δ (ppm) 181.80 (C=S), 172.45 (C=O), 143.76, 131.61, 130.92, 130.86, 127.29, 122.10 (C_{ar}), 50.17 (NCH_2), 32.16 ($\underline{C}H_2CO$). FTIR (ν, cm^{-1}): 1705 (C=O), 2583 (OH), 3358 (NH_2), Anal. Calc for

$C_{10}H_{11}BrN_2O_2S$ (303.17 g/mol): C, 39.62%; H, 3.66%; N, 9.24%; S, 10.57%. Found: C, 39.56%; H, 3.66%; N; 9.39%, S, 10.22%.

General procedure for the synthesis of 1,3-thiazole derivatives 5a–h.

A mixture of 3-(1-(3-bromophenyl)thioureido)propanoic acid (**4**) (1 mmol, 0.303g) corresponding to bromoacetophenone (1 mmol) and 20 ml of acetone was stirred at room temperature for 2–6 h. The precipitate was filtered, washed with acetone, then diethyl ether and dried. The corresponding crystals were dissolved in methanol by heating, then the solution was filtered and diluted with 10 ml of 10% sodium acetate aqueous solution; the precipitate was filtered and washed with water. The products **5a–h** was purified by crystallisation from propan-2-ol.

3-((3-Bromophenyl)(4-phenylthiazol-2-yl)amino)propanoic acid (5a)

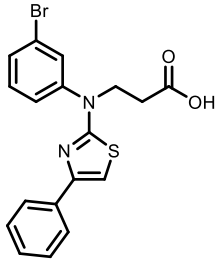

White solid, yield 0.19 g (62%), m. p. 105–106 °C, ^{1}H NMR (400 MHz, DMSO-d_6) δ (ppm) 12.34 (s, 1H, OH), 7.87 (d, J = 7.7 Hz, 2H, H_{ar}), 7.77 (s, 1H, H_{ar}), 7.54 (t, J = 8.9 Hz, 2H, H_{ar}), 7.48–7.36 (m, 3H, H_{ar}), 7.30 (t, J = 7.4 Hz, 1H, H_{ar}), 7.23 (s, 1H, H_{ar}), 4.21 (t, J = 7.1 Hz, 2H, NCH_2), 2.72 (t, J = 7.1 Hz, 2H, CH_2CO). ^{13}C NMR (101 MHz, DMSO-d_6) δ (ppm) 172.65 (C=O), 168.08 (C=N), 150.37, 146.03, 134.47, 131.77, 130.57, 129.96, 129.22, 128.61, 127.65, 125.68, 125.60, 122.77, 122.24, 103.30 (C_{ar}), 48.76 (NCH_2), 32.33 ($\underline{C}H_2CO$). FTIR (ν, cm^{-1}): 1700 (C=O), 2912 (OH), Anal. Calc for $C_{18}H_{15}BrN_2O_2S$ (403.29 g/mol): C, 53.61%; H, 3.75%; N, 6.96%; S, 7.95%. Found: C, 53.65%; H, 3.86%; N, 7.10%; S, 7.85%.

3-((3-Bromophenyl)(4-(4-hydroxyphenyl)thiazol-2-yl)amino)propanoic acid (**5b)**

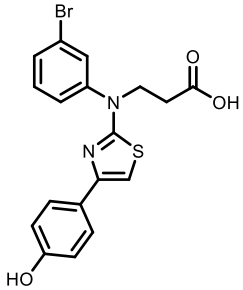

White solid, yield 0.20 g (65%), m. p. 158–160 °C, ^{1}H NMR (400 MHz, DMSO-d_6) δ (ppm) 12.32 (s, 1H, OH), 9.55 (s, 1H, OH), 7.77–7.63 (m, 3H, H_{ar}), 7.52 (t, J = 9.0 Hz, 2H, H_{ar}), 7.43 (t, J = 7.9 Hz, 1H, H_{ar}), 6.95 (s, 1H, H_{ar}), 6.79 (d, J = 8.1 Hz, 2H, H_{ar}), 4.18 (t, J = 7.2 Hz, 2H, NCH_2), 2.70 (t, J = 7.1 Hz, 2H, CH_2CO). ^{13}C NMR (101 MHz, DMSO-d_6) δ (ppm) 172.67 (C=O), 167.82 (C=N), 157.16, 150.67, 146.13, 131.72, 129.85, 129.81, 129.11, 127.09, 125.87, 125.54, 125.51, 122.20, 115.31, 100.35 (C_{ar}), 48.71, 32.36 ($2CH_2$). FTIR (ν, cm^{-1}): 3246 (OH), 1703 (C=O), Anal. Calc for $C_{18}H_{15}BrN_2O_3S$ (419.29 g/mol): C, 51.56%; H, 3.61%; N, 6.68%; S, 7.65%. Found: C, 51.41%; H, 3.29%; N, 6.39%; S, 6.85%.

3-((3-Bromophenyl)(4-(4-fluorophenyl)thiazol-2-yl)amino)propanoic acid (5c)

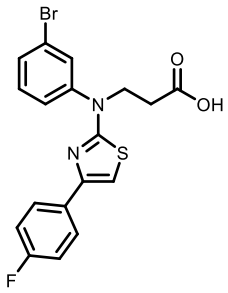

White solid, yield 0.195 g (64%), m. p. 123–125 °C, ^{1}H NMR (400 MHz, DMSO-d_6) δ (ppm) 12.38 (s, 1H, OH), 7.90 (t, J = 6.2 Hz, 2H, H_{ar}), 7.75 (s, 1H, H_{ar}), 7.58–7.40 (m, 3H, H_{ar}), 7.28–7.11 (m, 3H, H_{ar}), 4.19 (t, J = 7.2 Hz, 2H, NCH_2), 2.70 (t, J = 7.2 Hz, 2H, CH_2CO). ^{13}C NMR (101 MHz, DMSO-d_6) δ (ppm) 172.66 (C=O), 168.21 (C=N), 162.88, 160.46, 149.31, 145.98, 131.78, 131.10, 130.03, 129.26, 127.70, 125.66, 122.24, 115.56, 115.35, 103.01, (C_{ar}), 48.79 (NCH_2), 32.36 ($\underline{C}H_2CO$). FTIR (ν, cm^{-1}): 1700 (C=O), 2677 (OH). Anal. Calc for $C_{18}H_{14}BrFN_2O_2S$ (421.28 g/mol): C, 51.32%; H, 3.35%; N, 6.65%; S, 7.61%: Found: 51.47%; H, 3.32%; N, 6.55%, S, 7.41%.

3-((3-Bromophenyl)(4-(4-chlorophenyl)thiazol-2-yl)amino)propanoic acid (5d)

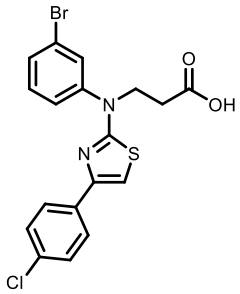

White solid, yield 0.20 g (67%), m. p. 83–85 °C, ^{1}H NMR (400 MHz, DMSO-d_6) δ (ppm) 12.37 (s, 1H, OH), 8.41 (s, 1H, H_{ar}), 8.05–7.87 (m, 3H, H_{ar}), 7.80 (s, 1H, H_{ar}), 7.60–7.44 (m, 3H, H_{ar}), 7.38 (s, 1H, H_{ar}), 4.27 (t, J = 7.1 Hz, 2H, NCH_2), 2.75 (t, J = 7.1 Hz, 2H, CH_2CO). ^{13}C NMR (101 MHz, DMSO-d_6) δ (ppm) 172.69 (C=O), 168.27 (C=N), 150.34, 145.97, 133.14, 132.52, 131.80, 130.04, 129.33, 128.11, 127.61, 126.46, 125.69, 124.20, 122.27, 104.14, 48.69, 32.42. FTIR (ν, cm^{-1}): 1705 (C=O), 2925 (OH), Anal. Calc for $C_{18}H_{14}BrClN_2O_2S$ (437.74 g/mol): C, 49.39%; H, 3.22%; N, 6.40%; S, 7.32%. Found: C, 49.76%; H, 3.54%; N, 6.23%; S, 7.52%.

3-((3-Bromophenyl)(4-(4-bromophenyl)thiazol-2-yl)amino)propanoic acid (5e)

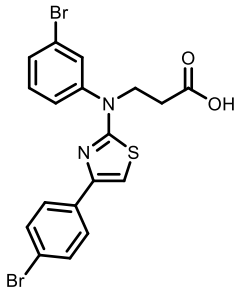

White solid, yield 0.19 g (62%), m. p. 112–114 °C, ^{1}H NMR (400 MHz, DMSO-d_6) δ (ppm) 12.33 (s, 1H, OH), 7.85–7.64 (m, 3H, H_{ar}), 7.64–7.34 (m, 5H, H_{ar}), 7.31 (s, 1H, H_{ar}), 4.19 (t, J = 7.2 Hz, 2H, NCH_2), 2.70 (t, J = 7.4 Hz, 2H, CH_2CO). ^{13}C NMR (101 MHz, DMSO-d_6) δ (ppm) 172.62 (C=O), 168.33 (C=N), 167.34, 149.15, 146.58, 145.91, 133.65, 131.82, 131.54, 130.15, 129.36, 127.67, 125.78, 120.65, 120.65, 104.16 (C_{ar}), 48.71 (NCH_2), 32.30 ($\underline{C}H_2CO$). FTIR (ν, cm^{-1}): 1695 (C=O), 2730 (OH). Anal. Calc for $C_{18}H_{14}Br_2N_2O_2S$ (479.91 g/mol): C, 44.84%; H, 2.93%; N, 5.81%; S, 6.65%. Found: C, 44.47%; H, 2.84%; N, 5.91%; S, 6.91%.

3-((3-Bromophenyl)(4-(4-nitrophenyl)thiazol-2-yl)amino)propanoic acid (5f)

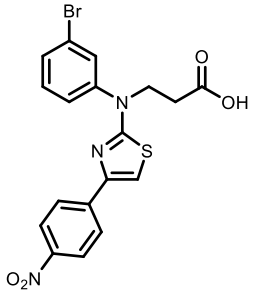

Yellow solid, 0.18 g (61%) m. p. 184–185 °C, ^{1}H NMR (400 MHz, DMSO-d_6) δ (ppm) 12.36 (s, 1H, OH), 8.27 (d, J = 8.9 Hz, 2H, H_{ar}), 8.12 (d, J = 8.8 Hz, 2H, H_{ar}), 7.77 (s, 1H, H_{ar}), 7.62–7.43 (m, 4H, H_{ar}), 4.22 (t, J = 7.2 Hz, 2H, NCH_2), 2.71 (t, J = 7.2 Hz, 2H, CH_2CO). ^{13}C NMR (101 MHz, DMSO-d_6) δ (ppm) 172.61 (C=O), 168.68 (C=N), 148.30, 146.30, 145.73, 140.44, 131.91, 130.40, 129.57, 129.52, 126.48, 126.00, 125.94, 124.12, 122.34, 108.03 (C_{ar}),

48.76 (NCH_2), 32.29 (CH_2CO). FTIR (ν, cm^{-1}): 1710 (C=O), 2950 (OH). Anal. Calc for $C_{18}H_{14}BrN_3O_4S$ (448.29 g/mol): C, 48.23%; H, 3.15%; N, 9.37%; S, 7.15%. Found: C, 47.95%; H, 2.99%; N, 9.40%; S, 6.95%.

3-((3-Bromophenyl)(4-(naphthalen-2-yl)thiazol-2-yl)amino)propanoic acid (5g)

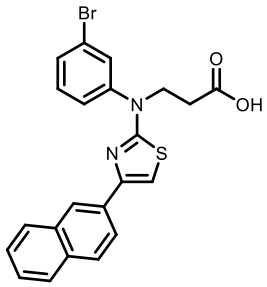

White solid, yield 0.20 g (68%), m. p. 89–91 °C, ^{1}H NMR (400 MHz, DMSO-d_6) δ (ppm) 12.36 (s, 1H, OH), 8.40 (s, 1H, H_{ar}), 8.05–7.87 (m, 4H, H_{ar}), 7.80 (s, 1H, H_{ar}), 7.60–7.42 (m, 5H, H_{ar}), 7.38 (s, 1H, H_{ar}), 4.27 (t, J = 7.1 Hz, 2H, NCH_2), 2.75 (t, J = 7.1 Hz, 2H, CH_2CO). ^{13}C NMR (101 MHz, DMSO-d_6) δ (ppm) 172.68 (C=O), 168.27 (C=N), 150.34, 145.97, 133.14, 132.51, 131.95, 131.81, 130.05, 129.33, 128.14, 128.11, 127.61, 126.46, 126.03, 125.69, 124.20, 124.07, 122.26, 104.14 (C_{ar}), 48.68 (NCH_2), 32.40 (CH_2CO). FTIR (ν, cm^{-1}): 1708 (C=O), 2924 (OH), 3421 (NH_2); Anal. Calc. for $C_{22}H_{17}BrN_2O_2S$ (453.35 g/mol): C, 58.29%, H, 3.78%, N, 5.18%, S,7.07%. Found: C, 58.51%; H, 3.58%; N, 5.32%; S, 6.81%.

3-((3-Bromophenyl)(4-(3,4-dimethoxyphenyl)thiazol-2-yl)amino)propanoic acid (5h)

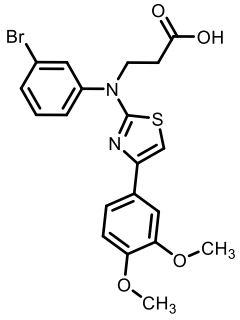

White solid, yield 0.19 g (62%), m. p. 150–151 °C, ^{1}H NMR (400 MHz, DMSO-d_6) δ (ppm) 12.33 (s, 1H, OH), 7.78 (s, 1H, H_{ar}), 7.56–7.39 (m, 5H, H_{ar}), 7.13 (s, 1H, H_{ar}), 6.98 (d, J = 8.4 Hz, 1H, H_{ar}), 4.20 (t, J = 7.1 Hz, 2H, NCH_2), 3.79 (d, J = 13.6 Hz, 6H, $2OCH_3$), 2.72 (t, J = 7.1 Hz, 2H, CH_2CO). ^{13}C NMR (101 MHz, DMSO-d_6) δ (ppm) 172.66 (C=O), 167.67 (C=N), 150.37, 148.69, 148.59, 146.02, 131.69, 129.71, 128.98, 127.57, 125.24, 122.17, 118.34, 111.75, 109.44, 101.58 (C_{ar}), 55.52 (OCH_3), 55.49 (OCH_3), 48.76 (NCH_2) 32.37 (CH_2CO). FTIR (ν, cm^{-1}): 1718 (C=O), 2642 (OH). Anal. Calc for $C_{20}H_{19}BrN_2O_4S$ (463.35 g/mol): C, 51.84%; H, 4.13%; N, 5.05%; S, 6.92%. Found: C, 52.00%; H, 4.01%; N; 5.21%; S, 6.83%.

Synthesis of 3-((3-bromophenyl)(4-oxo-4,5-dihydrothiazol-2-yl)amino)propanoic acid (6).

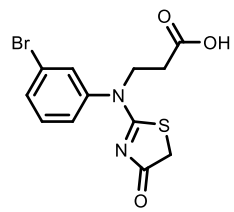

3-(1-(3-Bromophenyl)thioureido)propanoic acid (**4**) (3 mmol, 0.91 g) was dissolved in 10 ml of propan-2-ol. Sodium acetate (10 mmol, 0.82 g) was dissolved in 10 mL of water and added to the organic solution. Chloroacetic acid (5 mmol, 0.47 g) was then added, and the reaction mixture was stirred at 70 °C for 6 h. The mixture was cooled, and the precipitate was filtered and dissolved in a 5% sodium bicarbonate solution. The solution was filtered again and then acidified with acetic acid to pH 6. The resulting precipitate was collected by filtration and washed with water. Purification of thiazolone **6** was carried out by recrystallisation from propan-2-ol. White, yield 0.25 (73%) m. p. 169–171 °C, ^{1}H NMR (400 MHz, DMSO-d_6) δ (ppm) 12.48 (s, 1H, OH), 8.05–7.28 (m, 4H, H_{ar}),

4.16 (t, J = 7.4 Hz, 2H, NCH_2), 3.95 (s, 2H, SCH_2), 2.58 (t, J = 14.8 Hz, 2H, CH_2CO), ^{13}C NMR (101 MHz, DMSO) δ (ppm) 186.95 (C=N), 183.12 (C=O), 172.03, (C=O), 141.61, 132.63, 131.67, 131.09, 127.51, 121.99 (C_{ar}), 50.07 (NCH_2), 40.66 (CH_2CO), 31.96 (SCH_2). FTIR (ν, cm^{-1}): Anal. Calc for $C_{12}H_{11}BrN_2O_3S$: C, 42.00%; H, 3.23%; N, 8.16%; S, 9.36%. Found: C, 41.95%; H, 3.29%; N, 7.98%; S, 9.21%.

Synthesis of 3-((3-bromophenyl)(4,9-dioxo-4,9-dihydronaphtho-[2,3-*d*]thiazol-2yl)amino)-propanoic acid (7)

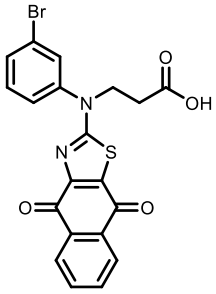

A mixture of 3-(1-(3-bromophenyl)thioureido)propanoic acid (**4**) (2 mmol, 0.61 g), 2,3-dichloronaphthalene-1,4-dione (1.9 mmol, 0.43 g), 20 ml of acetic acid and sodium acetate solution (30 mmol, 2.50 g) was stirred at 70 °C about 24h. Then, the reaction mixture was cooled down, and the precipitate was filtered. The filtrate was diluted with 50 ml of water, and the precipitate was filtered and washed with water. The product **7** was recrystallised from propan-2-ol. Brick red, yield 0.276 g (60%), m. p. 265–267 °C, ^1H NMR (400 MHz, DMSO-d_6) δ (ppm) 12.47 (s, 1H, OH), 8.00–7.84 (m, 3H, H_{ar}), 7.76 (dd, J = 17.3, 8.3 Hz, 2H, H_{ar}), 7.64–7.51 (m, 3H, H_{ar}), 4.34 (t, J = 7.2 Hz, 2H, NCH_2), 2.72 (t, J = 7.1 Hz, 2H, CH_2CO).^{13}C NMR (101 MHz, DMSO-d_6) δ (ppm) 179.85, 174.97, 172.29 (3C=O), 170.20 (C=N), 160.03, 153.25, 144.00, 135.19, 132.28, 132.20, 131.79, 130.85, 130.04, 128.92, 126.47, 125.87, 122.57, 120.94 (C_{ar}), 49.47 (NCH_2), 32.20 (CH_2CO). FTIR (ν, cm^{-1}): 1589 (C=N), 1700 (C=O), 3060 (COOH). Anal. Calc for $C_{20}H_{13}BrN_2O_4S$ (457.30 g/mol): C, 52.53%; H, 2.87%; N, 6.13%; S, 7.01%. Found: C, 52.30%; H, 2.67%, N, 5.97%; S, 7.24%.

Synthesis of 3-((5-acetyl-4-methylthiazol-2-yl)(3-bromophenyl)amino)propanoic acid (8)

A mixture of 3-(1-(3-bromophenyl)thioureido)propanoic acid (**4**) (1 mmol, 0.303.17g), 3-chloropentane-2,4-dione (1.3 mmol, 0.175g) and 20 ml of acetone was heated under reflux for 4 h. The reaction mixture was cooled down; the precipitate was filtered, washed with acetone and dried. The corresponding crystals were dissolved in 10 ml of methanol, filtered, and the filtrate was added to sodium acetate (3 mmol, 0.24 g), and diluted with water (30 ml). Then, the corresponding crystals were filtered and purified by crystallisation from propan-2-ol. White solid, yield 0.256 g (84.5%), m.

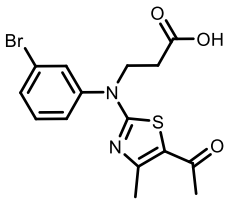

p. 108–110 °C, ^1H NMR (400 MHz, DMSO-d_6) δ (ppm) 12.34 (s, 1H, OH), 7.84–7.68 (m, 1H, H_{ar}), 7.64 (s, J = 6.1, 2.4 Hz, 1H, H_{ar}), 7.49 (d, J = 4.8 Hz, 2H, H_{ar}), 4.14 (t, J = 7.3 Hz, 2H, NCH_2), 2.61 (t, J = 7.3 Hz, 2H, CH_2CO), 2.33 (m, 3H, CH_3). ^{13}C NMR (101 MHz, DMSO-d_6) δ (ppm) 188.87 ($CH_3\underline{C}O$), 172.34 (C=O), 169.77 (C=N), 157.19, 144.68, 132.08, 131.33, 130.06, 126.50, 122.90, 122.41 (C_{ar}), 48.35 (NCH_2), 32.20 ($\underline{C}H_2CO$), 29.61 (CH_3), 18.52 (CH_3). FTIR (ν, cm^{-1}): 1717 (C=O), 3363 (OH), Anal. Calc for

$C_{15}H_{15}BrN_2O_3S$ (383.26 g/mol): C, 47.01%; H, 3.95%; N, 7.31%; S, 8.37%. Found: C, 46.87%; H, 4.10%; N, 7.18%; S, 8.36%.

General procedure for the synthesis of chalcone derivatives 9a–k

A mixture of 3-((5-acetyl-4-methylthiazol-2-yl)(3-bromophenyl)amino)propanoic acid (**8**) (1 mmol, 0.383 g), the corresponding benzaldehyde (1.30 mmol), and 20 mL of methanol was stirred at room temperature until completely dissolved. The solution was cooled to 0–5 °C, and 4 mL of 40% aqueous sodium hydroxide solution was added. The reaction mixture was allowed to warm to room temperature and stirred for 2–6 h. The resulting precipitate was filtered, washed with ethyl acetate, and dried. The obtained solid was dissolved in methanol, and the solution was filtered. The filtrate was subsequently acidified with acetic acid to approximately pH 6 and diluted with water. The solution was stored in a refrigerator overnight, and the precipitate was collected by filtration and washed with a large amount of water. The products **9a–k** were purified by recrystallisation from propan-2-ol.

3-((3-Bromophenyl)(5-cinnamoyl-4-methylthiazol-2-yl)amino)propanoic acid (9a)

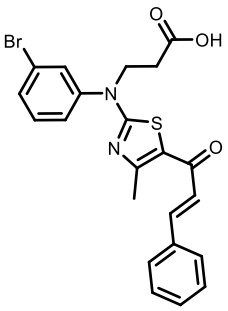

Yellow solid, yield 0.252 g (66.2%), m. p. 180–183 °C, ^{1}H NMR (400 MHz, DMSO-d_6) δ 12.40 (s, 1H, OH), 7.76 (d, J = 23.7 Hz, 3H, H_{ar}), 7.69–7.36 (m, 7H, H_{ar}), 7.25 (d, J = 15.5 Hz, 1H, H_{ar}), 4.17 (t, J = 7.3 Hz, 2H, NCH_2), 2.71–2.55 (m, J = 7.2 Hz, 5H, CH_2CO and CH_3). ^{13}C NMR (101 MHz, DMSO-d_6) δ (ppm) 180.46 (C=O), 172.32 (C=O), 170.10 (C=N), 158.49, 144.62, 141.91, 134.44, 132.12, 132.07, 131.43, 130.40, 130.11, 128.92, 128.59, 128.54, 126.58, 124.51, 122.68, 122.48 (C_{ar}), 48.53 (NCH_2), 32.18 ($\underline{C}H_2CO$), 19.02 (CH_3). FTIR (ν, cm^{-1}): 1650 (C=N), 1715 (C=O), 2540 (OH), Anal. Calc for $C_{22}H_{19}BrN_2O_3S$ (471.37 g/mol): C, 56.06%; H, 4.06%; N, 5.94%; S, 6.80%. Found: C, 56.23%; H, 3.94%; N, 6,17%; S, 6.56%.

(*E*)-3-((3-Bromophenyl)(5-(3-(4-fluorophenyl)acryloyl)-4-methylthiazol-2-yl)amino)propanoic acid (9b)

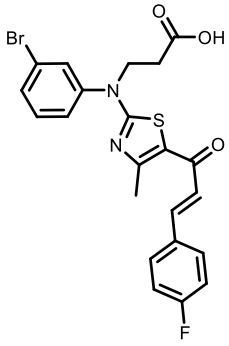

Yellowish solid, yield 0.266 g (70%), m. p. 178–179 °C, ^{1}H NMR (400 MHz, DMSO-d_6) δ (ppm) 12.43 (s, 1H, OH), 7.81 (d, J = 14.7 Hz, 2H, H_{ar}), 7.65 (d, J = 7.5 Hz, 1H, H_{ar}), 7.60–7.45 (m, 2H, H_{ar}), 7.28–7.17 (m, 5H, H_{ar}), 4.17 (t, J = 7.3 Hz, 2H, NCH_2), 2.62 (m, d, J = 8.3 Hz, 5H, CH_2CO and CH_3). ^{13}C NMR (101 MHz, DMSO-d_6) δ (ppm) 180.36 (C=O), 172.35 (C=O), 170.10 (C=N), 164.48, 162.01, 158.55, 144.63, 140.71, 132.12, 131.43, 131.14, 130.92, 130.12, 126.58, 124.42, 122.58, 122.48, 116.01, 115.79 (C_{ar}), 48.55 (NCH_2), 32.22 ($\underline{C}H_2CO$), 19.01 (CH_3). FTIR (ν, cm^{-1}): 1650 (C=N), 1757 (C=O), 2575 (OH), Anal. Calc for $C_{22}H_{18}BrFN_2O_3S$

(489.36 g/mol): C, 54.00%; H, 3.71%; N, 5.72%; S, 6.55%. Found: C, 53.76%; H, 3.79%; N, 5.88%; S, 6.63%.

(*E*)-3-((3-Bromophenyl)(5-(3-(4-chlorophenyl)acryloyl)-4-methylthiazol-2-yl)amino)propanoic acid (9c)

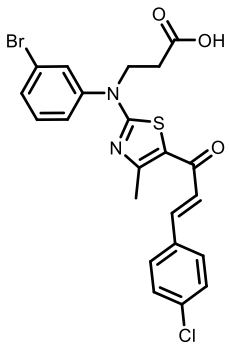

Yellowish solid, yield 0.255 g (67%), m. p. 178–179 °C, ^{1}H NMR (400 MHz, DMSO-d_6) δ (ppm) 12.38 (s, 1H, OH), 7.78 (d, J = 9.0 Hz, 3H, H_{ar}), 7.69–7.60 (m, 1H, H_{ar}), 7.59–7.40 (m, 5H, H_{ar}), 7.25 (dd, J = 15.4, 1.7 Hz, 1H, H_{ar}), 4.17 (t, J = 7.3 Hz, 2H, NCH_2), 2.62 (m, J = 10.8 Hz, 5H, CH_2CO and CH_3). ^{13}C NMR (101 MHz, DMSO-d_6) δ (ppm) 180.26 (C=O), 172.30 (C=O), 170.19 (C=N), 158.75, 144.59, 140.46, 134.82, 133.42, 132.13, 131.47, 130.39, 130.33, 130.32, 130.13, 128.92, 126.60, 125.26, 122.56, 122.49 (C_{ar}), 48.52 (NCH_2), 32.15 ($\underline{C}H_2CO$), 19.03 (CH_3). FTIR (ν, cm^{-1}): 1641 (C=N), 1757 (C=O), 2537 (OH), Anal. Calc for $C_{22}H_{18}BrClN_2O_3S$ (505.81 g/mol): C, 54.00%; H, 3.59%; N, 5.54%; S, 6.34%. Found: C, 53.76%; H, 3.58%; N, 5.83%; S, 6.26%.

(*E*)-3-((3-Bromophenyl)(5-(3-(2-chlorophenyl)acryloyl)-4-methylthiazol-2-yl)amino)propanoic acid (9d)

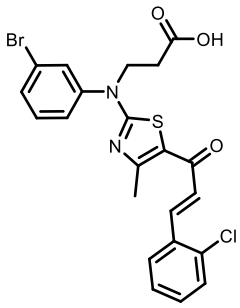

Yellowish sold, yield 0.232 (62%), m. p. 147–148 °C, ^{1}H NMR (400 MHz, DMSO-d_6) δ (ppm) 12.28 (s, 1H, OH), 7.87 (d, J = 7.8 Hz, 1H, H_{ar}), 7.76–7.21 (m, 8H, H_{ar}), 7.18 (d, J = 15.4 Hz, 1H, H_{ar}), 4.04 (m, J = 14.8, 6.9 Hz, 2H, NCH_2), 2.51 (m, J = 6.3 Hz, 5H, CH_2CO and CH_3. ^{13}C NMR (101 MHz, DMSO-d_6) δ (ppm) 180.02 (C=O), 172.30 (C=O), 170.40 (C=N), 159.25, 144.54, 136.55, 134.07, 132.15, 132.10, 131.75, 131.51, 130.14, 129.98, 128.47, 127.73, 127.33, 126.60, 122.50,122.37 (C_{ar}) 48.56 (NCH_2), 32.16 (CH_2CO), 19.08 (CH_3). FTIR (ν, cm^{-1}): 1646 (C=N), 1712 (C=O), Anal. Calc for $C_{22}H_{18}BrClN_2O_3S$: C, 52.24%; H, 3.59%; N, 5.54%; S, 5.63%. Found: C, 52.54%; 3.36%; N, 5.65%; S, 5.75%.

(*E*)-3-((3-Bromophenyl)(5-(3-(2,6-dichlorophenyl)acryloyl)-4-methylthiazol-2-yl)amino)propanoic acid (9e)

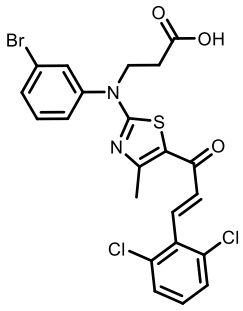

Yellowish solid, yield 0.288 g (75%). m. p. 182–183 °C, ^{1}H NMR (400 MHz, DMSO-d_6) δ (ppm) 12.30 (s, 1H, OH), 7.81–7.21 (m, 9H, H_{ar}), 4.17 (t, J = 7.2 Hz, 2H, NCH_2), 2.68–2.55 (m, 5H, CH_2CO and CH_3). ^{13}C NMR (101 MHz, DMSO-d_6) δ (ppm) 179.60 (C=O), 172.26 (C=O), 170.64(C=N), 160.64, 159.27, 144.43, 134.62, 134.04, 132.30, 132.11, 131.76, 131.52, 130.92, 130.91, 130.06, 129.17, 126.49, 122.70, 122.45(C_{ar}), 48.54, 32.12 (CH_2), 19.00 (CH_3). FTIR (ν,

cm^{-1}): 1649 (C=N), 1710 (C=O), 2531 (OH). Anal. Calc for $C_{22}H_{17}BrCl_2N_2O_3S$: C, 48.91%; H, 3.17%; N, 5.19%; S, 5.93%. Found: C, 48.62%; H, 3.19%; N, 5.13%, S, 5.64%:

(*E*)-3-((3-Bromophenyl)(5-(3-(4-bromophenyl)acryloyl)-4-methylthiazol-2-yl)amino)propanoic acid (9f)

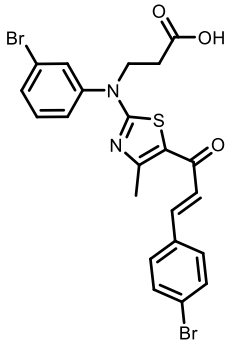

Yellowish solid, yield 0.245 g (64%), m. p. 163–164 °C, ^{1}H NMR (400 MHz, DMSO-d_6) δ (ppm) 12.45 (s, 1H, OH), 8.00–7.40 (m, 10H, H_{ar}), 7.26 (d, J = 15.4 Hz, 1H, H_{ar}), 4.17 (t, J = 7.3 Hz, 2H, NCH_2), 2.61 (m, J = 8.2 Hz, 5H, CH_2CO and CH_3).v^{13}C NMR (101 MHz, DMSO-d_6) δ (ppm) 180.25, 172.34 (C=O), 170.19, 158.79, 144.60, 140.55, 133.74, 132.13, 132.05, 131.85, 131.84, 131.46, 130.53, 130.12, 126.59, 125.31, 123.69, 122.54, 122.49 (C_{ar}), 48.59, 32.24 (CH_2), 19.03 (CH_3). FTIR (ν, cm^{-1}): 1636 (C=N), 1728 (C=O), 2684 (OH). Anal. Calc for $C_{22}H_{18}Br_2N_2O_3S$ (550.27 g/mol): C, 48.02%; H, 3.30%; N, 5.09%; S, 5.83%. Found: C, 48.12%; H, 3.35%; N, 5.18%; S, 5.76%.

(*E*)-3-((3-Bromophenyl)(4-methyl-5-(3-(naphthalen-1-yl)acryloyl)thiazol-2-yl)amino)propanoic acid (9g)

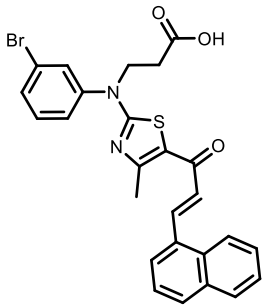

Yellowish solid, yield 0.254 g (67%), m. p. 174–175 °C, ^{1}H NMR (400 MHz, DMSO-d_6) δ (ppm) 12.40 (s, 1H, OH), 8.23 (s, 1H, H_{ar}), 7.92 (s, 4H, H_{ar}), 7.83–7.61 (m, 3H, H_{ar}), 7.62–7.44 (m, 4H, H_{ar}), 7.36 (d, J = 15.3 Hz, 1H, H_{ar}), 4.18 (t, J = 7.3 Hz, 2H, NCH_2), 2.64 (m, J = 6.5 Hz, 5H, CH_2CO and CH_3). ^{13}C NMR (101 MHz, DMSO-d_6) δ (ppm) 180.37 (C=O), 172.32 (C=O), 170.08 (C=N), 158.61, 144.63, 142.00, 133.80, 132.95, 132.13, 132.07, 131.45, 130.28, 130.12, 128.52, 128.49, 127.69, 127.35, 126.75, 126.59, 124.78, 124.27, 122.64, 122.50 (C_{ar}), 48.54 (NCH_2), 32.16 (CH_2CO) 19.07 (CH_3). FTIR (ν, cm^{-1}): 1716 (C=O), 1648 (N=C), 2887 (OH). Anal. Calc for $C_{26}H_{21}BrN_2O_3S$: C, 59.89%; H, 4.06%; N, 5.37%; S, 6.16%. Found: C, 59.53%; H, 4.15%; N, 5.34%; S, 6.12%.

(*E*)-3-((3-Bromophenyl)(4-methyl-5-(3-(thiophen-2-yl)acryloyl)thiazol-2-yl)amino)propanoic acid (9h)

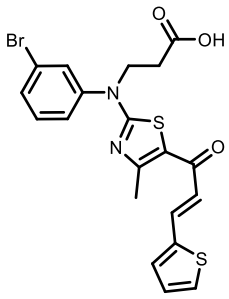

Yellowish solid, yield 0.275 g (72%), m. p. 191–193 °C, ^{1}H NMR (400 MHz, DMSO-d_6) δ (ppm) 12.39 (s, 1H, OH), 7.81–7.45 (m, 7H, H_{ar}), 7.14 (s, 1H, H_{ar}), 6.92 (d, J = 15.2 Hz, 1H, H_{ar}), 4.17 (t, J = 7.2 Hz, 2H, NCH_2), 2.61 (m, J = 16.5 Hz, 5H, CH_2CO and CH_3). ^{13}C NMR (101 MHz, DMSO-d_6) δ (ppm) 179.76 (C=O), 172.31 (C=O), 169.94 (C=N), 158.22, 144.60, 139.45, 134.72, 132.52, 132.11, 131.42, 130.06, 129.91, 128.74, 126.54, 122.74, 122.58, 122.47 (C_{ar}), 48.52 (NCH_2), 32.17 (CH_2CO), 18.94 (CH_3). FTIR (ν, cm^{-1}): 1722 (C=O), 3443 (OH), 1633 (C=N).

Anal. Calc for $C_{20}H_{17}BrN_2O_3S_2$: C, 50.32%; H, 3.59%; N, 5.87%; S, 13.43%. Found: C, 50.43%; H, 3.56%; N, 6.01%; S, 13.52%.

(*E*)-3-((3-Bromophenyl)(5-(3-(furan-2-yl)acryloyl)-4-methylthiazol-2-yl)amino)propanoic acid (9i)

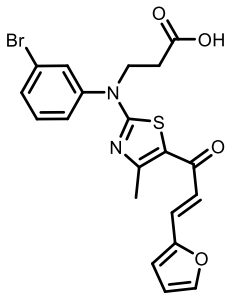

Yellowish solid, yield 0.268 (70%), m. p. 185–186 °C, ^{1}H NMR (400 MHz, DMSO-d_6) δ (ppm) 12.41 (s, 1H, OH), 7.90–7.32 (m, 6H, H_{ar}), 7.04–6.87 (m, 2H, H_{ar}), 6.63 (s, 1H, H_{ar}), 4.17 (t, J = 7.3 Hz, 2H, NCH_2), 2.61 (d, J = 17.3 Hz, 5H, CH_2CO and CH_3). ^{13}C NMR (101 MHz, DMSO-d_6) δ (ppm) 179.59 (C=O), 172.31 (C=O), 169.88 (C=N), 158.30, 150.83, 145.96, 144.61, 132.11, 131.42, 130.07, 128.55, 126.52, 122.52, 122.46, 121.17, 116.72, 113.02 (C_{ar}), 48.51 (NCH_2), 32.19 (CH_2CO), 18.89 (CH_3). FTIR (ν, cm^{-1}): 1713 (C=O), 1646 (C=N), 3383 (OH). Anal. Calc for $C_{20}H_{17}BrN_2O_4S$: C, 52.07%; H, 3.71%; N, 6.07%; S, 6.95%. Found: C, 52.12%; H, 3.39%; N, 5.79%; S, 7.14%.

(*E*)-3-((3-Bromophenyl)(5-(3-(4-bromothiophen-2-yl)acryloyl)-4-methylthiazol-2-yl)amino)propanoic acid (9j)

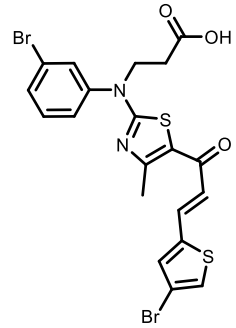

Yellowish solid, yield 0.264 g (77%), m. p. 205–207 °C, ^{1}H NMR (400 MHz, DMSO-d_6) δ (ppm) 12.32 (s, 1H, OH), 7.81–7.32 (m, 7H, H_{ar}), 6.92 (d, J = 15.2 Hz, 1H, H_{ar}), 4.08 (t, J = 7.3 Hz, 2H, NCH_2), 2.69–2.48 (m, 5H, CH_2CO and CH_3). ^{13}C NMR (101 MHz, DMSO-d_6) δ (ppm) 179.55 (C=O), 172.30 (C=O), 170.18 (C=N), 158.73, 144.55, 140.64, 133.20, 132.98, 132.12, 131.47, 130.08, 126.90, 126.55, 126.54, 124.08, 122.49, 110.21 (C_{ar}), 48.55 (NCH_2), 32.17 (CH_2CO), 18.99 (CH_3). FTIR (ν, cm^{-1}): 1646 (C=N), 1711 (C=O). Anal. Calc for $C_{20}H_{16}Br_2N_2O_3S_2$: C, 43.18%; H, 2.90%; N, 5.04%; S, 11.53%. Found: C, 42.97%; H, 3.12%; N, 4.98%, S, 11.23%.

(*E*)-3-((5-(3-(5-Bromofuran-2-yl)acryloyl)-4-methylthiazol-2-yl)(3-bromophenyl)amino)propanoic acid (9k)

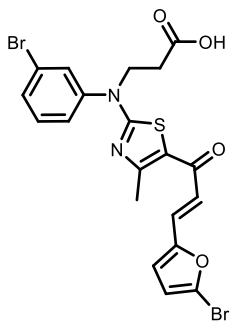

Yellowish solid, yield 0.265 g (69%). m. p. 164–165 °C, ^{1}H NMR (400 MHz, DMSO-d_6) δ (ppm) 12.39 (s, 1H, OH), 7.83–7.44 (m, 4H, H_{ar}), 7.31 (d, J = 15.2 Hz, 1H, H_{ar}), 7.05 (s, 1H, H_{ar}), 6.92–6.71 (m, 2H, H_{ar}), 4.17 (t, J = 7.2 Hz, 2H, NCH_2), 2.61 (d, J = 17.5 Hz, 5H, CH_2CO and CH_3). ^{13}C NMR (101 MHz, DMSO-d_6) δ (ppm) 179.37 (C=O), 172.29 (C=O), 169.99 (C=N), 158.58, 153.05, 144.55, 132.11, 131.45, 130.04, 127.41, 126.51, 125.49, 122.47, 122.38, 121.54, 118.84, 115.14 (C_{ar}), 48.53 (NCH_2), 32.15 (CH_2CO), 18.93 (CH_3). FTIR

(ν, cm^{-1}): 1708 (C=O), 1650 (C=N), 3126 (OH). Anal. Calc for $C_{20}H_{16}Br_2N_2O_4S$: C, 44.47%; H, 2.99%; N, 5.19; S, 5.93%. Found: C, 44.28%, H, 2.77%; N, 5.29%; S, 6.14%.

General procedure for the synthesis of compounds (10a, b)

A mixture of 3-bromoaniline (3 mmol, 0.52 g), the corresponding 2-bromoacetophenone (2.9 mmol), sodium bicarbonate (3 mmol, 0.36 g), and 10 mL of propan-2-ol was stirred at room temperature for 12–16 h. The resulting precipitate was filtered, washed with water, and dried. The product was purified by recrystallisation from ethyl acetate.

2-((3-Bromophenyl)amino)-1-(naphthalen-2-yl)ethan-1-one (10a)

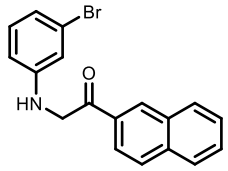

White solid, yield 0.412 g (80%), m. p. 160–162 °C, ^{1}H NMR (400 MHz, DMSO-d_6) δ (ppm) 7.33 (s, 1H, H_{ar}), 6.78 (dd, J = 43.3, 17.0, 8.4 Hz, 4H, H_{ar}), 6.49–6.35 (m, 2H, H_{ar}), 6.05 (s, 1H, H_{ar}), 5.87 (t, J = 8.0 Hz, 1H, H_{ar}), 5.68 (s, 2H, H_{ar}), 5.48 (d, J = 8.2 Hz, 1H, NH), 3.51 (s, 2H, CH_2). ^{13}C NMR (101 MHz, $CDCl_3$-d_6) δ (ppm), 194.45 (C=O), 148.38, 136.14, 132.60, 132.07, 130.77, 129.77, 129.69, 129.13, 129.05, 128.05, 127.30, 123.55, 123.41, 120.73, 115.50, 112.31, 50.20. (C_{ar}), 12.56 (CH_2). FTIR (ν, cm^{-1}): 1862 (C=O), 3368 (N-H). Anal. Calc for $C_{18}H_{14}BrNO$ (340.22 g/mol): C, 63.55%; H, 4.15%; N, 4.12%. Found: C, 63.74%; H, 3.98%; N, 4.19%.

2-((3-Bromophenyl)amino)-1-(3,4-dimethoxyphenyl)ethan-1-one (10b)

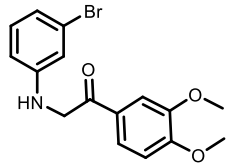

White solid, yield 0.174 g (85%) m. p. 106–107 °C, ^{1}H NMR (400 MHz, DMSO-d_6) δ (ppm) 7.78 (d, J = 8.4 Hz, 1H, H_{ar}), 7.52 (s, 1H, H_{ar}), 7.15–6.59 (m, 5H, H_{ar}), 6.18 (s, 1H, NH), 4.65 (d, J = 5.3 Hz, 2H, CH_2), 3.85 (m, J = 7.9, 2.3 Hz, 6H, CH_3). ^{13}C NMR (101 MHz, DMSO-d_6) δ (ppm) 194.62 (C=O), 153.40, 149.98, 148.63, 130.56, 127.83, 122.62, 122.33, 118.28, 114.47, 111.68, 110.99, 110.25 (C_{ar}), 55.83 (OCH_3), 55.64 (OCH_3), 49.21 (CH_2). FTIR (ν, cm^{-1}): 1681 (C=O), 3381 (C=N). Anal. Calc for $C_{16}H_{16}BrNO_3$ (350.21 g/mol): C, 54.87%; H, 4.61%, N, 4.00%. Found: C, 53.21%; H, 6.21%; N, 3.86%.

General procedure for the synthesis of compounds 11a, b

A mixture of the corresponding compound **10a** or **10b** (10 mmol), potassium thiocyanate (12 mmol, 1.16 g) and 40 mL acetic acid was stirred at room temperature for 24 h. The precipitate was filtered off, washed with water, then with propan-2-ol and dried. The products **11a, b** was purified by crystallisation from propan-2-ol.

1-(3-bromophenyl)-4-(naphthalen-2-yl)-1,3-dihydro-2*H*-imidazole-2-thione (11a)

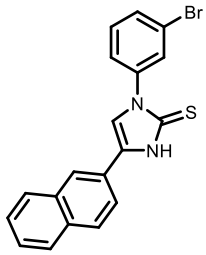

White solid, yield 0.451 g (80%), m. p. 223–225 °C, ^{1}H NMR (400 MHz, DMSO-d_6) δ (ppm) 13.19 (s, 1H, NH), 8.36 (s, 1H, H_{ar}), 8.10–7.24 (m, 11H, H_{ar}). ^{13}C NMR (101 MHz, DMSO-d_6) δ (ppm) 162.99 (C=S), 138.96, 132.95, 132.32, 130.69, 130.67, 128.54, 128.44, 127.85, 127.72, 126.89, 126.37, 124.99, 124.86, 124.81, 122.64, 122.49, 121.16, 116.51 ($C_{ar+imid.}$). FTIR (ν, cm^{-1}): 1590(C=C), Anal. Calc for $C_{19}H_{13}BrN_2S$ (381.29 g/mol): C, 59.85%; H, 3.44%; N, 7.35%; S, 8.41%. Found: C, 59.66%; H, 3.45%; N, 7.62%; S, 8.24%.

1-(3-Bromophenyl)-4-(3,4-dimethoxyphenyl)-1,3-dihydro-2*H*-imidazole-2-thione (11b)

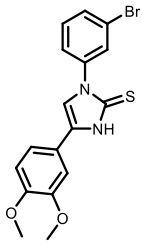

Orange solid, yield 0.308 g (88%) m. p. 219–220 °C, ^{1}H NMR (400 MHz, DMSO-d_6) δ (ppm) 12.94 (s, 1H, NH), 8.02 (t, J = 1.9 Hz, 1H, H_{ar}), 7.89–7.74 (m, 2H, H_{ar}), 7.64 (d, J = 8.0 Hz, 1H, H_{ar}), 7.50 (t, J = 8.0 Hz, 1H, H_{ar}), 7.44–7.28 (m, 2H, H_{ar}), 7.00 (d, J = 8.3 Hz, 1H, H_{ar}), 3.79 (dd, J = 13.8 Hz, 6H, CH_3). ^{13}C NMR (101 MHz, DMSO-d_6) δ (ppm) 162.11(C=S), 148.99, 148.62, 139.06, 130.69, 128.82, 128.28, 124.76, 121.13, 120.26, 116.77, 114.59, 112.02, 108.19, 66.38 ($C_{ar+imid.}$), 55.64 (OCH_3), 55.57 (OCH_3). FTIR (ν, cm^{-1}): 3568 (N-H). Anal. Calc for $C_{17}H_{15}BrN_2O_2S$ (391.28 g/mol): C, 52.18%; H, 3.86%, N, 7.16%, S, 8.19%. Found: C, 52.31%; H, 3.80%; N, 6.91%; S, 7.10%.

General methods of synthesis of derivatives 12–16a, b

A mixture of the corresponding compound **11a** and **11b** (0.5 mmol), the corresponding 2-bromoacetophenone (0.51 mmol), and 20 mL of acetone was stirred at room temperature for 2–4 h. The resulting precipitate was filtered, washed with acetone, then with a small amount of diethyl ether, and dried. The obtained solid was dissolved in methanol, and the solution was filtered and diluted with 10 mL of 10% aqueous sodium acetate solution. The precipitate was filtered and washed with water. The products **12–16a, b** were purified by recrystallisation from propan-2-ol.

2-((1-(3-Bromophenyl)-4-(naphthalen-2-yl)-1*H*-imidazol-2-yl)thio)-1-phenylethan-1-one 12a

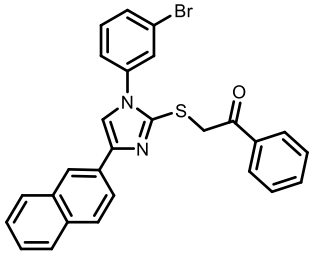

White solid, yield 0.138 g (72%), m. p. 130–132 °C, ^{1}H NMR (400 MHz, DMSO-d_6) δ (ppm) 8.21–8.06 (m, 4H, H_{ar}), 7.89–7.39 (m, 13H, H_{ar}), 4.85 (s, 2H, CH_2). ^{13}C NMR (101 MHz, DMSO-d_6) δ (ppm) 194.25 (C=O), 141.42, 141.12, 137.92, 135.96, 133.79, 133.55, 133.19, 132.14, 131.45, 131.39, 130.78, 128.79, 128.50, 128.02, 127.74, 127.67, 127.64, 126.37, 125.53, 124.16, 123.26, 122.05, 122.02, 119.80, 118.81 ($C_{ar+imid.}$), 38.89 (CH_2). FTIR (ν, cm^{-1}): 1602 (C=N), 1700 (C=O). Anal. Calc for $C_{27}H_{19}BrN_2OS$ (499.43 g/mol): C, 64.93%; H, 3.83%; N, 5.61%; S, 6.42%. Found: C, 65.84%; H, 3.86%; N, 5.64%; S, 6.65%.

2-((1-(3-Bromophenyl)-4-(3,4-dimethoxyphenyl)-1*H*-imidazol-2-yl)thio)-1-phenylethan-1-one (12b)

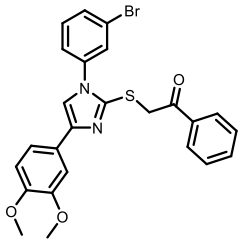

White solid, yield 0.243 g (62%), m. p. 138–140 °C, ^{1}H NMR (400 MHz, DMSO-d_6) δ (ppm) 8.06–7.49 (m, 10H, H_{ar}), 7.21 (d, J = 12.3 Hz, 2H, H_{ar}), 6.89 (d, J = 8.2 Hz, 1H, H_{ar}), 4.78 (s, 2H, CH_2), 3.73 (s, 3H, OCH_3), 3.63 (s, 3H, OCH_3). ^{13}C NMR (101 MHz, DMSO-d_6) δ (ppm) 193.93 (C=O), 148.73, 148.72, 147.86, 143.01, 141.34, 140.40, 138.01, 135.77, 133.46, 131.37, 131.19, 128.74, 128.37, 127.59, 126.27, 124.07, 121.97, 118.18, 116.57, 111.82, 108.12 ($C_{ar+imid.}$), 55.47 (OCH_3), 55.24 (OCH_3), 38.89 (CH_2). FTIR (ν, cm^{-1}): 1697 (C=O). Anal. Calc for $C_{25}H_{21}BrN_2O_3S$ (509.48 g/mol): C, 58.94%; H, 4.16%; N, 5.50%; S, 6.29% Found: C, 58.69%; H, 3.88%; N, 5.67%; S, 6.52%:

2-((1-(3-Bromophenyl)-4-(naphthalen-2-yl)-1*H*-imidazol-2-yl)thio)-1-(4-fluorophenyl)ethan-1-one (13a)

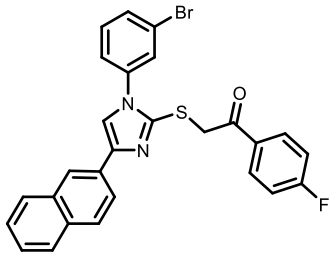

White solid, yield 0.132 g (69%), m. p. 146–147 °C, ^{1}H NMR (400 MHz, DMSO-d_6) δ (ppm) 8.22–8.11 (m, 3H, H_{ar}), 8.07 (s, 1H, H_{ar}), 7.88–7.80 (m, 4H), 7.72 (t, J = 8.9 Hz, 2H, H_{ar}), 7.63–7.38 (m, 6H, H_{ar}), 4.81 (s, 2H, CH_2).^{13}C NMR (101 MHz, DMSO- d_6) δ (ppm) 192.94 (C=O), 141.30, 141.13, 137.90, 133.18, 132.71, 132.68, 132.16, 131.62, 131.52, 131.45, 131.39, 130.78, 128.04, 127.75, 127.67, 127.61, 126.39, 125.56, 124.18, 123.26, 122.04, 122.00, 119.85, 115.92, 115.70 ($C_{ar+imid.}$), 39.52 (CH_2). FTIR (ν, cm^{-1}): 1591 (C=N), 1686 (C=O). Anal. Calc for $C_{27}H_{18}BrFN_2OS$ (517.42 g/mol): C, 62.68%; H, 3.51; N, 5.41; S, 6.20%. Found: C, 62.45%; H, 3.60%; N, 5.43%; S, 6.12%.

2-((1-(3-Bromophenyl)-4-(3,4-dimethoxyphenyl)-1*H*-imidazol-2-yl)thio)-1-(4-fluorophenyl)ethan-1-one (13b)

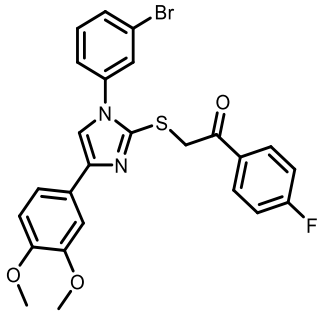

White solid, yield 0.272 g (70%) m. p. 132–133 °C, ^{1}H NMR (400 MHz, DMSO-d_6) δ (ppm) 8.15–7.90 (m, 3H, H_{ar}), 7.79–7.17 (m, 8H, H_{ar}), 6.90 (d, J = 8.2 Hz, 1H, H_{ar}), 4.75 (s, 2H, CH_2), 3.74 (s, 3H,CH_3), 3.66 (s, 3H,CH_3). ^{13}C NMR (101 MHz, DMSO-d_6) δ (ppm) 192.59, (C=O), 166.41, 163.91, 148.74, 147.96, 141.18, 140.25, 137.93, 132.45, 131.49, 131.40, 131.25, 127.65, 126.04, 124.13, 121.95, 118.32, 116.65, 115.86, 115.64, 111.83, 108.19 ($C_{ar+imid.}$), 55.48 (OCH_3), 55.24 (OCH_3), 38.89 (CH_2). FTIR (ν, cm^{-1}): 1592 (C=N), 1699 (C=O). Anal. Calc for $C_{25}H_{20}BrFN_2O_3S$ (527.41 g/mol): C, 56.93%; H, 3.82%; N, 5.31%; S, 5.89%. Found: C, 56.81%; H, 3.68%; N, 5.46%; S, 5.69%.

2-((1-(3-Bromophenyl)-4-(naphthalen-2-yl)-1*H*-imidazol-2-yl)thio)-1-(4-chlorophenyl)ethan-1-one (14a)

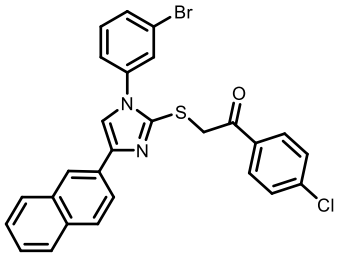

White solid, yield 0.132 g (69%), m. p. 145–150 °C, ^{1}H NMR (400 MHz, DMSO-d_6) δ (ppm) 8.20 (s, 1H, H_{ar}), 8.09 (d, J = 8.2 Hz, 2H, H_{ar}), 7.99 (s, 1H, H_{ar}), 7.83 (q, J = 8.5 Hz, 4H, H_{ar}), 7.74–7.41 (m, 8H, H_{ar}), 4.80 (s, 2H, CH_2). ^{13}C NMR (101 MHz, DMSO-d_6) δ (ppm) 193.46 (C=O), 141.32, 141.11, 138.49, 137.89, 134.72, 133.17, 132.14, 131.48, 131.39, 130.74, 130.45, 128.91, 128.02, 127.69, 127.66, 127.64, 126.38, 125.56, 124.11, 123.23, 122.06, 121.99, 120.71, 119.84, 115.82 ($C_{ar+imid.}$), 39.31 (CH_2). FTIR (ν, cm^{-1}): 1632 (C=N), 1666 (C=O). Anal. Calc for $C_{27}H_{18}BrClN_2OS$ (533.87 g/mol): C, 60.74%; H, 3.40%; N, 5.25%; S, 6.01%. Found: C, 60.59%; H, 3.28%; N, 5.56%; S, 6.02%.

2-((1-(3-Bromophenyl)-4-(3,4-dimethoxyphenyl)-1*H*-imidazol-2-yl)thio)-1-(4-chlorophenyl)ethan-1-one (14b)

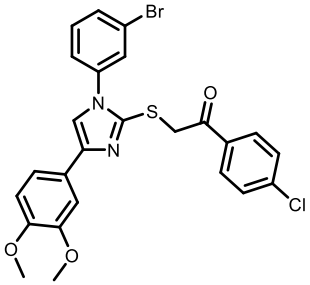

White solid, yield 0.256 g (65.5%), m. p. 156–157 °C, ^{1}H NMR (400 MHz, DMSO-d_6) δ (ppm) 8.05–7.96 (m, 3H, H_{ar}), 7.79–7.49 (m, 6H, H_{ar}), 7.18 (d, J = 14.4 Hz, 2H, H_{ar}), 6.89 (d, J = 8.3 Hz, 1H, H_{ar}), 4.74 (s, 2H, CH_2), 3.74 (s, 3H, OCH_3), 3.64 (s, 3H, OCH_3).^{13}C NMR (101 MHz, DMSO-d_6) δ (ppm) 193.10 (C=O), 148.71, 147.89, 141.34, 140.22, 138.39, 137.96, 134.45, 131.37, 131.19, 130.30, 128.83, 127.58, 126.20, 124.23, 124.06, 121.96, 118.25, 116.61, 116.60, 111.81, 108.13 ($C_{ar+imid.}$), 55.47 (OCH_3), 55.18 (OCH_3), 38.89 (CH_2). FTIR (ν, cm^{-1}): 1691 (C=O), 1610 (C=N). Anal. Calc for $C_{25}H_{20}BrClN_2O_3S$ (543.86 g/mol): C, 55.21%; H, 3.71%; N,5.15%; S, 5.89%. Found: C, 54.92%; H, 3.72%; N, 5.27%; S, 5.65%.

1-(4-Bromophenyl)-2-((1-(3-bromophenyl)-4-(naphthalen-2-yl)-1H-imidazol-2-yl)thio)ethan-1-one 15a

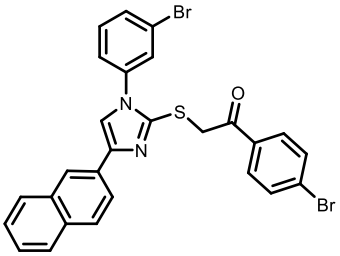

White solid, yield 0.128 g (67%), m. p. 140–143 °C, ^{1}H NMR (400 MHz, DMSO-d_6) δ (ppm) 8.19 (s, 1H, H_{ar}), 8.05–7.95 (m, 3H, H_{ar}), 7.89–7.76 (m, 6H), 7.70 (t, J = 7.6 Hz, 2H, H_{ar}), 7.63–7.41 (m, 4H, H_{ar}), 4.79 (s, 2H, CH_2).^{13}C NMR (101 MHz, DMSO-d_6) δ (ppm) 193.69 (C=O), 141.34, 141.10, 137.89, 135.08, 135.03, 133.16, 132.14, 131.87, 131.49, 131.39, 130.73, 130.54, 128.02, 127.73, 127.67, 126.38, 125.57, 124.09, 123.22, 122.07, 122.07, 121.99, 119.90, 119.86, 119.83 ($C_{ar+imid.}$), 39.73 (CH_2). FTIR (ν, cm^{-1}): 1632 (C=N), 1669 (C=O). Anal. Calc for $C_{27}H_{18}Br_2N_2OS$ (578.32 g/mol): C, 56.08%; H, 3.14%; N, 4.84%; S, 5.54%. Found: C, 55.87%; H, 2.95%; N, 5.01%, 5.74%.

1-(4-Bromophenyl)-2-((1-(3-bromophenyl)-4-(3,4-dimethoxyphenyl)-1*H*-imidazol-2-yl)thio)ethan-1-one (15b)

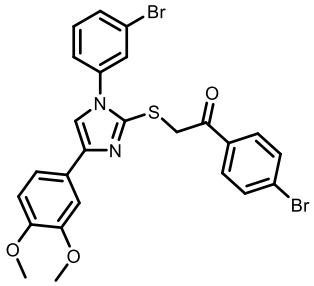

White solid, yield 0.257 g (66%) m. p. 170–172 °C, ^{1}H NMR (400 MHz, DMSO-d_6) δ (ppm) 8.04–7.46 (m, 9H, H_{ar}), 7.24–7.13 (m, 2H, H_{ar}), 6.89 (d, J = 8.3 Hz, 1H, H_{ar}), 4.73 (s, 2H, CH_2), 3.74 (s, 3H, CH_3), 3.64 (s, 3H, CH_3). ^{13}C NMR (101 MHz, DMSO-d_6) δ (ppm) 193.33 (C=O), 148.71, 147.88, 141.33, 140.22, 137.99, 137.95, 136.83, 134.79, 131.79, 131.37, 131.19, 130.38, 127.60, 127.57, 126.20, 124.04, 121.97, 118.23, 116.60, 111.80, 108.11 ($C_{ar+imid.}$), 55.47 (OCH_3), 55.19 (OCH_3), 38.89, (CH_2). FTIR (ν, cm^{-1}): 1610 (C=N), 1690 (C=O). Anal. Calc for $C_{25}H_{20}Br_2N_2O_3S$ (588 g/mol): C, 51.04%; H, 3.43%; N, 4.75%; S, 5.43%. Found: C, 50.85%; H, 3.42%; N, 4.82%; S, 4.54%:

2-((1-(3-Bromophenyl)-4-(naphthalen-2-yl)-1*H*-imidazol-2-yl)thio)-1-(naphthalen-2-yl)ethan-1-one (16a)

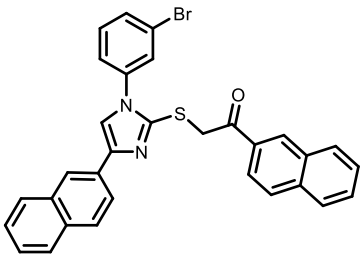

White solid, yield 0.134 g (70%), m. p. 135–145 °C. ^{1}H NMR (400 MHz, DMSO-d_6) δ (ppm) 8.87 (s, 1H, H_{ar}), 8.19–7.59 (m, 14H, H_{ar}), 7.56–7.28 (m, 4H, H_{ar}), 4.97 (s, 2H, CH_2). ^{13}C NMR (101 MHz, DMSO-d_6) δ (ppm) 194.33 (C=O), 141.53, 141.13, 137.92, 135.22, 133.35, 133.08, 132.22, 132.06, 131.44, 131.36, 130.71, 130.67, 129.77, 128.88, 128.38, 127.94, 127.77, 127.68, 127.54, 127.51, 127.06, 126.19, 125.46, 124.11, 123.91, 123.20, 122.04, 122.01, 119.80 ($C_{ar+imid.}$), 39.86 (CH_2). FTIR (ν, cm^{-1}): 1627 (C=N), 1678 (C=O). Anal. Calc for $C_{31}H_{21}BrN_2OS$ (549.49 g/mol): C, 67.76%; H, 3.85%; N, 5.10%; S, 5.83%. Found: C, 67.49%; H, 3.68%; N, 5.18%; S, 5.57%.

2-((1-(3-Bromophenyl)-4-(3,4-dimethoxyphenyl)-1*H*-imidazol-2-yl)thio)-1-(naphthalen-2-yl)ethan-1-one (16b)

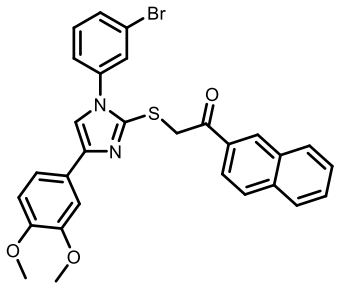

White solid, yield 0.278 g (71%) m. p. 153–155 °C, ^{1}H NMR (400 MHz, DMSO-d_6) δ (ppm) 8.78 (s, 1H, H_{ar}), 8.14–7.14 (m, 13H, H_{ar}), 6.80 (d, J = 8.4 Hz, 1H, H_{ar}), 4.90 (s, 2H, CH_2), 3.70 (s, 3H, OCH_3), 3.45 (s, 3H, OCH_3).^{13}C NMR (101 MHz, DMSO-d_6) δ (ppm) 193.92 (C=O), 148.66, 147.81, 141.38, 140.44, 138.00, 135.14, 133.06, 132.16, 131.35, 131.17, 130.52, 129.65, 128.83, 128.34, 127.69, 127.58, 127.00, 126.23, 124.08, 123.80, 121.95, 118.23, 116.61, 111.76, 108.05 ($C_{ar+imid.}$), 55.43 (OCH_3), 54.99 (OCH_3), 38.89 (CH_2). FTIR (ν, cm^{-1}): 1626 (C=N), 1684 (C=O). Anal. Calc for $C_{29}H_{23}BrN_2O_3S$ (559.48 g/mol): C, 62.26%; H, 4.14%; N, 5.01%; S, 5.73%. Found: C, 62.05%; H, 4.01%; N, 5.240%; S, 5.52%:

General method of synthesis of compounds 17a, b

A mixture of the corresponding compound **11a** or **11b** (1 mmol), 2-(chloromethyl)-1*H*-benzo[*d*]imidazole (1.2 mmol, 0.20 g), sodium bicarbonate (2 mmol, 0.168 g), and 7 ml of DMF was stirred at room temperature for 48 h. Then the reaction mixture was diluted with 20 mL of water. The precipitate was filtered, washed with water, then with a small amount of propan-2-ol, and dried. The products **17a, b** were purified by recrystallisation from methanol.

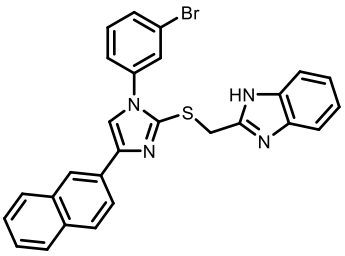

Light orange, yield 0.378 g (74%), m. p. 193–196 °C, ^{1}H NMR (400 MHz, DMSO-d_6) δ (ppm) 12.50 (s, 1H, NH), 8.36 (s, 1H, H_{ar}), 8.24 (s, 1H), 8.01–7.40 (m, 12H, H_{ar}), 7.15 (s, 2H, H_{ar}), 4.65 (d, J = 1.7 Hz, 2H, CH_2). ^{13}C NMR (101 MHz, DMSO-d_6) δ (ppm) 150.35, 143.12, 143.11, 141.41, 140.97, 137.91, 134.39, 133.31, 132.25, 131.42, 131.22, 130.87, 128.16, 128.12, 127.86, 127.68, 126.45, 125.63, 124.51, 123.40, 122.26, 121.90, 121.34, 120.27, 118.56, 111.24 ($C_{ar + imid. + benzimid.}$), 31.47 ($CH_2$). FTIR (ν, cm^{-1}): 3117 (N-H), 1627 (C=N). Anal. Calc for $C_{27}H_{19}BrN_4S$ (511.44 g/mol): C, 63.41%; H, 3.74%; N, 10.95%; S, 6.27%; Found: C, 63.39%; H, 3.62%; N, 10.99%; S, 6.48%:

2-(((1-(3-Bromophenyl)-4-(2,3-dimethoxyphenyl)-1*H*-imidazol-2-yl)thio)methyl)-1*H*-benzo[*d*]imidazole (17b)

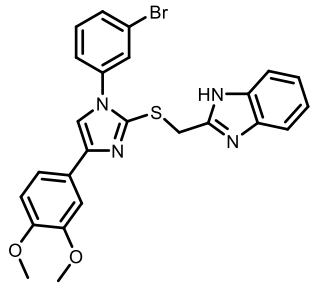

Pinkish white solid, yield 0.236 g (60%), m. p. 110–113 °C, ^{1}H NMR (400 MHz, DMSO-d_6) δ (ppm) 12.48 (s, 1H, NH), 8.02 (s, 1H, H_{ar}), 7.75–7.59 (m, 2H, H_{ar}), 7.52–7.30 (m, 6H, H_{ar}), 7.14 (s, 2H, H_{ar}), 6.98 (d, J = 8.3 Hz, 1H, H_{ar}), 4.57 (s, 2H, CH_2), 3.79 (s, 3H, CH_3), 3.77 (s, 3H, CH_3). ^{13}C NMR (101 MHz, DMSO-d_6) δ (ppm) 150.45, 148.85, 148.01, 147.98, 141.67, 141.64, 139.99, 138.01, 131.28, 131.23, 131.12, 127.98, 126.32, 124.42, 121.82, 121.62, 121.58, 118.75, 118.70, 116.77, 111.91, 108.35 ($C_{ar + imid. + benzimid}$), 55.51 ($OCH_3$), 55.47 ($OCH_3$), 31.60 ($CH_2$). FTIR (ν, cm^{-1}): 1613 (C=O). Anal. Calc for $C_{25}H_{21}BrN_4O_2S$ (521.43 g/mol): C, 57.59%; H, 4.06%; N, 10.75%; S, 6.15%. Found: C, 57.56%, H, 4.04%; N, 10.55%; S, 6.22%.

2.2. Biological Evaluation by the MTT Cytotoxicity Assay

The in vitro anticancer activity of compounds **4–17** was evaluated using A549 human pulmonary adenocarcinoma cells (ATCC CCL-185). The cells were cultured in DMEM/F12 medium supplemented with GlutaMAX, 10% heat-inactivated fetal bovine serum (FBS), and penicillin/streptomycin (Thermo Fisher Scientific) at 37 °C in a humidified atmosphere containing 5% CO_2. For the MTT assay, the cells were seeded in 96-well plates and incubated overnight. The test compounds were dissolved in DMSO (stock solution: 10 mM) and added to the wells at a final concentration of 100 μM, with the DMSO content maintained at ≤0.1%. Doxorubicin (DOX),

cisplatin (CP), and cytarabine (AraC) were used as positive controls. After 20 h of exposure to the compounds, MTT solution (0.5 mg/mL) was added to each well, and the plates were incubated for 4 h at 37 °C. The resulting formazan crystals were dissolved in anhydrous DMSO, and the absorbance was measured at 580 nm using a Multiskan microplate reader (Thermo Fisher Scientific). Cell viability was calculated according to the following equation: $([A_e - A\_b] / [A\_c - A\_b]) \times 100\%$, where A_e represents the absorbance of treated cells, A_c corresponds to untreated control cells, and A_b denotes the blank. All experiments were performed in triplicate, and the data are presented as the mean ± standard deviation (SD). Statistical analysis was carried out using GraphPad Prism v9 (unpaired t-test), and differences were considered statistically significant at $p < 0.05$.

3. Results and discussion

3.1 Synthesis of 3-(1-(3-bromophenyl)thioureido)propanoic acid (4)

The precursor of thioureic acid **4** was synthesised using a literature procedure [66], which was adapted to 3-bromoaniline. The synthesis was carried out in a multistep manner, starting from commercially available 3-bromoaniline (**1**), as shown in Scheme 3.1. Compound **2** was obtained by a classical aza-Michael coupling reaction between 3-bromoaniline (**1**) and acrylic acid. The reaction was carried out in toluene at 50 °C for 24 h. Subsequently, 1-(3-bromophenyl)-2-thioxotetrahydropyrimidin-4(1*H*)-one (**3**) was synthesised from 3-((3-bromophenyl)amino)propanoic acid (**2**) by reaction with potassium thiocyanate in glacial acetic acid. Compound **4** was obtained by alkaline hydrolysis from compound **3**. After acidification of the alkaline solution with dilute acetic acid, the intermediate free base was converted to the target 3-(1-(3-bromophenyl)thioureido)propanoic acid (**4**) in 87% yield Scheme 3.1.

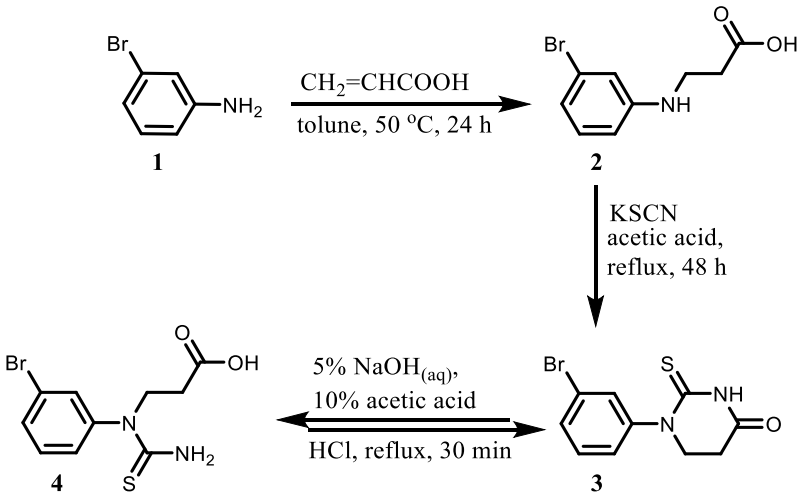

Scheme 3.1. The synthesis of thioureido acid **4**.

The structures of the synthesised compounds **3** and **4** were confirmed by ^{1}H and ^{13}C NMR, FTIR spectroscopy and elemental analysis. In the ^{1}H NMR spectrum, two triplets with a coupling constant $J = 7.6$ Hz at δ 4.15 and 2.54 ppm were assigned to methylene (CH_2) protons. A broad singlet observed at δ 6.93 ppm was assigned to the NH_2 group, confirming the structure of compound **4**.

In the ^{1}H NMR spectrum of compound **3**, the NH signals were observed to be sharp and not broadened, as shown in Fig. 3.1., suggesting that no tautomerisation of exchangeable protons takes place in DMSO. This interpretation is further supported by the FTIR spectrum, in which an absorption band characteristic of an NH group was detected at 3141 cm^{-1}. Taken together, these findings indicate that 1-(3-bromophenyl)-2-thioxotetrahydropyrimidin-4(1*H*)-one (**3**) predominantly exists in the thione form.

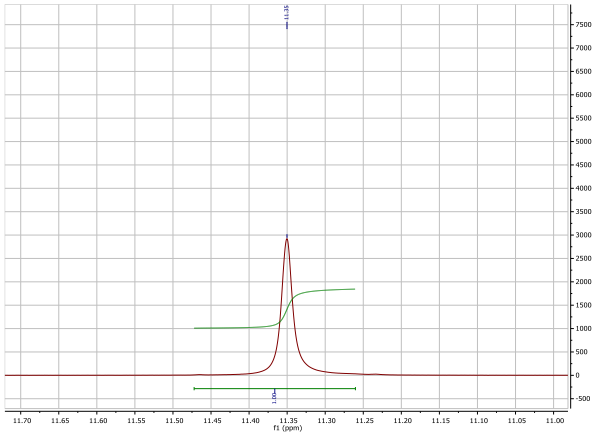

Fig. 3.1. The NH proton signal in the ^{1}H NMR spectrum of compound **3**

The ^{1}H NMR spectrum of compound **4** was characterised by a doublet at δ 7.25 ppm, a triplet at δ 7.39 ppm, and doublets at δ 7.49 and 7.55 ppm, which were assigned to aromatic protons. In addition, a broad singlet at δ 12.25 ppm was assigned to the hydroxyl (OH) proton. An expanded region of the ^{1}H NMR spectrum of 3-(1-(3-bromophenyl)thioureido)propanoic acid (**4**) is presented in Fig. 3.2.

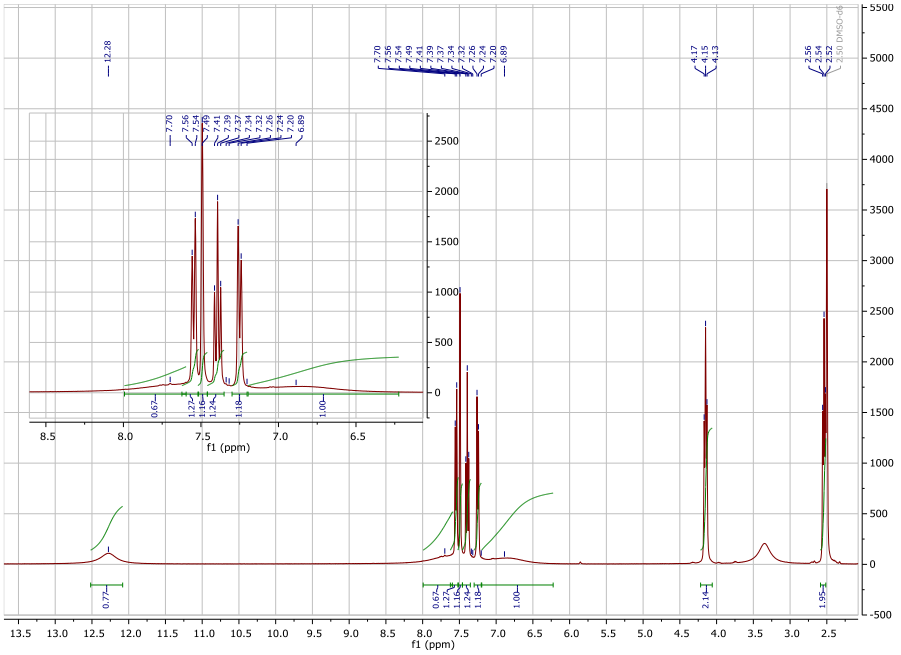

Fig. 3.2. Section of the ^{1}H NMR spectrum of 3-(1-(3-bromophenyl)thioureido)propanoic acid (**4**)

The thiol-thione tautomerism effect was also observed, as the migration of the NH_2 proton to the sulphur atom led to the appearance of two broad singlets in the aromatic region, which is consistent with proton exchange processes. The characteristic resonance at δ 181.80 ppm in the ^{13}C NMR spectrum, corresponding to the C=S group, indicated that thioureic acid **4** in DMSO solution exists predominantly in the thione tautomeric form. This assignment was further supported by FTIR data, where the absorption band characteristic of the NH_2 group at 3358 cm^{-1} confirmed the dominance of the thione form in the solid state.

3.2Thioureic acid 4 reaction with α-haloketones

A literature review indicates that thiazoles bearing a 4-aryl substituent exhibit significant anticancer activity [66]. In this study, thiazole derivatives were synthesised from thioureic acid **4** by reacting various 2-bromoacetophenone derivatives using a Hantzsch-type cyclisation mechanism. It has also been reported [67] that in the absence of a base catalyst and when the reactions are carried out in aprotic solvents, the reaction produces hydrogen bromide, and the products form insoluble salts. Accordingly, treatment of thioureic acid **4** with various 2-bromoacetophenones in acetone at room temperature gave the corresponding thiazole salts **5a–h**. These salts **5a–h** was subsequently converted to the corresponding free bases by dissolving them in methanol and treating with sodium acetate. The yields of the final products **5a–h** ranged from 62% to 68% (Scheme 3.2). The structures of the resulting compounds **5a–h** were confirmed by ^{1}H NMR spectroscopy, as indicated by an increased number of signals in the chemical shift region corresponding to aromatic protons, along with the absence of signals attributed to the NH_2 group.

In this project, the reactions of compound **5a** were also tested in tetrahydrofuran and acetonitrile solvents. During the work, it was found that the products were also formed quickly, but the reaction mixture was obtained in lower yields compared to acetone. It was also observed that impurities may form when dissolving the corresponding hydrobromide salts of the products for a longer time and at higher temperatures. This is most likely related to the heating conditions under which Fischer esterification can occur. In addition, it was observed that a small amount of water can initiate an acid-catalysed cyclocondensation, resulting in the formation of 1-(3-bromophenyl)-2-thioxotetrahydropyrimidin-4(1*H*)-one (**3**), which can further participate in side reactions. Therefore, the use of dry aprotic solvents is recommended. In addition, the conversion to free bases should be carried out by dissolving the salts in methanol at room temperature, avoiding heating.

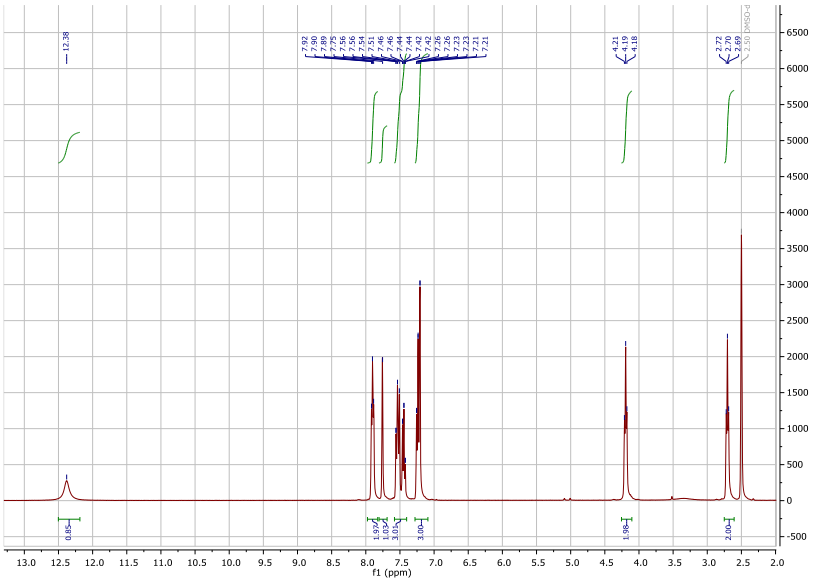

Fig. 3.3. Section of the ^{1}H NMR spectrum of compound **5c**

In the ^{1}H NMR spectrum of compound **5c**, a broad singlet at δ 12.38 ppm was observed and attributed to the OH group proton. Additionally, signals corresponding to nine aromatic protons were detected within the characteristic chemical shift region. In the ^{13}C NMR spectrum, a signal at approximately δ 172 ppm was assigned to a carbonyl carbon (C=O), confirming the presence of a carbonyl functional group.

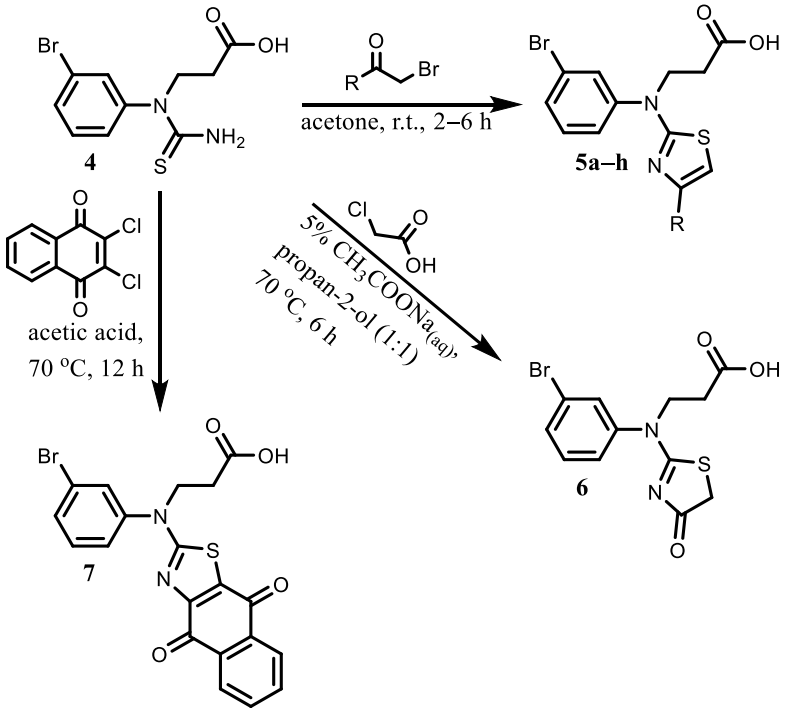

R = 5a) C_6H_5; **5b)** 4-HOC_6H_4; **5c)** 4-FC_6H_4; **5d)** 4-ClC_6H_4; **5e)** 4-BrC_6H_4; **5f)** 4-$NO_2C_6H_4$; **5g)** 2-naphthyl; **5h)** 3,4-di(CH_3O)C_6H_3.

Scheme 3.1. General synthesis of 2-aminothiazole derivatives **5**, **7** and thiazolone **6**.

The thiazole acid **4** was treated with chloroacetic acid in 5% aqueous sodium acetate in propan-2-ol at 70 °C for 6 h to give the 4-oxothiazoline derivative **6** in 73% yield (Scheme 3.2). The reaction was further investigated in aqueous systems using potassium carbonate, sodium carbonate and sodium bicarbonate, as well as in a mixture of water and propanol containing sodium bicarbonate. In all cases, the target products were not isolated or only very small amounts were obtained.

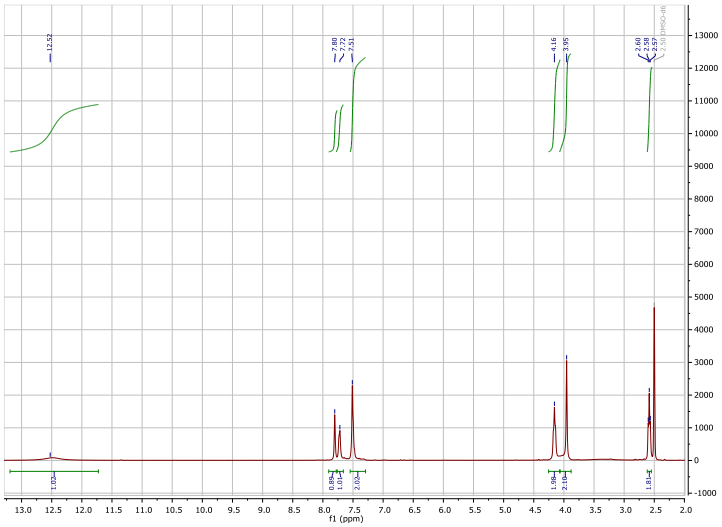

Fig. 3.4. The ^{1}H NMR spectrum of 4-thiazolinone derivative **6**

In the ^{1}H NMR spectrum of compound **6**, a singlet was observed at δ 3.95 ppm, which was assigned to the protons of SCH_2 group. However, the remaining signals in the spectrum were not well resolved into individual multiplets, which can be attributed to the presence of several nucleophilic centers in the molecule **6** (Fig. 3.4). This interpretation was supported by the ^{13}C NMR data, in which signals

corresponding to carbonyl-type carbon atoms were detected at δ 186.95 ppm (C=N), 183.12 ppm (C=O) and 172.03 ppm (C=O), indicating to thiazolone structure **6** formation.
According to the literature[68], it is known that thiazole derivatives fused to a naphthoquinone moiety exhibit notable biological activity. In the project, the target naphthoquinone-thiazole hybrid **7** was obtained by treating thioureic acid **4** with 2,3-dichloronaphthalene-1,4-dione in acetic acid/sodium acetate at 70 °C for 12 h (Scheme 3.2). According to the literature, acetonitrile and potassium carbonate under reflux are suitable conditions for the synthesis of this class of compounds. However, the application of these conditions did not give the desired result, and the target products were not isolated from the reaction mixture. The formation of the thiazole ring in all compounds was confirmed by ^{1}H NMR spectroscopy, as indicated by the appearance of a characteristic aromatic CH_2 signal at δ 6.95–7.23 ppm, accompanied by an increase in the number of signals in the aromatic region and the disappearance of the thioureic acid **4** NH_2 proton signal.

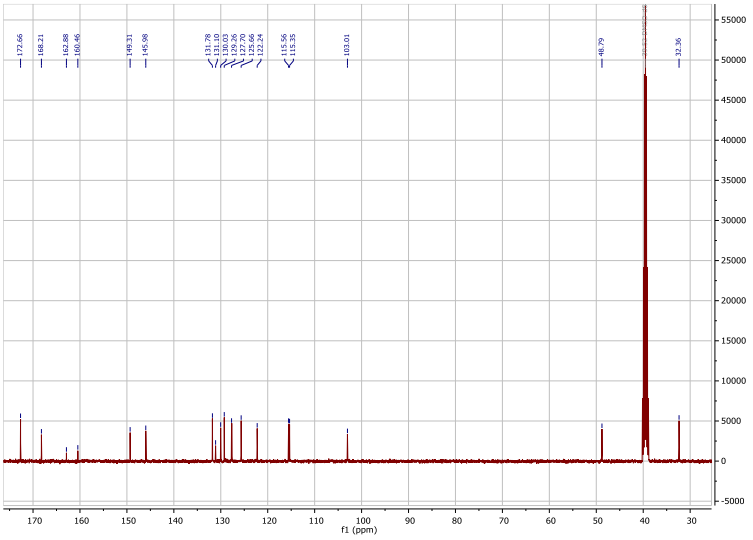

Fig. 3.5. Expanded region of the ^{13}C NMR spectrum of compound **7**

In the ^{13}C NMR spectrum, signals assigned to the NCH_2 carbon atoms were observed in the range of δ 48.7–32.3 ppm, and the corresponding resonances of aromatic carbon atoms appeared between δ 100 and 155 ppm. In the case of compound **7**, the formation of the naphthoquinone-thiazole bicyclic system was confirmed by three carbonyl signals at δ 179.85, 174.97 and 172.29 ppm, corresponding to two naphthoquinone carbonyl groups and one carboxylic acid group, as shown in Figure 3.5. In addition, the compound was characterised by a characteristic brick-red colour. FTIR absorptions confirmed the formation of the bicyclic system at 1700 cm^{-1} (C=O) and 1588 cm^{-1} (C=N).

3.3 Synthesis of chalcone-type derivatives 9a-k

The bifunctional intermediate **8**, bearing both a reactive 5-acetyl group suitable for Claisen–Schmidt condensation and a carboxylic acid moiety, was synthesised from thioureic acid **4** and 3-chloropentane-2,4-dione in acetone under reflux with 85% yield (Scheme 3.3). The reaction proceeds via a regioselective Hantzsch-type cyclisation of the unsymmetrical α-chlorodiketone. The mechanism is involved where nucleophilic attack of the thiourea sulphur occurs at the less hindered α-chlorocarbon, followed by intramolecular cyclisation to afford the 4-methyl-5-acetylthiazole scaffold in derivative **8**, in agreement with literature reports [62].

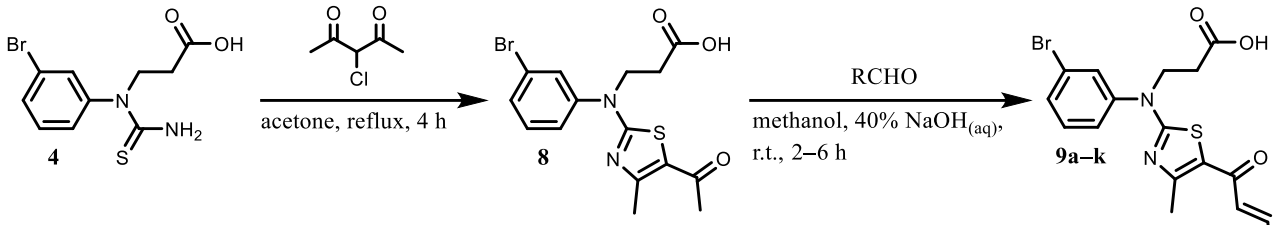

R = 9a) C_6H_5; **R = 9b)** 4-FC_6H_4; **R = 9c)** 2-ClC_6H_4; **R = 9d)** 4-ClC_6H_4; **R = 9e)** 2,6-diClC_6H_3; **R = 9f)** 4-BrC_6H_4; **R = 9g)** 2-naphthyl; **R = 9h)** 2-thienyl; **R = 9i)** 2-furyl; **R = 9j)** 3-bromothien-2-yl; **R = 9k)** 5-bromofur-2-yl.

Scheme 3.3. Synthesis of derivatives **9a–k** by Claisen-Schmidt condensation reaction.

Compound **8** was subsequently subjected to base-mediated Claisen-Schmidt condensation with a series of aryl and heteroaryl aldehydes in methanol using aqueous NaOH, affording chalcone–thiazole hybrids **9a–k** in 62–77% yield (Scheme 3.3). The transformation proceeds via enolate formation at the acetyl group, nucleophilic addition to the aldehyde, and subsequent dehydration to yield the thermodynamically favoured *E* isomer of chalcone products. The formation of chalcones was confirmed by ^{1}H NMR spectroscopy through the appearance of two characteristic –CH=CH– group absent in compound **8**, with coupling constants ($J \approx 15$–16 Hz) consistent with *E*-configuration[63] . In contrast, compound **8** exhibited only the acetyl methyl singlet at δ 2.33 ppm. According to the literature, thiazole-chalcone hybrids preferentially adopt the *E* configuration. In the present study, no signal splitting attributable to isomerisation was observed in the NMR spectra of the synthesised chalcones, indicating the exclusive formation of the *E*-isomers.

To obtain compounds **9a–k**, a Claisen–Schmidt condensation was carried out in a small volume of an alcoholic solvent by adding saturated aqueous sodium hydroxide to the reaction mixture. Notably, the products crystallised directly from the reaction mixture as the corresponding sodium salts, which were readily converted into the free acids by dissolution in methanol followed by acidification with acetic acid. However, this procedure proved unsuitable for several chalcone-type derivatives **9a–k**. Therefore, calcium carbonate was employed as an alternative base. Under these conditions, the reaction proceeded significantly more slowly, and reflux was required to obtain compounds **9c** and **9j**. The solvent selection was found to play an important role in both the reaction rate and the yield of compound **9a**. Prolonged reaction times were associated with an increased formation of side products, which consequently diminished the formation of the desired compound.

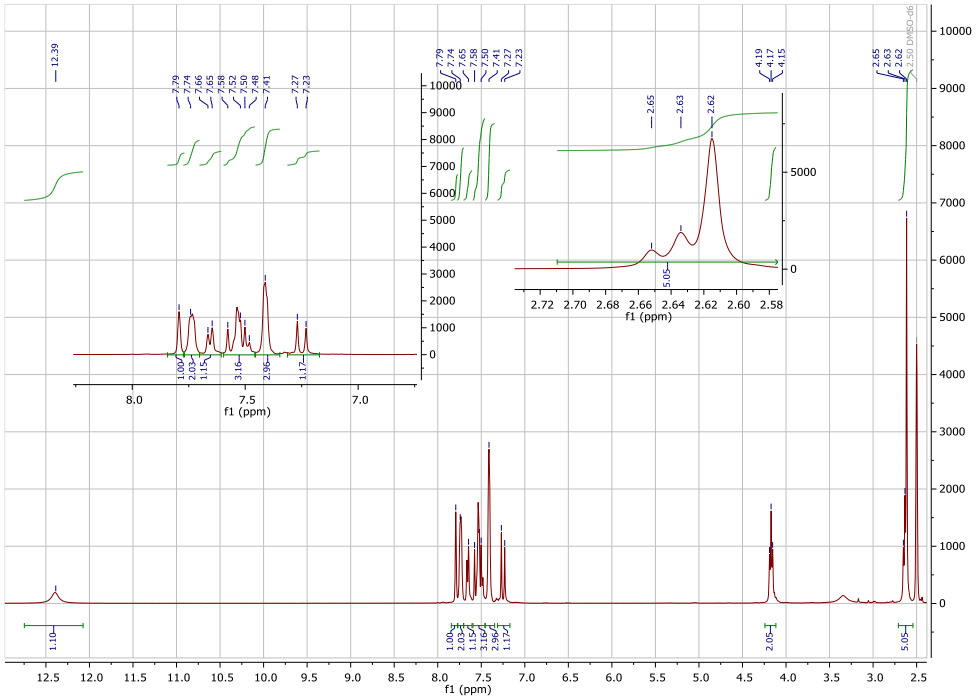

Fig. 3.6. Expanded region of the ^{1}H NMR spectrum of compound **9a**

In the ^{1}H NMR spectrum of compound **9a**, a broad singlet at δ 12.39 ppm was attributed to the hydroxyl proton. Signals in the region δ 7.79–7.25 ppm were observed predominantly as multiplets and were assigned to the aromatic protons of the phenyl ring. A triplet at δ 4.17 ppm was attributed to the CH_2 group, while an additional multiplet at δ 2.71–2.55 ppm further supports the formation of the chalcone structure in molecule **9a** (Fig. 3.6).

3.4 Synthesis of imidazole-2-thione derivatives 11–17a,b

It is well established in the literature that compounds containing an imidazole ring exhibit significant anticancer activity [69]. Therefore, in the present study, imidazole derivatives based on a 3-bromoaniline scaffold were synthesised, and their properties were investigated. Compounds **10a,b** were obtained by the reaction of 3-bromoaniline (**1**) with the corresponding 2-bromoacetophenones in propan-2-ol with sodium bicarbonate The imidazole-2-thione precursors **11a,b** were subsequently prepared by treating the 2-aminoketone intermediates **10a,b** with potassium thiocyanate in glacial acetic acid at room temperature for 24 h.

In this study, several *N*-alkylation reaction conditions were investigated by varying both the solvent and the base. It was observed that the reaction could proceed via competing pathways, leading to the formation of side products. In particular, the use of methanol or stronger bases resulted in an increased formation of by-products. The structure of compound **10b** was confirmed by ^{1}H and ^{13}C NMR spectroscopy. In the ^{1}H NMR spectrum, a characteristic NH group proton resonance was observed at δ 6.18 ppm, along with a singlet at δ 4.65 ppm attributed to the CH_2 group protons.

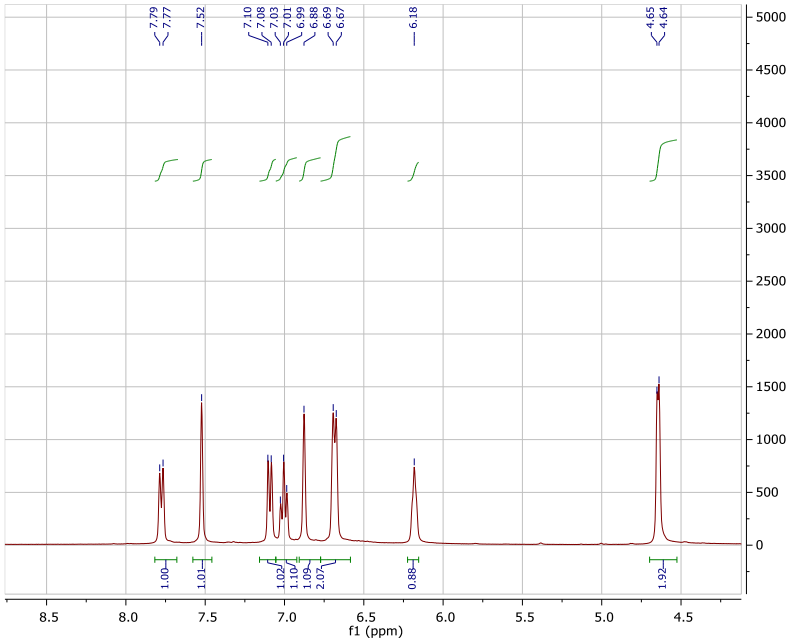

Fig. 3.7. The part of the ^{1}H NMR spectrum of compound **10b**

The ^{13}C NMR spectrum showed signals at δ 194.62 ppm and 49.21 ppm, assigned to the carbonyl (C=O) and methylene (CH_2) carbons, respectively. Additionally, an increased number of signals in the aromatic region further supported the proposed structure **10b**.

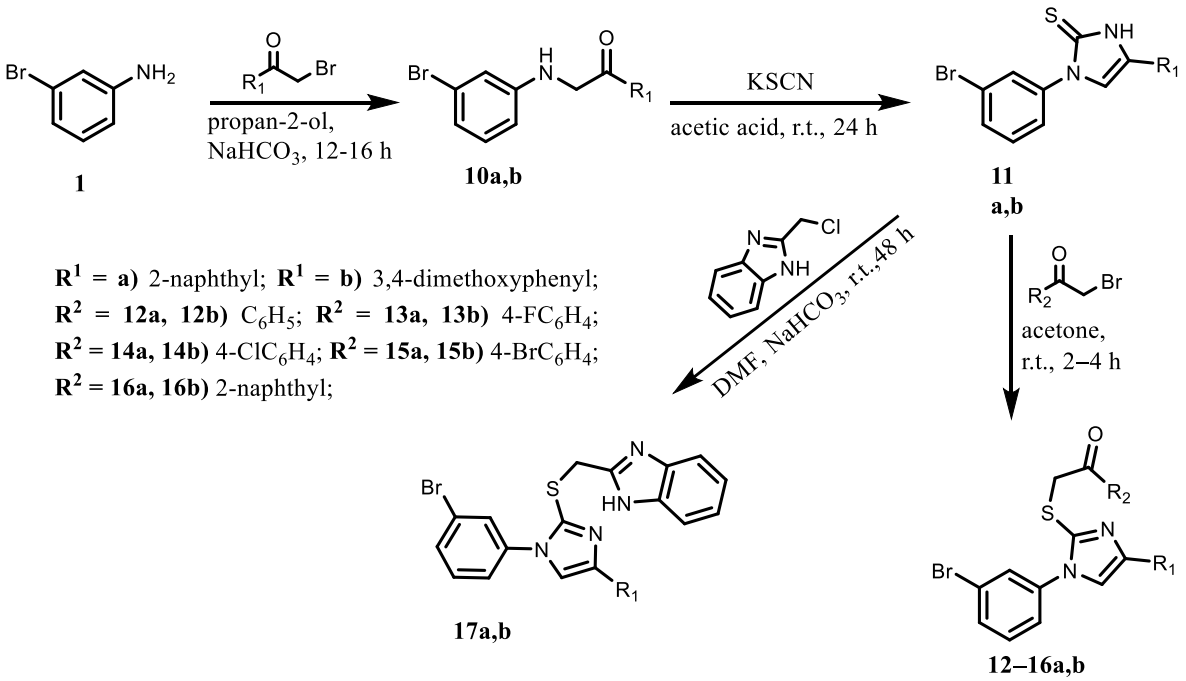

Scheme 3.4. Synthesis of imidazole-2-thione derivatives **12–16a,b**.

According to the literature, alkylation of imidazole-2-thiones with bromoacetophenone derivatives affords compounds that exhibit promising anticancer activity against various cancer cell lines. Therefore, in this study, a series of *S*-alkylated imidazole-2-thione derivatives **12–16** was synthesised. These reactions were efficiently carried out in polar aprotic solvents, where in situ-generated hydrogen halides formed salts with the products. These salts are usually precipitated directly from the reaction mixtures and can be easily converted to the corresponding free bases by treatment with

sodium acetate. Imidazole-2-thiones **11a** and **11b** were then reacted with various 2-bromoacetophenones to yield *S*-alkylated imidazole derivatives **12-16a,b**.

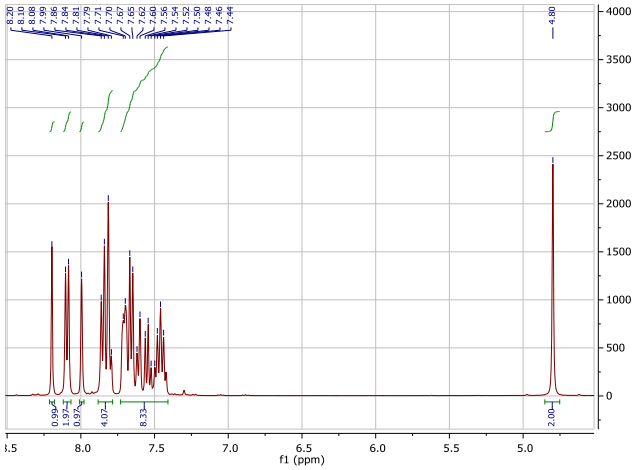

Fig. 3.8. The part of the ^{1}H NMR spectrum of compound **14a**

The ^{1}H NMR spectrum exhibited a singlet at δ 4.80 ppm, confirming the presence of a proton of the NCH_2 group. Signals in the region δ 7.0–8.5 ppm were attributed to aromatic protons, indicating the presence of phenyl and heteroaromatic moieties. Compounds **17a** and **17b** were synthesised from precursors **11a** and **11b** via reaction with 2-(chloromethyl)-1*H*-benzo[*d*]imidazole in the presence of sodium bicarbonate in DMF at room temperature for 48 h, leading to the formation of benzimidazole-substituted derivatives (Scheme 3.4). The reaction mixture was stirred at room temperature for 2–4 h. The *S*-alkylated products were obtained after standard work-up, treated with sodium acetate, and subsequently crystallised from methanol, affording yields in the range of 67–72%.
It is also known that compounds containing a benzimidazole moiety exhibit favourable biological properties and often enhance overall biological activity [65]. 2-(Chloromethyl)-1*H*-benzo[*d*]imidazole was synthesised from 2-chloroacetic acid and o-phenylenediamine and then used in *S*-alkylation reactions of imidazole-2-thiones **11a,b** to give the corresponding derivatives **17a,b**. All obtained compounds were converted to free bases before analysis. Structural confirmation was based on spectroscopic data, which were consistent with those of structurally related compounds described in the literature [66].

The structures of the obtained compounds were confirmed by NMR spectroscopy, as presented in fig. 3.9.

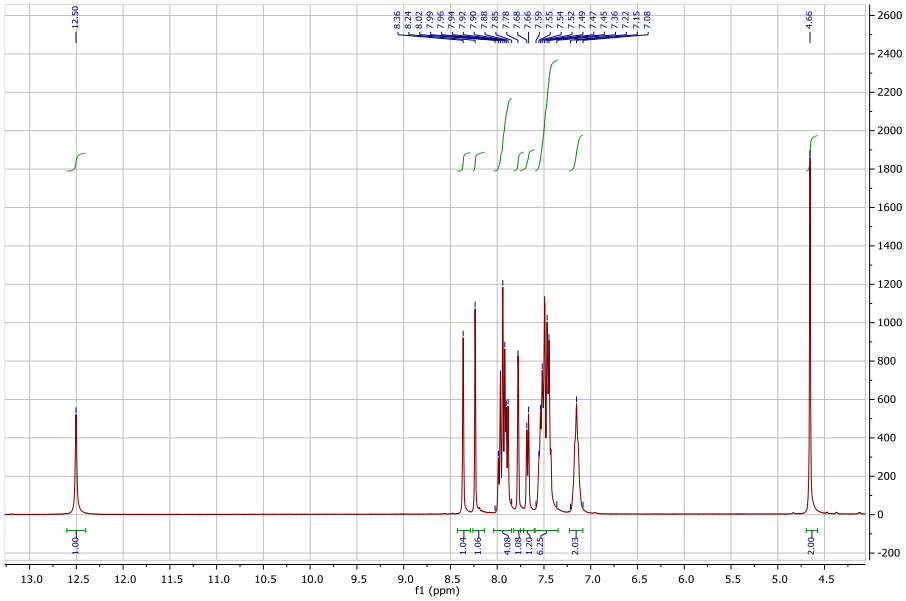

Fig. 3.9. The part of the ^{1}H NMR spectrum of compound **17a**

The ^{1}H NMR spectrum exhibited a signal at δ 12.50 ppm, which was attributed to NH protons, confirming the presence of a heterocyclic thione moiety. Signals in the δ 7.0–8.5 ppm region were assigned to aromatic protons, while a signal at approximately δ 4.5 ppm was attributed to a proton of the methylene (CH_2) group.

3.5 Biological activity studies of synthesised compounds 4-17 on A549 cells

The synthesised compounds were evaluated for their potential *in vitro* antiproliferative activity. The assays were carried out using the human lung cancer cell line A549 at a fixed concentration of 100 µM. The A549 cell line is widely employed in preliminary anticancer screening studies.

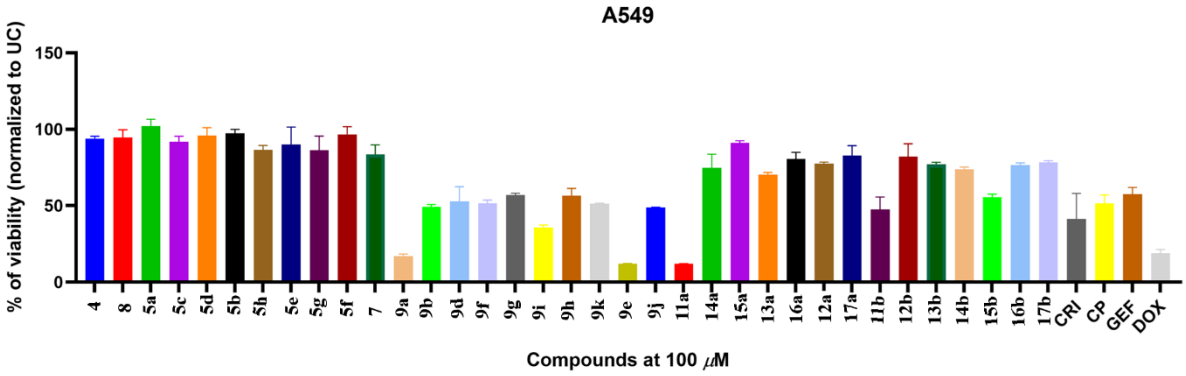

Fig. 3.10. Antiproliferative activity of all synthesised compounds (corresponding to series **4**, **5a–h**, **9a–k** and **12–17a, b**) against A549 human non-small cell lung cancer cells at 100 µM. The cell viability (%) is normalised with the untreated control (UC). Reference drugs: cytarabine (CRI/AraC), cisplatin (CP), gefitinib (GEF) and doxorubicin (DOX) are shown for comparison. Data are mean ± SD (n = 3). Viability < 50% (dashed threshold) is considered active.

Cell viability was normalised to the untreated control (set at 100%) and compared with reference anticancer agents, including crizotinib (CRI), cisplatin (CP), gefitinib (GEF), and doxorubicin

(DOX). Reduced cell viability was interpreted as indicative of enhanced antiproliferative activity. The obtained data demonstrate a discernible structure–activity relationship. Early-stage intermediates and selected heterocyclic derivatives (compounds **4**, **8**, **5a–5h**, and **7**) exhibited minimal activity against A549 cells, as evidenced by high viability values (83–102%). These findings indicate that, at 100 µM, the compounds exert negligible inhibitory effects on cancer cell proliferation. Therefore, under the applied experimental conditions, these derivatives may be classified as biologically inactive or weakly active. Conversely, several later-stage derivatives demonstrated pronounced inhibition of A549 cell growth. The most active compounds – **9e**, **9a**, and **11a** – reduced cell viability to approximately 12%, indicating strong antiproliferative activity. These results suggest that compounds **9e**, **9a**, and **11a** possess significant anticancer potential. Notably, compound **9a** exhibited a cell viability of approximately 17%, which is comparable to that of the reference drug doxorubicin (DOX), for which cell viability was approximately 18%. Furthermore, compounds **9a**, **9b**, and **11a** demonstrated superior activity relative to the reference agents crizotinib (CRI), cisplatin (CP), gefitinib (GEF), and doxorubicin (DOX) in this preliminary screening assay.

In conclusion, the antiproliferative activity of the compounds may be ranked as **9e** > **11a** > **9a**. These results indicate a clear correlation between biological activity and molecular structure. In particular, the presence of a chalcone moiety, as observed in compounds **9a–9j**, appears to contribute significantly to enhanced antiproliferative effects, with compound **9e** exhibiting the highest activity. Similarly, compounds bearing imidazole-based frameworks **11a–15b** demonstrated measurable anticancer activity; however, their efficacy was generally lower than that of the chalcone-containing derivatives. As the present evaluation was conducted at a single concentration (100 µM), further studies are required to comprehensively assess the therapeutic potential of these compounds. Such investigations should include IC_{50} determination, apoptosis assays, and selectivity profiling against normal cell lines prior to any consideration of their further development.

3.5.1 Activity of thiazole derivative compounds

Thiazole is an important heterocyclic compound that contains nitrogen and sulfur atoms on its core. The area of thiazole derivatives is widely studied in medicinal chemistry since their ability to interact with diverse biological targets through different interactions related with its SAR. Several thiazole-containing molecules display different biological activities, such as anti-cancer [70], ant-microbial [71], anti-inflammatory [72]. Therefore, thiazole might be considered as a useful scaffold in anti-cancer drug design.

In this synthesised sequence of compounds having a thiazole ring from **5a-h** and **7,** tested against A549 cell lines. The results confirm that the thiazole ring alone is adequate for better antiproliferative activity. The results from the bar graph show that the synthesised compounds did not significantly reduce A549 cancer cell growth in the test. The action could be affected by the absence of strongly active pharmacophore clusters.

3.5.2 Activity of chalcone derivatives

Chalcones are very important compounds in anti-cancer research due to the occurrence of α,β-unsaturated carbonyl system. This enone scheme may act as a Michel acceptor, which may interact with nucleophilic sites in the biological targets. Chalcones are well recognised for their anti-cancer properties [73].

In my work, the chalcone-bearing thiazole hybrid series from **9a-9k** shows good anti-cancer properties. Compared to the different reference drugs, in contradiction of A549 cell lines and some compounds show activity better than Doxorubicin (DOX). Most of the compounds show in this series a medium range cell viability of approximately 36–57%, which shows moderate activity at 100 µM. The most active compound in our entire series of synthesis was found to be compound **9e,** which reduces lung cancer A549 cell line viability to nearly **12%,** which is stronger than that of the reference drug doxorubicin, which demonstrates an activity range of **18%** of viability. The strong activity of compound **9e** could be based on its structural properties. Mostly related to the presence of the 2,6-dichlorophenyl substituent. The two chlorine atoms are strong electron-withdrawing groups, and they might be improving the electrophilic character of this α,β-unsaturated carbonyl arrangement. This helps the compound to advance the interaction with the biological target and increases the cytotoxic action. Similarly, compound **9a**, a phenyl-substituted chalcone derivative, also shows strong activity with 17% viability. This is almost equivalent to that of doxorubicin. Moreover, the derivatives **9b, 9d, 9f, 9h, 9i, 9j**, and **9k** display a weaker effect compared to the compounds **9e** and **9a**. We could say that the substation on the aromatic ring plays a significant part in the biological activity. Throughout, chalcone derivatives exhibited better anticancer activity than the simple thiazole intermediate. The results show the chalcone moiety plays a major role in improving biological activity. Among these compounds, **9e** and **9a** show strong activity against lung cancer A549 in the cell viability test.

3.5.3 Activity of imidazole and imidazole derivatives

Five-membered heterocyclic rings covering two nitrogen atoms are a core in medicinal chemistry due to their capability to form hydrogen bond exchanges with receptors, enzymes and improve binding capability with biological targets. Many imidazole derivatives have shown decent anti-cancer[74], ant-inflammatory [75], anti-fungal properties [76]. In my study, compound **11a, which** belongs to imidazole derivatives, shows good anti-proliferative activity against A549 cell lines with a viability range of around **12%**. The activity was stronger than that of doxorubicin and much stronger than other reference drugs in the same screening assessment. The activity of **11a** could be related to the presence of an imidazole ring bearing a 2-naphthyl substituent. The imidazole ring can expand the interaction with biological targets with the help of nitrogen atoms, while the naphthyl group increases the aromatic surface and improves hydrophobicity by π-π interaction. In a comparison with thiazole derivatives, imidazole displays good activity against the A549 cell line. The imidazole series compound **11a** shows good activity, while some other derivatives from **12a,b–17a,b** show reasonable activity. which states that the imidazole core is not only sufficient for strong anti-cancer activity. The attached substituted groups are also very important for their activity.

3.6 SAR of active compounds

Structure-activity relationship analysis revealed a clear dependence of antiproliferative activity on the nature of the substituents. Of the tested compounds, the 2,6-dichlorophenyl-substituted chalcone-thiazole derivative **9e** exhibited the highest activity, which can be attributed to the presence of an α,β-unsaturated carbonyl system and electron-withdrawing chlorine atoms, which enhance electrophilicity and interaction with biological targets. However, this compound exhibited slightly reduced drug similarity due to its higher molecular weight (537.95), increased lipophilicity (LogP = 5.07), and one violation of Lipinski's rule.

The unsubstituted phenyl chalcone-thiazole derivative **9a** also exhibited potent antiproliferative activity, indicating that the chalcone-thiazole system itself is intrinsically favourable for anticancer activity. Compared to compound **9e**, compound **9a** exhibited better drug similarity, lower molecular weight (380), LogP 4.67, and no Lipinski rule violations, indicating a more balanced pharmacological profile. The naphthalenyl-substituted imidazole derivative **11a** also exhibited significant activity, which may be related to the ability of the imidazole ring to form hydrogen bonds and polar interactions, along with enhanced hydrophobic interactions provided by the naphthalene moiety. Although compound **11a** exhibited acceptable drug similarity (MW = 470.03, LogP = 4.49), the expected CYP inhibition, high plasma protein binding, and potential toxicity require further investigation. Overall, structure-dependent activity was observed in the A549 cell screening, and compounds **9e**, **9a**, and **11a** were identified as the most active. Chalcone-thiazole hybrids **9e** and **9a** exhibited potent anticancer activity due to their electrophilic α,β-unsaturated system, while the imidazole derivative **11a** exhibited activity related to its heterocyclic interaction capabilities

3.7 ADMET analysis of active compounds 9a, 9e, and 11a

The ADMET profiles of compound **9e,9a** and 11a were compared using very important drug-related activities such as physicochemical, pharmacokinetics, drug likeness and toxicity parameters.

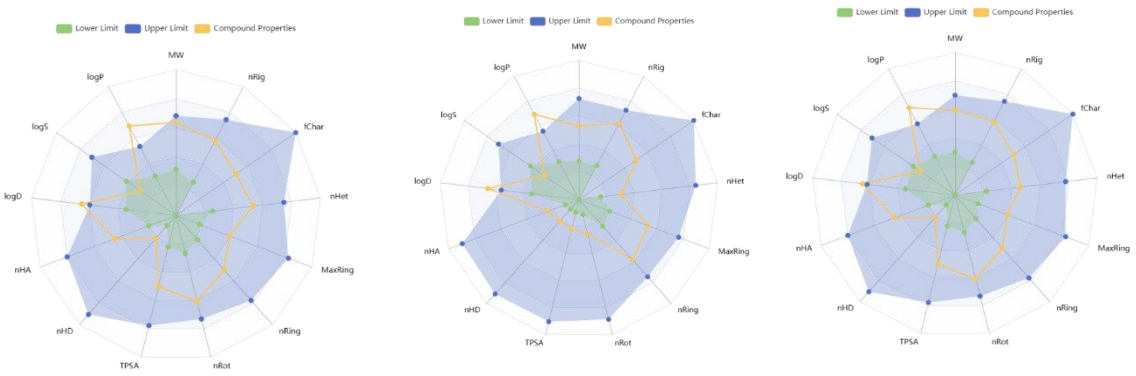

A **B** **C**

Fig. 3.11 Radar plot comparing physicochemical and drug-likeness properties of compounds **9a (A)**, **9e (B)**, and **11a (C).**

All three compounds exhibited high plasma protein binding (>90%), indicating that only a small free fraction is available for pharmacological activity. The blood–brain barrier (BBB) permeability was predicted to be low for all compounds, suggesting limited central nervous system penetration.

In these compared compounds, compounds **11a** and **9a** showed better Lipinski-drug-likeness, and compound **9e** shows 1 violation due to high molecular weight and lipophilicity. The rest of the 2

compounds have molecular weights within the range. All 3 compounds showed hydrogen bond acceptance and donations and TPSA values, which remark their basic physicochemical properties are more likely within drug-like range. In terms of absorption, compound **9a** shows better Caco-2 permeability, while compound **11a** shows less permeability. And compounds **9a** and **11a** showed a higher probability of P-gp inhibition. The predicted oral bioavailability profile was acceptable. But very high lipophilicity
and high plasma protein of all 3 compounds may affect their free drug availability in systemic circulation.

Table 3.1. Selected ADMET parameters and drug-likeness comparison of the most active compounds **9a**, **9e**, and **11a**.

ADMET parameter	Compound number 9e	Compound number 9a	Compound number 11a	Observations
Molecular weight	537.95	380	470.03	Compound number 9a,11a are following Lipinski limit, 9e is slightly high
Log p	5.07	4.670	4.492	11a have most acceptable lipophilicity
Lipinski rule violation	1	0	0	Compound number 9a, 11a has the highest predicted drug likeness
BBB penetration	0.270	0.198	0.186	All have low BBB penetration probability
Plasma protein binding	99.546%	98.252%	99.267%	All compounds have high plasma protein binding
CYP inhibition risk	High	Moderate	High	Compound number 9e and 11a inhibit more CYP enzymes
Plasma clearance	0.782	4.681	0.525	All 3 compounds show low clearance
P-gp inhibitor	0.505	0.957	0.864	Compound number 9a and 11a strongly inhibit p-gp
DILI risk	0.995	0.995	0.967	All shows predicted liver injury risk
Caco-2 permeability	-5.153	-4.928	-5.387	11a shows better predictable permeability
Half-life	1,8h	0.584h	1.434h	9e shows longest half-life
hERG blocker risk	0.142	0.243	0.148	All show low basic hERG blocker probability
Genotoxicity	0.998	0.994	0.997	All shown high predicted genotoxicity
Skin sensitization	0.804	0.447	0.815	Compound 9e and 11a maybe skin sensitizer

In terms of metabolism, compounds **9e** and **11a** were predicted to inhibit several cytochrome P450 (CYP) enzymes, indicating a potential risk of drug–drug interactions. In contrast, compound **9a** exhibited comparatively lower CYP inhibition, particularly toward CYP1A2 and CYP2C8.
The excretion profile indicated generally low clearance for all compounds, although compound **9a** showed relatively higher plasma clearance compared with the others.
Toxicity assessment revealed several concerns, including predicted high risk of drug-induced liver injury (DILI) and potential genotoxicity. Additionally, compounds **9e** and **11a** showed a higher

probability of skin sensitisation, whereas the risk of hERG channel inhibition was low for all compounds.

Overall, compound **11a** demonstrated a balanced profile between biological activity and ADMET properties, whereas compound **9e**, despite its high activity, showed reduced drug-likeness due to its higher molecular weight and violation of Lipinski's rule. All compounds exhibited promising activity, although further optimisation is required to improve their pharmacokinetic and toxicity profiles.

3.8 *In silico* study of active compounds 9a, 9e, and 11a.

A structure-based pharmacophore modelling and molecular docking study was performed to evaluate the binding potential of selected compounds against the bacterial DNA gyrase B active site. The crystal structure of the target protein was obtained from the Protein Data Bank (PDB ID: 3RHK), which represents the ATP-binding domain complexed with a known inhibitor, 1-[(3*R*,4*R*)-4-(1*H*-indol-3-yl)-2,5-dioxopyrrolidin-3-yl]pyrrolo[3,2,1-ij]quinolinium (PubChem CID: 53322946). The target protein was selected based on literature data [74], which indicates that benzimidazole derivatives exhibit inhibitory activity against DNA gyrase B. Due to the essential role of this enzyme in bacterial DNA replication and the structural features of the ATP-binding pocket, DNA gyrase B represents a well-established target for the design of novel antibacterial agents. The protein–ligand complex was imported into LigandScout 4.5 Advanced, and a structure-based pharmacophore model was generated. Key interaction features, including hydrogen bond donors and acceptors, hydrophobic regions, and aromatic interactions, were identified and refined to retain only the most relevant binding elements.

A set of synthesised compounds (**9a**, **9e**, and **11a**) was prepared as SDF structures using Chem3D 15.1 and energy-minimised by MMFF94 before analysis. These compounds were subjected to pharmacophore screening and molecular docking within the active site of the 3RHK protein. Docking results were evaluated based on binding affinity (kcal/mol) and RMSD values. The results are provide to table 3.2.

Table 3.1. Docking results were evaluated based on binding affinity (kcal/mol) and RMSD values.

Compound	Affinity(kcal/mol)	Conformer	RMSD
M971 (reference)	-13.20	1	0.00
11a	-10.70	1	0.00
9e	-10.10	1	0.00
9a	-9.70	1	0.00

The reference ligand (M971) exhibited the strongest binding affinity with a docking score of -13.20 kcal/mol, confirming the reliability of the docking protocol. Among the tested compounds, compound **11a** demonstrated the highest binding affinity (-10.70 kcal/mol), indicating a strong interaction with the active site. Compound **9e** showed moderate binding (-10.10 kcal/mol), while compound **9a** exhibited weaker interaction (-9.70 kcal/mol).

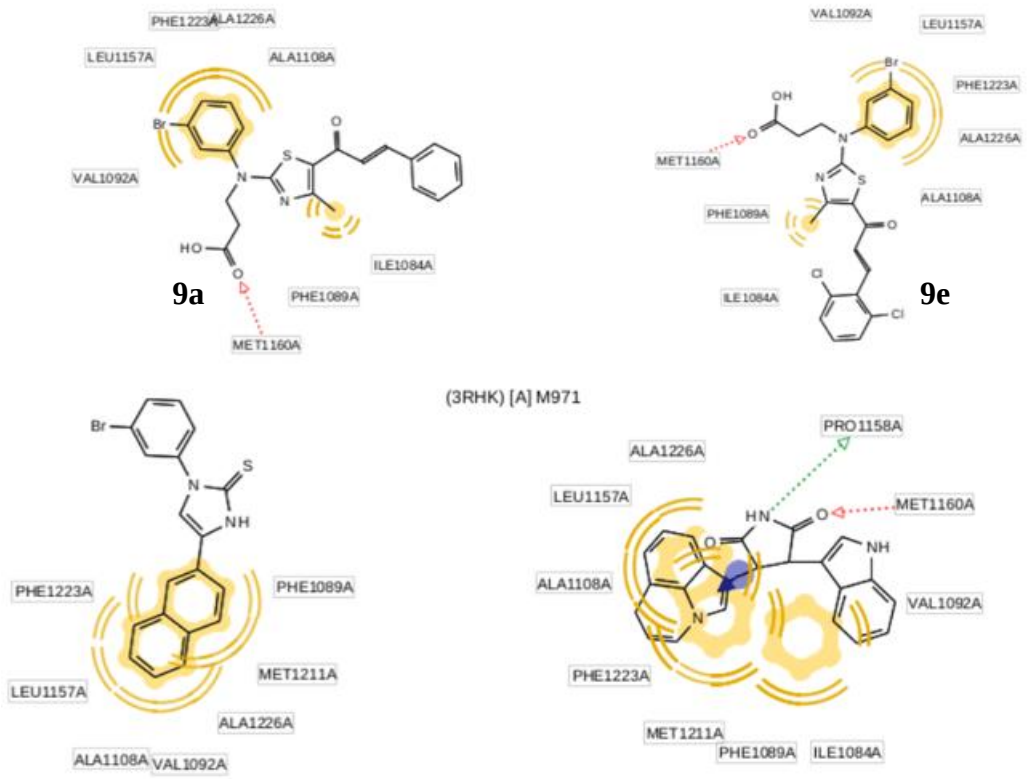

Fig. 3.10. Binding interactions of compounds **9a**, **9e and 11a** within the active site of the 3RHK binding pocket. The ligand forms key contacts with amino acid residues through hydrogen bonding and hydrophobic interactions, contributing to its stabilisation within the ATP-binding site of DNA gyrase B.

All best-ranked conformations showed RMSD values of 0.00 Å, indicating optimal docking poses without structural deviation from the predicted orientation. The observed ranking suggests that compound **11a** most effectively mimics the key pharmacophoric features required for binding.
The *in silico* analysis demonstrated that compound **11a** is the most promising candidate among the tested molecules, exhibiting the binding affinity closest to the reference inhibitor. The results suggest that effective binding within the 3RHK active site is primarily driven by key hydrogen bonding interactions (notably with Asp73) and hydrophobic contacts within the binding pocket. Compounds **9e** and **9a** showed moderate to weak binding, indicating partial compatibility with the pharmacophore model.

Recommendations

Based on the results of my project, future studies are highly recommended to prove the anticancer potential of the synthesised thiazole, imidazole and chalcone derivatives based on 3-bromoaniline. Some of the synthesised compounds were highly active against the lung cancer cell line A549. Therefore, further studies are needed to prove their therapeutic suitability as a commercial drug. Future studies can also be extended to different cancer cell lines as well as normal cell lines to determine their safety profile. Further automated studies, such as apoptosis assay, molecular target validation, etc., molecular docking could also be considered to determine how the active compounds bind to the receptor and how important this is for different targets. It is also recommended to modify the existing structure to determine how electron attraction or acceptance in the heterocyclic rings can affect the activity. It would also be possible to analyse how this property improves potency, selectivity, solubility, etc., and pharmacokinetics could be analysed. Analysis of the most promising compounds for IC50 studies could be considered. This could be done in light of advanced preclinical studies. These recommendations will help in future studies to obtain a good anticancer drug synthesised from 3-bromoaniline.

Conclusions

1. The synthesis of novel thiazole and imidazole derivatives was carried out, revealing that 3-bromoaniline possesses favourable properties and can be considered a suitable synthon as well as a biologically relevant fragment for the development of new potential anticancer agents.
2. Structural modification of 3-bromoaniline derivatives containing thiazole or imidazole moieties demonstrated that these scaffold are not only convenient for the synthesis of new compounds but also play a significant role in determining biological activity.
3. The analysis of the synthesised derivatives demonstrated antiproliferative activity against A549 human non-small cell lung cancer cells. The highest activity was exhibited by (*E*)-3-((3-bromophenyl)(5-(3-(2,6-dichlorophenyl)acryloyl)-4-methylthiazol-2-yl)amino)propanoic acid (**9e**), 3-((3-bromophenyl)(5-cinnamoyl-4-methylthiazol-2-yl)amino)propanoic acid (**9a**), and 1-(3-bromophenyl)-4-(naphthalen-2-yl)-1,3-dihydro-2*H*-imidazol-2-thione (**11a**).
4. The structure–activity relationship analysis, supported by ADMET studies and molecular modelling, indicated that specific structural features contribute significantly to anticancer activity. Among the investigated compounds, 1-(3-bromophenyl)-4-(naphthalen-2-yl)-1,3-dihydro-2*H*-imidazol-2-thione (**11a**) was identified as a promising candidate for further development.

List of references

[1] Y. Ouyang, J. Li, X. Chen, X. Fu, S. Sun, and Q. Wu, "Chalcone Derivatives: Role in Anticancer Therapy," *Biomolecules*, vol. 11, no. 6, p. 894, Jun. 2021, doi: 10.3390/biom11060894.

[2] D. Hanahan, "Hallmarks of Cancer: New Dimensions," *Cancer Discov.*, vol. 12, no. 1, pp. 31–46, Jan. 2022, doi: 10.1158/2159-8290.CD-21-1059.

[3] P. Martins *et al.*, "Heterocyclic Anticancer Compounds: Recent Advances and the Paradigm Shift towards the Use of Nanomedicine's Tool Box," *Molecules*, vol. 20, no. 9, pp. 16852–16891, Sep. 2015, doi: 10.3390/molecules200916852.

[4] H. E. N. Khasawneh *et al.*, "A novel thiazole-sulfonamide hybrid molecule as a promising dual tubulin/carbonic anhydrase IX inhibitor with anticancer activity," *Front. Chem.*, vol. 13, Jun. 2025, doi: 10.3389/fchem.2025.1606848.

[5] C. T. Supuran, "Carbonic anhydrases: novel therapeutic applications for inhibitors and activators," *Nat. Rev. Drug Discov.*, vol. 7, no. 2, pp. 168–181, Feb. 2008, doi: 10.1038/nrd2467.

[6] F. Ciardiello and G. Tortora, "EGFR Antagonists in Cancer Treatment," *New England Journal of Medicine*, vol. 358, no. 11, pp. 1160–1174, Mar. 2008, doi: 10.1056/NEJMra0707704.

[7] M. A. Jordan and L. Wilson, "Microtubules as a target for anticancer drugs," *Nat. Rev. Cancer*, vol. 4, no. 4, pp. 253–265, Apr. 2004, doi: 10.1038/nrc1317.

[8] F. Bray *et al.*, "Global cancer statistics 2022: GLOBOCAN estimates of incidence and mortality worldwide for 36 cancers in 185 countries," *CA Cancer J. Clin.*, vol. 74, no. 3, pp. 229–263, May 2024, doi: 10.3322/caac.21834.

[9] D. Hanahan, "Hallmarks of Cancer: New Dimensions," *Cancer Discov.*, vol. 12, no. 1, pp. 31–46, Jan. 2022, doi: 10.1158/2159-8290.CD-21-1059.

[10] L. Vadlakonda, M. Pasupuleti, and R. Pallu, "Role of PI3K-AKT-mTOR and Wnt Signaling Pathways in Transition of G1-S Phase of Cell Cycle in Cancer Cells," *Front. Oncol.*, vol. 3, 2013, doi: 10.3389/fonc.2013.00085.

[11] G. H. Lyman, N. M. Kuderer, and M. Aapro, "Improving Outcomes of Chemotherapy: Established and Novel Options for Myeloprotection in the COVID-19 Era," *Front. Oncol.*, vol. 11, Jul. 2021, doi: 10.3389/fonc.2021.697908.

[12] Sahil, K. Kaur, and V. Jaitak, "Thiazole and Related Heterocyclic Systems as Anticancer Agents: A Review on Synthetic Strategies, Mechanisms of Action and SAR Studies," *Curr. Med. Chem.*, vol. 29, no. 29, pp. 4958–5009, Sep. 2022, doi: 10.2174/0929867329666220318100019.

[13] P. Sharma, C. LaRosa, J. Antwi, R. Govindarajan, and K. A. Werbovetz, "Imidazoles as Potential Anticancer Agents: An Update on Recent Studies," *Molecules*, vol. 26, no. 14, p. 4213, Jul. 2021, doi: 10.3390/molecules26144213.

[14] Y. Ouyang, J. Li, X. Chen, X. Fu, S. Sun, and Q. Wu, "Chalcone Derivatives: Role in Anticancer Therapy," *Biomolecules*, vol. 11, no. 6, p. 894, Jun. 2021, doi: 10.3390/biom11060894.

[15] D. Hanahan and R. A. Weinberg, "The Hallmarks of Cancer," *Cell*, vol. 100, no. 1, pp. 57–70, Jan. 2000, doi: 10.1016/S0092-8674(00)81683-9.

[16] A. Glaviano *et al.*, "PI3K/AKT/mTOR signaling transduction pathway and targeted therapies in cancer," *Mol. Cancer*, vol. 22, no. 1, p. 138, Aug. 2023, doi: 10.1186/s12943-023-01827-6.

[17] A. Fassl, Y. Geng, and P. Sicinski, “CDK4 and CDK6 kinases: From basic science to cancer therapy,” *Science (1979).*, vol. 375, no. 6577, Jan. 2022, doi: 10.1126/science.abc1495.

[18] M. V. Liberti and J. W. Locasale, “The Warburg Effect: How Does it Benefit Cancer Cells?,” *Trends Biochem. Sci.*, vol. 41, no. 3, pp. 211–218, Mar. 2016, doi: 10.1016/j.tibs.2015.12.001.

[19] A. A. Cluntun, M. J. Lukey, R. A. Cerione, and J. W. Locasale, “Glutamine Metabolism in Cancer: Understanding the Heterogeneity,” *Trends Cancer*, vol. 3, no. 3, pp. 169–180, Mar. 2017, doi: 10.1016/j.trecan.2017.01.005.

[20] T. Mashima, H. Seimiya, and T. Tsuruo, “De novo fatty-acid synthesis and related pathways as molecular targets for cancer therapy,” *Br. J. Cancer*, vol. 100, no. 9, pp. 1369–1372, May 2009, doi: 10.1038/sj.bjc.6605007.

[21] S. Qian, Z. Wei, W. Yang, J. Huang, Y. Yang, and J. Wang, “The role of BCL-2 family proteins in regulating apoptosis and cancer therapy,” *Front. Oncol.*, vol. 12, Oct. 2022, doi: 10.3389/fonc.2022.985363.

[22] B. J. Druker *et al.*, “Efficacy and Safety of a Specific Inhibitor of the BCR-ABL Tyrosine Kinase in Chronic Myeloid Leukemia,” *New England Journal of Medicine*, vol. 344, no. 14, pp. 1031–1037, Apr. 2001, doi: 10.1056/NEJM200104053441401.

[23] M. Hojjat-Farsangi, “Small-Molecule Inhibitors of the Receptor Tyrosine Kinases: Promising Tools for Targeted Cancer Therapies,” *Int. J. Mol. Sci.*, vol. 15, no. 8, pp. 13768–13801, Aug. 2014, doi: 10.3390/ijms150813768.

[24] N. C. Turner *et al.*, “Palbociclib in Hormone-Receptor–Positive Advanced Breast Cancer,” *New England Journal of Medicine*, vol. 373, no. 3, pp. 209–219, Jul. 2015, doi: 10.1056/NEJMoa1505270.

[25] J. M. Adams and S. Cory, “The BCL-2 arbiters of apoptosis and their growing role as cancer targets,” *Cell Death Differ.*, vol. 25, no. 1, pp. 27–36, Jan. 2018, doi: 10.1038/cdd.2017.161.

[26] D. Kaloni, S. T. Diepstraten, A. Strasser, and G. L. Kelly, “BCL-2 protein family: attractive targets for cancer therapy,” *Apoptosis*, vol. 28, no. 1–2, pp. 20–38, Feb. 2023, doi: 10.1007/s10495-022-01780-7.

[27] W. Xiang, C.-Y. Yang, and L. Bai, “MCL-1 inhibition in cancer treatment,” *Onco. Targets. Ther.*, vol. Volume 11, pp. 7301–7314, Oct. 2018, doi: 10.2147/OTT.S146228.

[28] N. Kerru, L. Gummidi, S. Maddila, K. K. Gangu, and S. B. Jonnalagadda, “A Review on Recent Advances in Nitrogen-Containing Molecules and Their Biological Applications,” *Molecules*, vol. 25, no. 8, p. 1909, Apr. 2020, doi: 10.3390/molecules25081909.

[29] L. J. Lombardo *et al.*, “Discovery of *N* -(2-Chloro-6-methyl- phenyl)-2-(6-(4-(2-hydroxyethyl)- piperazin-1-yl)-2-methylpyrimidin-4- ylamino)thiazole-5-carboxamide (BMS-354825), a Dual Src/Abl Kinase Inhibitor with Potent Antitumor Activity in Preclinical Assays,” *J. Med. Chem.*, vol. 47, no. 27, pp. 6658–6661, Dec. 2004, doi: 10.1021/jm049486a.

[30] J. S. Tokarski *et al.*, “The Structure of Dasatinib (BMS-354825) Bound to Activated ABL Kinase Domain Elucidates Its Inhibitory Activity against Imatinib-Resistant ABL Mutants,” *Cancer Res.*, vol. 66, no. 11, pp. 5790–5797, Jun. 2006, doi: 10.1158/0008-5472.CAN-05-4187.

[31] T. R. Rheault *et al.*, “Discovery of Dabrafenib: A Selective Inhibitor of Raf Kinases with Antitumor Activity against B-Raf-Driven Tumors,” *ACS Med. Chem. Lett.*, vol. 4, no. 3, pp. 358–362, Mar. 2013, doi: 10.1021/ml4000063.

[32] D. Budman, “Novel microtubule-targeting agents – the epothilones,” *Biologics*, p. 789, Oct. 2008, doi: 10.2147/BTT.S3487.

[33] V. B. Siramshetty *et al.*, "NCATS Inxight Drugs: a comprehensive and curated portal for translational research," *Nucleic Acids Res.*, vol. 50, no. D1, pp. D1307–D1316, Jan. 2022, doi: 10.1093/nar/gkab918.

[34] R. Ferraldeschi, N. Sharifi, R. J. Auchus, and G. Attard, "Molecular Pathways: Inhibiting Steroid Biosynthesis in Prostate Cancer," *Clinical Cancer Research*, vol. 19, no. 13, pp. 3353–3359, Jul. 2013, doi: 10.1158/1078-0432.CCR-12-0931.

[35] Y. Ouyang, J. Li, X. Chen, X. Fu, S. Sun, and Q. Wu, "Chalcone Derivatives: Role in Anticancer Therapy," *Biomolecules*, vol. 11, no. 6, p. 894, Jun. 2021, doi: 10.3390/biom11060894.

[36] Sahil, K. Kaur, and V. Jaitak, "Thiazole and Related Heterocyclic Systems as Anticancer Agents: A Review on Synthetic Strategies, Mechanisms of Action and SAR Studies," *Curr. Med. Chem.*, vol. 29, no. 29, pp. 4958–5009, Sep. 2022, doi: 10.2174/0929867329666220318100019.

[37] S. H. Ali and A. R. Sayed, "Review of the synthesis and biological activity of thiazoles," *Synth. Commun.*, vol. 51, no. 5, pp. 670–700, Mar. 2021, doi: 10.1080/00397911.2020.1854787.

[38] S. Jain *et al.*, "Anticancer Potential of Thiazole Derivatives: A Retrospective Review," *Mini-Reviews in Medicinal Chemistry*, vol. 18, no. 8, pp. 640–655, Apr. 2018, doi: 10.2174/1389557517666171123211321.

[39] A. F. Kassem, R. H. Althomali, M. M. Anwar, and W. I. El-Sofany, "Thiazole moiety: A promising scaffold for anticancer drug discovery," *J. Mol. Struct.*, vol. 1303, p. 137510, May 2024, doi: 10.1016/j.molstruc.2024.137510.

[40] M. R, P. M, S. Pandey, R. Nayak, K. S. R. Pai, and S. L. Gaonkar, "Novel pyridine and 1,3,4-oxadiazole-linked 1,3-thiazole hybrids: Synthesis, anticancer evaluation, and computational insights," *J. Mol. Struct.*, vol. 1352, p. 144465, Feb. 2026, doi: 10.1016/j.molstruc.2025.144465.

[41] A. Boualli *et al.*, "Design, Hemisynthesis, Computational, and Biological Evaluation of Novel Totarol-1,3-Thiazol Derivatives as Anticancer Agents," *Chem. Biol. Drug Des.*, vol. 107, no. 4, Apr. 2026, doi: 10.1111/cbdd.70288.

[42] M. D. Altıntop *et al.*, "Development of a new series of thiazoles as EGFR-targeted anticancer agents for NSCLC therapy through nanotechnological and computer-aided approaches," *Bioorg. Chem.*, vol. 178, p. 109938, Aug. 2026, doi: 10.1016/j.bioorg.2026.109938.

[43] E. M. Radwan, M. M. Omran, A. H. A. Almaaty, M. A. El-Hawashey, N. A. Farouk, and M. A. E. Sophy, "Synthesis, characterization and anticancer investigation of some novel 2,5-disubstituted-1,3-thiazol-4-(5H)-ones and 1-substituted-1H-pyrazolo[3,4-d] thiazole derivatives," *J. Mol. Struct.*, vol. 1322, p. 140352, Feb. 2025, doi: 10.1016/j.molstruc.2024.140352.

[44] Y. Ouyang, J. Li, X. Chen, X. Fu, S. Sun, and Q. Wu, "Chalcone Derivatives: Role in Anticancer Therapy," *Biomolecules*, vol. 11, no. 6, p. 894, Jun. 2021, doi: 10.3390/biom11060894.

[45] T. Constantinescu and C. N. Lungu, "Anticancer Activity of Natural and Synthetic Chalcones," *Int. J. Mol. Sci.*, vol. 22, no. 21, p. 11306, Oct. 2021, doi: 10.3390/ijms222111306.

[46] E. C. McLoughlin and N. M. O'Boyle, "Colchicine-Binding Site Inhibitors from Chemistry to Clinic: A Review," *Pharmaceuticals*, vol. 13, no. 1, p. 8, Jan. 2020, doi: 10.3390/ph13010008.

[47] N. A. A. Elkanzi, H. Hrichi, R. A. Alolayan, W. Derafa, F. M. Zahou, and R. B. Bakr, "Synthesis of Chalcones Derivatives and Their Biological Activities: A Review," *ACS Omega*, vol. 7, no. 32, pp. 27769–27786, Aug. 2022, doi: 10.1021/acsomega.2c01779.

[48] M. Zhu *et al.*, "Design, synthesis, and evaluation of chalcone analogues incorporate α,β-Unsaturated ketone functionality as anti-lung cancer agents via evoking ROS to induce pyroptosis," *Eur. J. Med. Chem.*, vol. 157, pp. 1395–1405, Sep. 2018, doi: 10.1016/j.ejmech.2018.08.072.

[49] K. V. Sashidhara *et al.*, "Novel Chalcone–Thiazole Hybrids as Potent Inhibitors of Drug Resistant *Staphylococcus aureus*," *ACS Med. Chem. Lett.*, vol. 6, no. 7, pp. 809–813, Jul. 2015, doi: 10.1021/acsmedchemlett.5b00169.

[50] K. V. Sashidhara, K. B. Rao, V. Kushwaha, R. K. Modukuri, R. Verma, and P. K. Murthy, "Synthesis and antifilarial activity of chalcone–thiazole derivatives against a human lymphatic filarial parasite, Brugia malayi," *Eur. J. Med. Chem.*, vol. 81, pp. 473–480, Jun. 2014, doi: 10.1016/j.ejmech.2014.05.029.

[51] T. A. Farghaly, G. S. Masaret, Z. A. Muhammad, and M. F. Harras, "Discovery of thiazole-based-chalcones and 4-hetarylthiazoles as potent anticancer agents: Synthesis, docking study and anticancer activity," *Bioorg. Chem.*, vol. 98, May 2020, doi: 10.1016/j.bioorg.2020.103761.

[52] Md. M. Alam *et al.*, "Design, synthesis and cytotoxicity of chimeric erlotinib-alkylphospholipid hybrids," *Bioorg. Chem.*, vol. 84, pp. 51–62, Mar. 2019, doi: 10.1016/j.bioorg.2018.11.021.

[53] P. Sharma, C. LaRosa, J. Antwi, R. Govindarajan, and K. A. Werbovetz, "Imidazoles as Potential Anticancer Agents: An Update on Recent Studies," *Molecules*, vol. 26, no. 14, p. 4213, Jul. 2021, doi: 10.3390/molecules26144213.

[54] I. Ali, M. N. Lone, and H. Y. Aboul-Enein, "Imidazoles as potential anticancer agents," *Med. Chem. Commun.*, vol. 8, no. 9, pp. 1742–1773, 2017, doi: 10.1039/C7MD00067G.

[55] Z. Murtazaeva *et al.*, "Imidazole Hybrids: A Privileged Class of Heterocycles in Medicinal Chemistry with New Insights into Anticancer Activity," *Molecules*, vol. 30, no. 10, p. 2245, May 2025, doi: 10.3390/molecules30102245.

[56] I. de Toledo, T. A. Grigolo, J. M. Bennett, J. M. Elkins, and R. A. Pilli, "Modular Synthesis of Di- and Trisubstituted Imidazoles from Ketones and Aldehydes: A Route to Kinase Inhibitors," *J. Org. Chem.*, vol. 84, no. 21, pp. 14187–14201, Nov. 2019, doi: 10.1021/acs.joc.9b01844.

[57] A. Maleki, J. Rahimi, and K. Valadi, "Sulfonated Fe superparamagnetic nanostructure: Design, in-situ preparation, characterization and application in the synthesis of imidazoles as a highly efficient organic–inorganic Bronsted acid catalyst," *Nano-Structures & Nano-Objects*, vol. 18, p. 100264, Apr. 2019, doi: 10.1016/j.nanoso.2019.100264.

[58] N. Xue *et al.*, "Synthesis and biological evaluation of imidazol-2-one derivatives as potential antitumor agents," *Bioorg. Med. Chem.*, vol. 16, no. 5, pp. 2550–2557, Mar. 2008, doi: 10.1016/j.bmc.2007.11.048.

[59] S. Nashaat, M. A. Henen, S. M. El-Messery, and H. Eisa, "Synthesis, state-of-the-art NMR-binding and molecular modeling study of new benzimidazole core derivatives as Pin1 inhibitors: Targeting breast cancer," *Bioorg. Med. Chem.*, vol. 28, no. 11, p. 115495, Jun. 2020, doi: 10.1016/j.bmc.2020.115495.

[60] S. Venugopal *et al.*, "Recent advances of benzimidazole as anticancer agents," *Chem. Biol. Drug Des.*, vol. 102, no. 2, pp. 357–376, Aug. 2023, doi: 10.1111/cbdd.14236.

[61] V. Mickevičius *et al.*, "Synthesis and Biological Activity of 3-[Phenyl(1,3-thiazol-2-yl)-amino]propanoic Acids and Their Derivatives," *Molecules*, vol. 18, no. 12, pp. 15000–15018, Dec. 2013, doi: 10.3390/molecules181215000.

[62] U. Nagel, G. Radau, and A. Link, “Short Synthesis of Ethyl 3-(3-aminophenyl)propanoate,” *Arch. Pharm. (Weinheim).*, vol. 344, no. 12, pp. 840–842, Dec. 2011, doi: 10.1002/ardp.200900164.

[63] V. V. Kotova, V. Z. Maslosh, T. M. Pekhtereva, and A. Yu. Chervinskii, “Hantzsch reaction in urea-formaldehyde resins,” *Russian Journal of Applied Chemistry*, vol. 81, no. 5, pp. 901–903, May 2008, doi: 10.1134/S1070427208050388.

[64] T. Nakamori, T. Saito, and T. Kasai, “Synthesis of Naphthoquinone Derivatives. XIII. Reaction of 2,3-Dihydro-2-thioxo-1 *H* -naphth[2,3- *d*]imidazole-4,9-dione with Dimethyl Acetylenedicarboxylate,” *Bull. Chem. Soc. Jpn.*, vol. 61, no. 6, pp. 2019–2023, Jun. 1988, doi: 10.1246/bcsj.61.2019.

[65] A.-M. Borcea, I. Ionuț, O. Crișan, and O. Oniga, “An Overview of the Synthesis and Antimicrobial, Antiprotozoal, and Antitumor Activity of Thiazole and Bisthiazole Derivatives,” *Molecules*, vol. 26, no. 3, p. 624, Jan. 2021, doi: 10.3390/molecules26030624.

[66] D. Dotta *et al.*, “Chalcone Synthesis by Green Claisen–Schmidt Reaction in Cationic and Nonionic Micellar Media,” *J. Org. Chem.*, vol. 90, no. 8, pp. 2915–2926, Feb. 2025, doi: 10.1021/acs.joc.4c02616.

[67] P. Sharma, C. LaRosa, J. Antwi, R. Govindarajan, and K. A. Werbovetz, “Imidazoles as Potential Anticancer Agents: An Update on Recent Studies,” *Molecules*, vol. 26, no. 14, p. 4213, Jul. 2021, doi: 10.3390/molecules26144213.

[68] B. Pathare and T. Bansode, “Review- biological active benzimidazole derivatives,” *Results Chem.*, vol. 3, p. 100200, Jan. 2021, doi: 10.1016/j.rechem.2021.100200.

[69] E. Kocabas, A. Burak Sarıguney, and A. Coskun, “A Rapid and High-Yielding Synthesis of Thiazoles and Aminothiazoles Using Tetrabutylammonium Salts,” *Heterocycles*, vol. 81, no. 12, p. 2849, 2010, doi: 10.3987/COM-10-12067.

[70] A. Chakraborti, S. Garg, R. Kumar, H. Motiwala, and P. Jadhavar, “Progress in COX-2 Inhibitors: A Journey So Far,” *Curr. Med. Chem.*, vol. 17, no. 15, pp. 1563–1593, May 2010, doi: 10.2174/092986710790979980.

[71] Y. Li *et al.*, “Identification of 5,6-dihydroimidazo[2,1-b]thiazoles as a new class of antimicrobial agents,” *Bioorg. Med. Chem.*, vol. 24, no. 21, pp. 5633–5638, Nov. 2016, doi: 10.1016/j.bmc.2016.09.027.

[72] R. Buathong and S. Duangsrisai, “Plant ingredients in Thai food: a well-rounded diet for natural bioactive associated with medicinal properties,” *PeerJ*, vol. 11, p. e14568, Mar. 2023, doi: 10.7717/peerj.14568.

[73] T. T. Komoto *et al.*, “Exploring the Therapeutic Potential of trans-Chalcone: Modulation of MicroRNAs Linked to Breast Cancer Progression in MCF-7 Cells,” *Int. J. Mol. Sci.*, vol. 24, no. 13, p. 10785, Jun. 2023, doi: 10.3390/ijms241310785.

[74] I. Ali, M. N. Lone, and H. Y. Aboul-Enein, “Imidazoles as potential anticancer agents,” *Med. Chem. Commun.*, vol. 8, no. 9, pp. 1742–1773, 2017, doi: 10.1039/C7MD00067G.

[75] M. V. P. S. Nascimento *et al.*, “A Novel Tetrasubstituted Imidazole as a Prototype for the Development of Anti-inflammatory Drugs,” *Inflammation*, vol. 41, no. 4, pp. 1334–1348, Aug. 2018, doi: 10.1007/s10753-018-0782-y.

[76] K. Ichise, T. Tanio, I. Saji, and T. Okuda, “Activity of SM-4470, a new imidazole derivative, against experimental fungal infections,” *Antimicrob. Agents Chemother.*, vol. 30, no. 3, pp. 366–369, Sep. 1986, doi: 10.1128/AAC.30.3.366.

[77] V. Vainauskas *et al.*, “Synthesis and Characterization of Sulfonamide-Imidazole Hybrids with In Vitro Antiproliferative Activity against Anthracycline-Sensitive and Resistant H69 Small

Cell Lung Cancer Cells," *ChemMedChem*, vol. 20, no. 16, Aug. 2025, doi: 10.1002/cmdc.202500260.